The copyright of this thesis vests in the author. No quotation from it or information derived from it is to be published without full acknowledgement of the source. The thesis is to be used for private study or non-commercial research purposes only.

Published by the University of Cape Town (UCT) in terms of the non-exclusive license granted to UCT by the author.

University of Cape Town

University of Cape Town

Department of Mechanical Engineering

Optimised combustion control for different diesel fuels

University of Cape Town

A dissertation submitted to the Department of Mechanical Engineering, University of Cape Town, in partial fulfilment of the requirements for the degree of Master of Science in Engineering

Author: Mark Wattrus

Supervisor: Paul Schaberg

Date: 14 September 2007

Acknowledgements

The author wishes to thank Mr Paul Schaberg who proposed and supervised this project. His guidance and technical advice throughout the project were greatly appreciated.

Additionally, the author's gratitude must go to the Sasol Advanced Fuels Laboratory who initiated and funded this exciting project.

Finally, the electrical advice of Mr Samuel Ginsberg is gratefully acknowledged.

University of Cape Town

Declaration

1. I know that plagiarism is to use another's work and pretend that it is one's own
2. I have used the Harvard convention for citation and referencing. Each significant contribution to, and quotation in, this project from the work(s) of other people has been attributed, and has been cited and referenced.
3. This project is my own work
4. I have not allowed, and will not allow anyone to copy my work with the intention of passing it off as his or her own work.

Signature Signed by candidate

Mark Craig Wattrus

Summary

This project shows the development of a flexible, re-configurable electronic control unit (ECU) fitted to a diesel engine. The engine in question was a single cylinder Ricardo Hydra research engine. It was configured in the direct injection diesel mode using a high pressure common rail fuel injection system.

The ECU was built around a platform consisting of a PC and FPGA (Field-Programmable Gate Array) data acquisition card. This PC runs a host program and performs in a supervisory capacity. It reads in the data from the FPGA card and displays it on a graphical user interface; additionally, does calculations and updates the injection parameters. The FPGA program runs on the data acquisition card which does all the deterministic control and data capture. The relevant front-end circuitry was designed and built to mimic current production ECU's. This system now becomes a useful tool for flexible fuel research and rapid development of control strategies.

A control strategy was developed with two fuels in mind. Namely, a European specified diesel (EN590) and a Gas-to-Liquid (GTL) diesel from Sasol Ltd, as well as blends of these two fuels.

The focus of the control strategy hypothesis was to minimise the emissions based on the fuel's properties. The thinking behind this was that with the addition of new fuels into the market place, from various alternative sources, the engine manufacturers can no longer rely on open-loop control using a traditional engine map. Each fuel has different combustion characteristics that need to be exploited by the ECU in order to benefit from any possible emission reductions. This inherently implies the introduction of closed-loop control systems.

Control Strategy Hypothesis

The control strategy hypothesis was defined as follows: Firstly, to detect a change in the fuel type. Thereafter, the controller would use this knowledge of the fuel to optimise the engine emissions.

University of Cape Town

In order to detect a change of the fuel type going into the engine, a parameter was defined based on the fuel's Hydrogen/Carbon (H/C) ratio. This was calculated only once the controller had adjusted the injection settings to yield the same load (as was produced by the reference fuel for a known set point) and combustion phasing; thereafter, the calculation was done using the aspirated air-mass flow, gravimetric fuel flow and the oxygen content in the exhaust, in the form of lambda. After the H/C ratio was calculated in the aforementioned manner, a supervisory controller can optimise the combustion based on this information.

As is known with Nitrous Oxides (NO_x) and Soot/Particulate Mass (PM) exhaust emissions, there is a trade-off. Additionally, there is an approximately linear relationship between H/C ratio and Soot/PM. This, in turn, implies that there are different NO_x – PM trade-off curves based on the fuel's H/C ratio, which therefore can be traversed to minimise the emissions as shown in the graphic below, by changing the injection timing. There are timing limits on either end of these curves that the controller would not be allowed to exceed. The timing advance would be limited by the maximum allowable cylinder pressure that the engine was designed for. On the other end, the timing retardation would be limited by unburned hydrocarbons or BSFC (brake specific fuel consumption) for example.

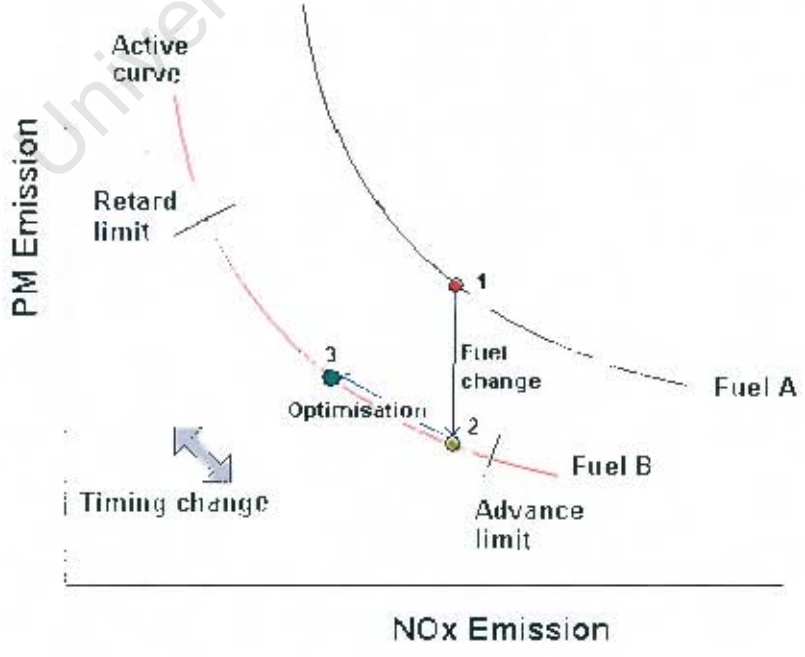

University of Cape Town

Validation

In order to validate the control algorithm five different fuels (EN590, GTL, and 3 blends in between) were used with varying H/C ratios and cetane numbers. These were run at the same engine operating point with and without the control; the control-off operating point for all the fuels was the chosen point for EN590. Additionally, a timing sweep was done for each fuel to ascertain its NO_x-Soot trade-off curve, and where the operating point was on this curve. Furthermore, the tests were run with and without pilot injections to gain further insight into the performance of the controller. Emission data, fuel consumption and power output were recorded to highlight the benefits of the control system. The success would be judged on the controller's ability to identify the fuel in use, and what emission improvements could potentially be achieved.

Conclusions

The ECU was fully functional and fulfilled all its requirements. Additionally, satisfactory control over the combustion phasing as well as the load was achieved. This control technique compensated for any differences in fuel energy content, injection delay and ignition delay.

Different Soot - NO_x trade-off curves were clearly identified based on the fuel's H/C ratio. These distinct curves have the potential to be traversed, with knowledge of the H/C ratio and the end limits, to significantly optimise emissions performance in favour of either NO_x or soot.

Furthermore the results confirmed that there was a clear linear relationship between soot concentration and H/C ratio – reducing soot with increasing H/C ratio. An insignificant change between the NO_x emissions and the H/C ratio was noticed, despite the difference in cetane numbers. It is speculated that this may be caused by the increased flame radiation heat loss for EN590 combustion, due to its higher soot levels.

The H/C ratio detection followed the trend of the actual fuel's H/C ratio, but to an unsatisfactory level without correction. An empirical correction factor was developed

University of Cape Town

Contents

University of Cape Town

University of Cape Town

List of Illustrations

Figures

University of Cape Town

University of Cape Town

Tables

University of Cape Town

Glossary

Lambda (λ) This is defined as the excess-air factor, or the ratio of the actual air/fuel ratio (AFR) to the theoretical stoichiometric AFR.

Acronyms

AFR	Air/fuel ratio
B50	50% point of the fuel's heat release
BDC	Bottom Dead Centre (prefix A represents After, conversely B is Before)
BSFC	Brake Specific Fuel Consumption
CAD	Crank Angle Degrees
CDM	Crank-angle Degree Marker
DMA	Direct Memory Access
ECU	Electronic Control Unit
EGR	Exhaust gas recirculation
FPGA	Field-Programmable Gate Array
FSN	Filter smoke number
GTL	Gas-to-Liquid
GUI	Graphical User Interface
H/C	Hydrogen/Carbon ratio
HC	Hydrocarbon
HIL	Hardware-in-the-loop
IMEP	Indicated mean effective pressure
LFM	Laminar flow meter
MOSFET	Metal–Oxide–Semiconductor Field-Effect Transistor
NO_x	Nitrous Oxides
PC	Personal Computer
PI	Proportional Integral
PM	Particulate Mass
PV	Pressure Volume
SOC	Start-of-combustion
SOI	Start-of-Injection
TDC	Top Dead Centre (prefix A represents 'after', conversely B is 'before')

University of Cape Town

1. Introduction

With ever stricter diesel exhaust emission legislation being implemented there is great demand for cost competitive solutions to achieve these emission levels. The easy way out would be to use expensive exhaust gas after-treatment systems, but a more challenging way is to implement a novel engine control strategy to optimise the combustion process.

Optimisation of the combustion process is most effectively achieved in a closed-loop control environment. Combustion parameters, like peak pressure, maximum pressure rise rate, heat release and start-of-combustion, need to be measured and controlled.

In order to develop these strategies it is therefore advantageous to have a flexible, re-configurable electronic control unit (ECU) fitted to the engine in question. Current production ECUs would obviously not provide this since they are hard coded and do not give access to their lookup tables.

A platform like this would allow the user to develop strategies to optimise exhaust pollutant emission levels while the engine is running, regardless of ambient conditions or what fuel is being used. The two fuels that were concentrated on in this report were a fuel meeting the EN590 specification and a gas-to-liquid (GTL) diesel fuel. This natural gas derived diesel was chosen on the basis of it being speculated that this will be a reliable future fuel source. Bio-diesel is also making inroads with the implementation of mandatory blending into conventional diesel; but there is still a lot of research to be done to allay fears of food crop offsets and other engine effects not yet known. As this transition happens there will, more than likely, be a gradual increase in GTL blending, rather than an overnight switch.

There are a few closed-loop control strategies built into the more modern ECUs, but these involve the control of more localised variables (i.e. start-of-injection or idle speed). Combustion analysis is a relatively new concept for production ECUs. Media reports have suggested that the engine manufacturers are on the verge of implementing full combustion control in some of their engines.

University of Cape Town

This document describes the development of such a flexible, re-configurable electronic control unit (ECU), and aims to demonstrate a control strategy hypothesis to help meet the stringent emission levels.

Report Structure

The layout of this report starts in the next section with a table containing the terms of reference that had to be achieved. Thereafter, a brief theoretical background is given followed by the literature review.

Next, the design solution is presented which is broken down into two subsections; the electronic control unit design and the control strategy. Following that, the validation process of the controller is described. Included in this section is the engine setup that was used for the validation.

This report concludes with the discussion of the various results and draws conclusions based on these results.

University of Cape Town

2. Terms of Reference

Table 2-1 shows the terms of reference that will guide the scope of this project. It will be seen that there are two main parts to this project; Firstly, to design and build a versatile PC-based ECU for the Ricardo Hydra, and secondly to implement a novel injection control strategy which can capitalise on cleaner-burning characteristics of diesel fuels with lower aromatics content.

Table 2-1: High level specifications

No.	Specification	Status
	Part 1 - Design and build a versatile PC-based ECU for the Ricardo Hydra	
1.1	Normal diesel engine ECU features	Achieved
1.2	Production standard injector driver	Achieved
1.3	Pilot and main injection events	Achieved
1.4	PC based	Achieved
1.5	Fail safe	Achieved
1.6	Programmed in LabVIEW	Achieved
1.7	User friendly interface	Achieved
	Part 2 - Implement a novel injection control strategy into the ECU	
2.1	Control load and injection timing to a desired set point	Achieved
2.2	Develop a parameter to identify fuel type during normal operation	Achieved
2.3	Demonstrate the control system's potential through a suitable validation process	Achieved

Refer to Appendix A for more detail on the contents of the above table.

Once the ECU with control algorithm support is completed, various conclusions will be drawn about how the control strategies interacted with the fuels.

University of Cape Town

3. Background and Literature Review

Electronic Control Unit (ECU)

An ECU, also known as an Electronic Diesel Control (EDC) in a diesel engine, is a control unit which controls various aspects of an internal combustion engine's operation.

Some of the first generation ECUs only controlled the injected fuel quantity for each cylinder, each engine cycle - previously this was done mechanically. ECUs have evolved and taken on more tasks as the fuel injection systems have become more flexible. [15] Nowadays advanced ECUs found on most modern diesel passenger cars also control the injection timing, rail pressure, exhaust gas recirculation, boost level of the turbocharger and other peripherals. These control parameters are calculated by monitoring the various engine sensors. These can include engine speed, fuel rail pressure, manifold-air pressure, intake-air mass flow, intake-air temperature, accelerator position, exhaust lambda and various others. This enhanced functionality and flexibility lets the ECU designers implement complex injection strategies; for example, the several small pilot injections (used to precondition the cylinder for the main combustion) that can be injected before the main injection. Additionally, the occasional late injection for regeneration of exhaust catalysts would just not have been possible without this level of control.

Currently, most ECUs do not implement closed-loop control of the combustion process. Mostly the injection settings are provided from lookup tables. These tables consist of two-dimensional or multi-dimensional data maps that have injection settings mapped as a function of engine speed and load. Correction factors and multipliers are used to account for changes in ambient conditions and transient operation.

There are closed-loop elements in modern ECU's (i.e. control of idle speed, start-of-injection, lambda) but there are still many development areas related to this. In particular, combustion analysis, which along with other closed-loop control strategies are discussed later in this Literature Review section.

To summarise, there are three primary functions that an automotive ECU fulfils.

University of Cape Town

Firstly, to detect the current engine operating conditions. Secondly, these variables need to be processed in a control unit which decides on an appropriate action and generates the required output signals for the actuators. Finally, the actuators convert the signals from the control unit into the physical world.

A more complex actuator that needs more explanation is the solenoid-valve injector driver. This is expanded on below.

Injector Driver

A solenoid-valve injector is a high current, electro-hydraulically activated device. This device needs to be controlled to a great level of accuracy and repeatability to ensure reliable fuel delivery. In order to achieve these needs a complex driver system is required. The driver circuit activates the injectors by the use of a current waveform consisting of several phases [15], as shown in Figure 3-1 below.

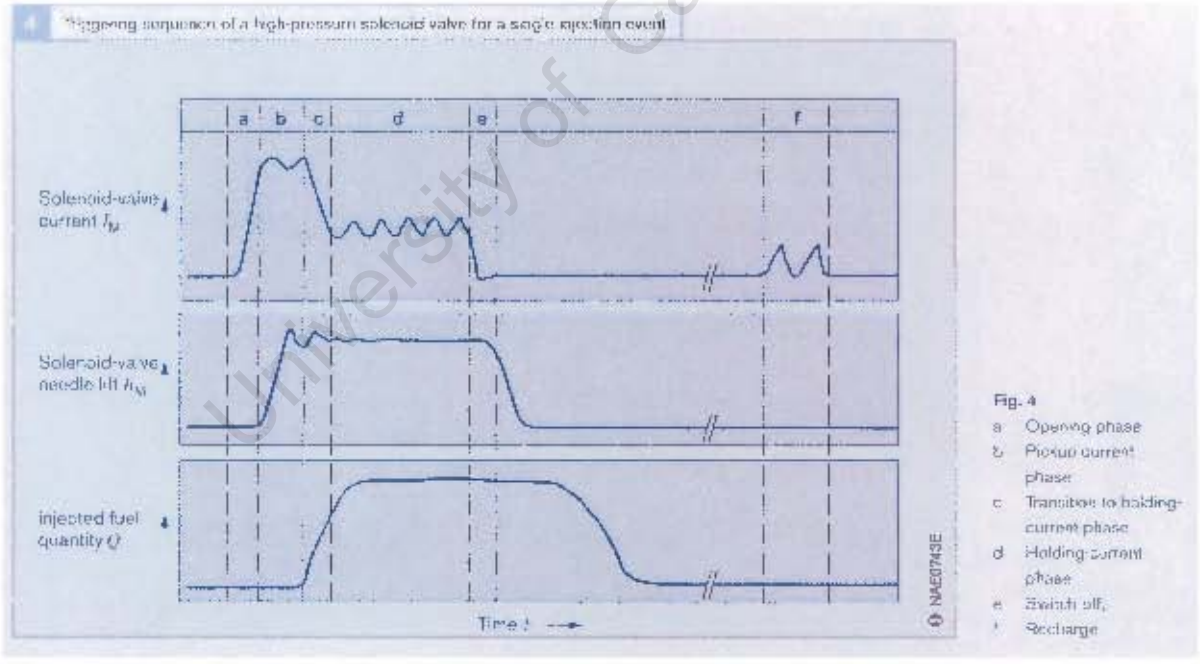

Figure 3-1: Triggering sequence of a solenoid-valve injector [15]

Opening phase

The rapid opening of the solenoid injector is achieved by applying a high voltage from a boost capacitor, up to 100 V, until the injector current reaches approximately 20 A. By using a high voltage this current level is achieved much faster than when

University of Cape Town

conventional battery voltage is used. This current ramp-up takes in the region of 30 μs.

Pickup-current phase

Once the peak current is achieved by the previous step, the high voltage is turned off and the battery voltage is applied. The current is held at this 20 A level for the remainder of the pickup phase which assists in opening the valve rapidly. This phase is usually around 200-250 μs.

Holding-current phase

After the previous two phases are complete the injector is guaranteed to be open. Implying that the armature of the solenoid has pulled in completely, thus reducing the air-gap to the stator. This consequently reduces the required current to maintain the injector open. The current is now dropped to around 12 A for the remainder of the injection duration to conserve power and prevent overheating.

Switch off

Once the injection event is complete the injector is required to close as quickly as possible. The back EMF (electromotive force) that is generated from switching off the solenoid is usually directed to the high voltage boost capacitor.

University of Cape Town

Closed-Loop Control of Combustion Process

With the current demand for continued reduction in emissions and fuel consumption, any improvement in diesel engine control is welcome. One area that would be influential in meeting this demand is more direct control of the combustion process. The current industry norm is open-loop control, which is probably explained by the expense and added complexity of adding the necessary feedback sensors for closed-loop combustion control.

These sensors would primarily come in the form of a pressure transducer, accelerometer and/or wide-band lambda sensor. There is a lot of focus on bringing down the cost of in-cylinder pressure transducers for this very purpose. Moriwaki et al. (2003) [13] developed a combustion pressure sensor installed inside a glow plug which showed good accuracy at a low cost. Ricardo UK (2006) [10] also found this

when investigating the current sensor technologies that would be fit-for-purpose in closed-loop combustion control systems, and found a glow plug mounted pressure sensor as the target sensor option. It has been subsequently announced by GM [11], who worked in conjunction with Ricardo, that these sensors will be implemented in the 2009 Cadillac GTS. Alternatively, there has been good progress in simple optical sensing techniques. This sensor consists of a silicon diaphragm which responds to the applied pressure, and the deflection is detected using an optical interferometer. Fitzpatrick (2000) [12] showed good performance with this sensor type, and low cost production capability.

These sensors will enable cycle-by-cycle combustion analysis on which new control strategies can be designed. The necessity for this is the current inability of open-loop control systems to adapt to changing environmental conditions, as well as to detect faults or performance reductions in the engine with more accuracy. As the engine ages its tolerances change through wear or deposition which could result in cycle-to-cycle and cylinder-to-cylinder variations. Additionally, there are substantial differences in the EN590 fuel specification; e.g. fuel density varies from 820-845 kg/m^3 (Yates and Rabe [14] observed a slight drop in power from this density change). All these changes could potentially be detected and compensated for. The benefit of reducing these variations is that the engine could always operate at some optimum point. Beasley et al. [10] have demonstrated a control strategy which deals with these variations, and have shown significant reductions in exhaust emission dispersion. The strategy involved, among other things, controlling the B50 point (50% point of the fuel's heat release) rather than the SOI (start-of-injection) point. This improves combustion phasing between cylinders and cycles by compensating for changes in injection and ignition delay.

The previous few paragraphs have been discussing the injection control strategies. Another method of closed-loop control, developed by Bosch, is the lambda-based exhaust gas recirculation (EGR) control. Lambda control is imperative for the regeneration of NO_x storage devices. This type of catalytic converter is regenerated when the overall AFR is rich and stores the NO_x when the engine is running lean ($\lambda>1$), as in normal diesel operation. Rich conditions ($\lambda<1$), are achieved by periodically increasing the amount of EGR, retarding injection and/or throttling the intake. There is quite a challenge in doing all this without affecting driveability.

University of Cape Town

Nevertheless, it has been done quite successfully and enables significant emission reductions.

Fuel Effects

With the threat of diminishing crude oil supplies, it is likely that fuels for internal combustion engines will be produced from a wider variety of feedstocks (e.g. natural gas, biomass, waste animal fats) in future. A particular challenge facing automotive manufacturers is to ensure optimal engine operation with fuels from these diverse sources.

Thus, it would be beneficial to detect, while running, different types of diesel fuel, and optimise the injection settings to suit the change in fuel properties.

This would require a method or an on-board sensor that could detect the change in fuel composition. A news report [17] has made mention to a company (SP3H) that is developing an in-tank near-infrared (NIR) sensor which categorises the composition of the fuel by hydrocarbon family. They intend on going into commercial production for the 2010 model year. This would give the ECU estimations of valuable fuel property information (i.e. Density, viscosity, heavy aromatic content, bio-fuel type and content, Distillation curve and cetane).

To get an idea of how these fuel properties will change with different fuels, a comparison is made between GTL diesel and the typical range for crude oil derived diesel (See Figure 3-2 below). Appendix C contains a full comparison of the fuels used in this project.

University of Cape Town

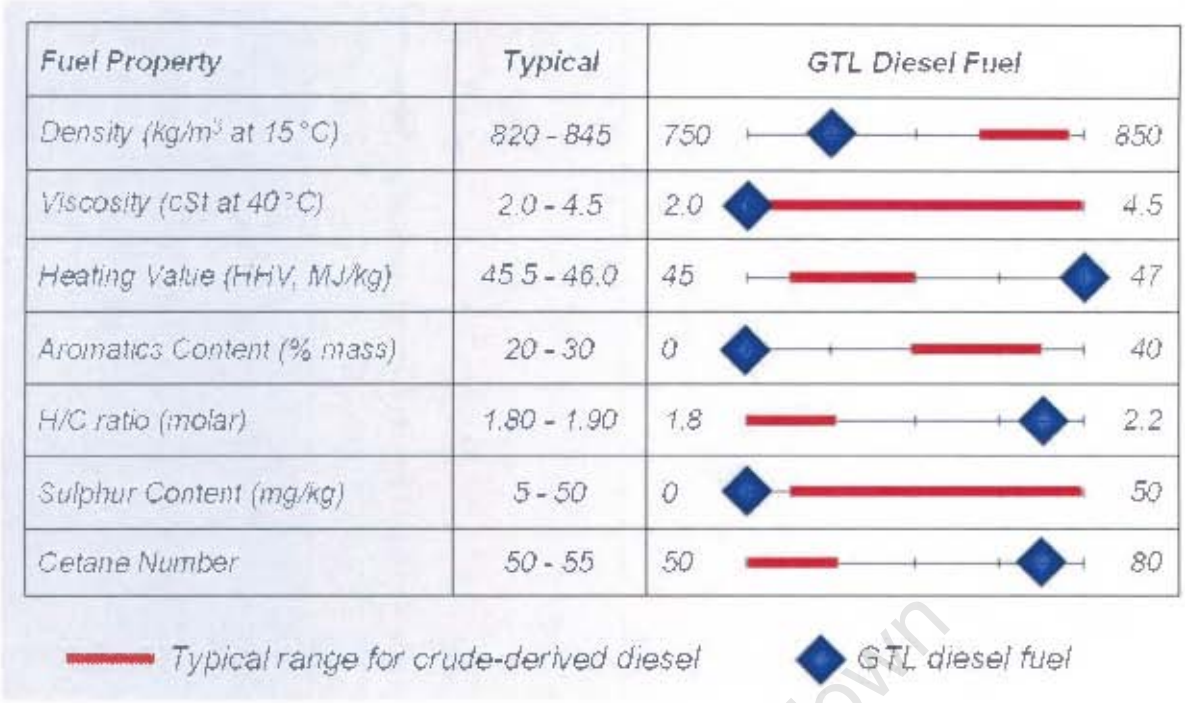

Figure 3-2: GTL diesel fuel properties comparison [17]

University of Cape Town

Cetane number (CN)

The cetane number is described as the fuel's propensity to auto-ignite. Thus GTL diesel with an estimated cetane number of greater than 74 would have a shorter ignition delay than the EN590 diesel (54.8 Cetane). A shorter ignition delay implies that less fuel is burned during the uncontrolled premixed combustion phase – responsible for high pressure rise rates - thus reducing the peak pressures and temperatures. There are additional benefits from the shorter ignition delay such as reduced engine noise.

Density (ρ)

Fuels are metered to the combustion chamber by volume. So if there is a reduction in density, as in GTL diesel, there will be a reduction in energy content for a hydrocarbon fuel. Consequently lower power and, in some cases, a decreased soot emission will be observed.

Heating Value (HV)

The heating value is the amount of chemical energy released by combustion of a unit quantity of a fuel.

The gross heating value is obtained when all products of the combustion are cooled down to the temperature before the combustion. Also, the water vapor formed during combustion is therefore condensed.

The net or lower heating value is obtained by subtracting the latent heat of vaporisation, of the water vapour formed during combustion, from the gross or higher heating value.

GTL's higher heating value compensates slightly for the lower power due to its lower density.

Hydrogen to Carbon Ratio (H/C Ratio)

The H/C ratio is the hydrogen to carbon ratio of the fuel on a molar basis (mol/mol). The H/C ratio is determined from the molecular structure of the fuel, which is the fundamental property that affects all other fuel properties. The affected properties are, among other things, the heating value, density and stoichiometric air/fuel ratio (AFR) of the fuel. As seen in Figure 3-2 the H/C ratio varies from 1.87 with crude oil derived diesel to 2.11 with GTL diesel.

It has been shown that there is an approximately linear relationship in pure hydrocarbon fuels between its H/C ratio and particulate matter (PM) exhaust emission [2], as shown below in Figure 3-3.

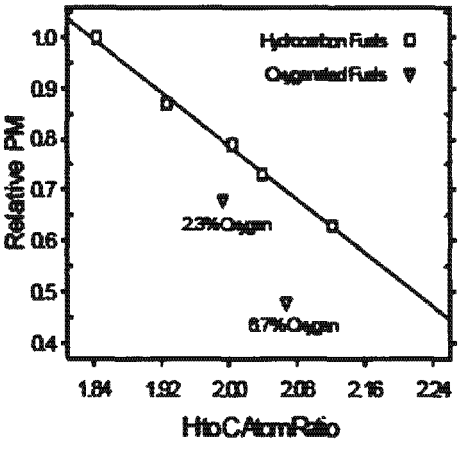

Figure 3-3: Linear relationship between PM and H/C ratio [2]

University of Cape Town

Particulates are formed in two stages; particle formation and particle growth, which include surface growth, coagulation and aggregation. Particulates are formed through the oxidation and/or pyrolysis products of a fuel. These products typically include unsaturated hydrocarbons which are the most likely precursors to soot formation. Throughout this process these products are dehydrogenated. The addition of mass occurs when the soot particles react with gas-phase molecules, thereafter growth continues with coagulation and aggregation [1]. Fundamentally the formation of soot is primarily from the carbon content of the fuel. Thus with a higher H/C ratio there is less carbon available for this process. It can be seen from the figure above that the linear relationship only holds for hydrocarbon fuels, and excludes oxygenated fuels.

Additionally, the H/C ratio affects the NO_x emissions. The heating value per stoichiometric air-fuel mixture becomes lower for a higher H/C ratio fuel; thus, reducing the adiabatic flame temperature. Since NO_x production has strong temperature dependency [18], the main effect of this is lower NO_x emission. Figure 3-4 shows how the adiabatic flame temperature is lowered with increasing H/C ratio fuels. It must be noted that an improved ignition quality can also contribute to lower burned gas temperatures.

University of Cape Town

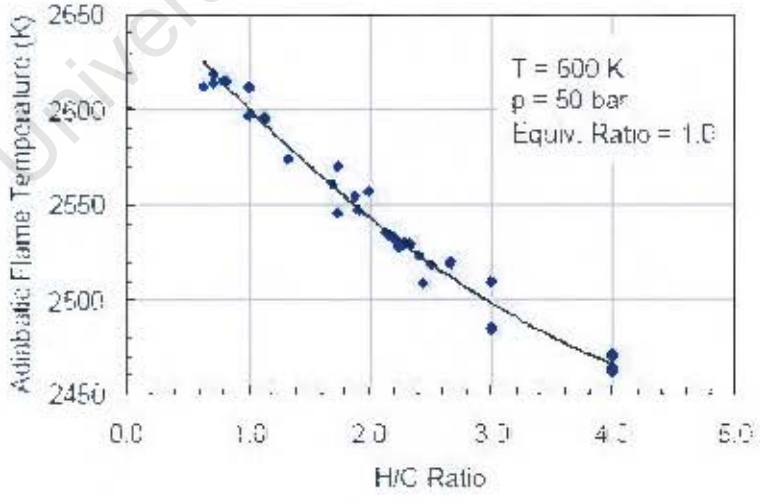

Figure 3-4: Calculated adiabatic flame temperature as a function of atomic H/C ratio for a variety of hydrocarbon fuels [20]

The same effect is achieved by retarding the injection timing, which also lowers peak temperatures and pressures. Also, by reducing peak temperatures and

reducing the effective time before the exhaust valves open, the rate and time for soot oxidation decreases, yielding increased levels of particulate emissions. Conversely, if the timing is advanced the NOx emissions will increase due to the higher temperatures, and the particulate emissions will decrease due to increased soot oxidation rates. This leads to the NO_x – Soot trade-off in diesel engines.

GTL is not yet commonly found in the forecourts but it is certainly headed for large scale integration into the market as it reduces dependence on crude oil [22]. More importantly it lowers exhaust emissions with virtually zero percent sulphur; this aids in reducing particulates and prevents catalyst poisoning. It can be appreciated that there will not be a transition overnight, but rather a gradual increase in the blending of the GTL diesel into conventional diesel. This implies that without some novel control strategy the fuel benefits would go largely unnoticed, that is until there are engines that are modified for GTL diesel and this diesel is freely available.

It is possible to run an unmodified engine on neat GTL diesel and notice emission reductions without noticing a significant performance change [3-7]. But, as mentioned above, it would be more advantageous to optimise the engine to suit the fuel. While hardware changes would yield a higher reduction in emissions [8, 9], injection control would be much easier to implement in the form of ECU software upgrades.

University of Cape Town

4. The Design Solution

The following sections describe the final solution that was implemented for each of the sub-systems.

4.1. Electronic Control Unit

The existing Bosch ECU was removed from the engine, leaving the original sensors and actuators in place, and designed from this state. The following chapter goes into the details of these electronic systems.

Essentially there are three functions that an automotive ECU fulfils:-

- Firstly, to detect the current engine operating conditions. This is done by acquiring feedback from the various sensors on an engine – Discussed in Sections 4.1.1 and 4.1.2.

- Secondly, these variables need to be processed in a control unit; thereafter, generate the required output signals for the actuators – Shown in Section 4.1.3.

- Finally, the actuators convert the signals from the control unit into the physical world – Explained in Section 4.1.4.

University of Cape Town

4.1.1. Hardware Platform

The hardware platform that was selected for the project needed to meet quite a high specification. It needed to fulfil several roles; along with capturing the data, it needed to control the various actuators at a high speed and to high accuracy. Flexibility was another requirement. This was needed to ensure a user-friendly platform to rapidly prototype the control algorithm.

There were several options that could potentially fulfil the requirements. One option was to use a standard PC with a traditional data acquisition card. This

would have been a user-friendly, flexible and an inexpensive solution, but lacked severely in the high speed and determinism areas. This was due to the fact that Microsoft Windows™ cannot perform true deterministic control as it prioritises system processes over software timing loops. A second option would be to use a microcontroller. Here there would have been high speed and accuracy, but this solution was discarded due to insufficient flexibility and user-unfriendliness.

The option that fulfilled all the requirements was achieved by using a PCI data acquisition card from National Instruments (NI 7831R) with a Field-Programmable Gate Array (FPGA) chip. This is a reconfigurable chip that rewires its internal gate array to perform the function of a program written in the LabVIEW® FPGA software. In short this is a hybrid between the first two options mentioned above. The PC provides the flexible and user-friendly platform, while the FPGA card provides true deterministic control over the actuators. Additionally, fast and accurate data capture is supported. The only disadvantage to this system was the higher price over the other solutions.

University of Cape Town

Figure 4-1: NI 7831R data acquisition card

The following list gives the specifications of the NI 7831R device (Figure 4-1):-

- 8 Analogue inputs, 16-bit resolution, 200 kHz simultaneous sampling, ±10 V
- 8 Analogue outputs, 16-bit resolution, 1MHz simultaneous updating, ±10 V

- 96 Digital input/output/counter lines, 40 MHz, 3.3 V / 5 V
- 1 Million gate FPGA chip

The analogue and digital channel assignment for the data acquisition card is shown in Appendix A.

4.1.2. Engine Sensors

As mentioned above this PC-based ECU was developed using all the existing sensors. Appropriate interface circuitry was designed and connected up to these sensors. All input signals were isolated from the data acquisition card as a precautionary measure. Additionally thermocouples were multiplexed to save on the analogue channel count. Refer to Appendix D for the circuit diagrams, additionally to Appendix E for the Bosch sensor information. All sensors are listed below.

University of Cape Town

Type of Sensor

Engine Speed

- Crankshaft encoder (AVL 364)

Engine Phase

- Proximity sensor mounted on the fuel pump driveshaft (Bosch 0 281 002 406)

Thermocouples

- Intake-air temperature (K-type)
- Exhaust-air temperature (K-type)
- Air-flow Meter temperature (K-type)
- Coolant temperature (K-type)

Pressures

- Rail pressure sensor (Bosch 0 281 002 260)

- Intake-air pressure Sensor (KISTLER 7505)
- Cylinder pressure (AVL QH32C Quartz Pressure Transducer)

Flow

- Laminar air-flow meter (Cussons P7200)
- Gravimetric fuel-flow meter (AVL 730)

Emissions

- Lambda (Horiba MEXA 110λ)
- NO_x (Horiba MEXA 720NO_x)
- Smoke meter (AVL 415)

4.1.3. Software

The programming language that was chosen for this project was LabVIEW®. This is a graphical based language which is easy to learn and very powerful. The development time is drastically reduced by using a language in this form. Additionally LabVIEW® easily integrates with all National Instruments data acquisition cards, thus giving the user a reliable PC-based control and acquisition system.

All the systems in the design solution were mapped in the following block diagram (Figure 4-2) to show the underlying system structure behind the user interface.

University of Cape Town

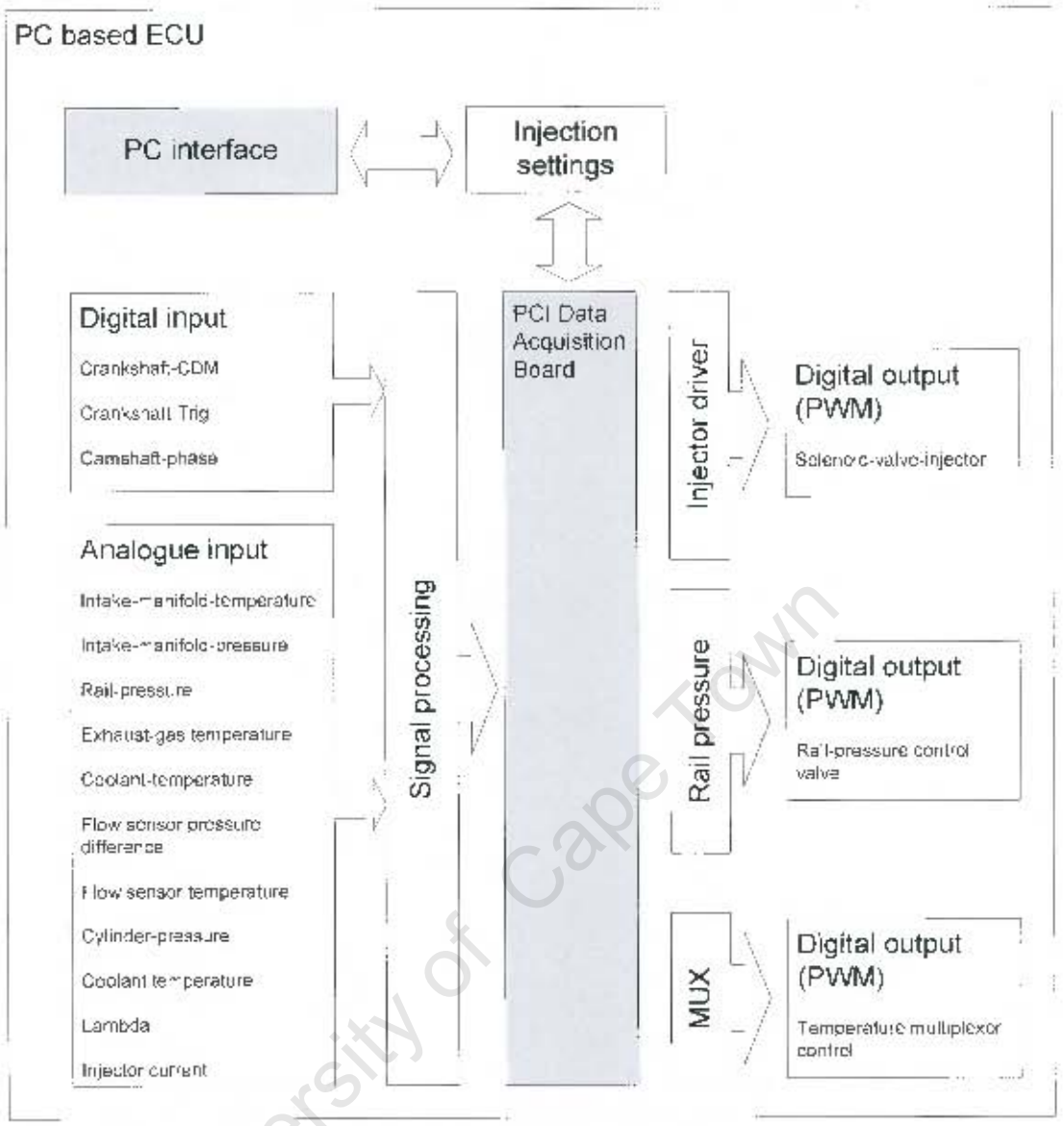

Figure 4-2: Systems structure

A host program runs on the PC and performs in a supervisory capacity. It reads in the data from the FPGA card and displays it on the graphical user interface (GUI), does calculations and updates the injection parameters. Figure 4-3 below is a screenshot of the user interface that was programmed for the ECU.

University of Cape Town

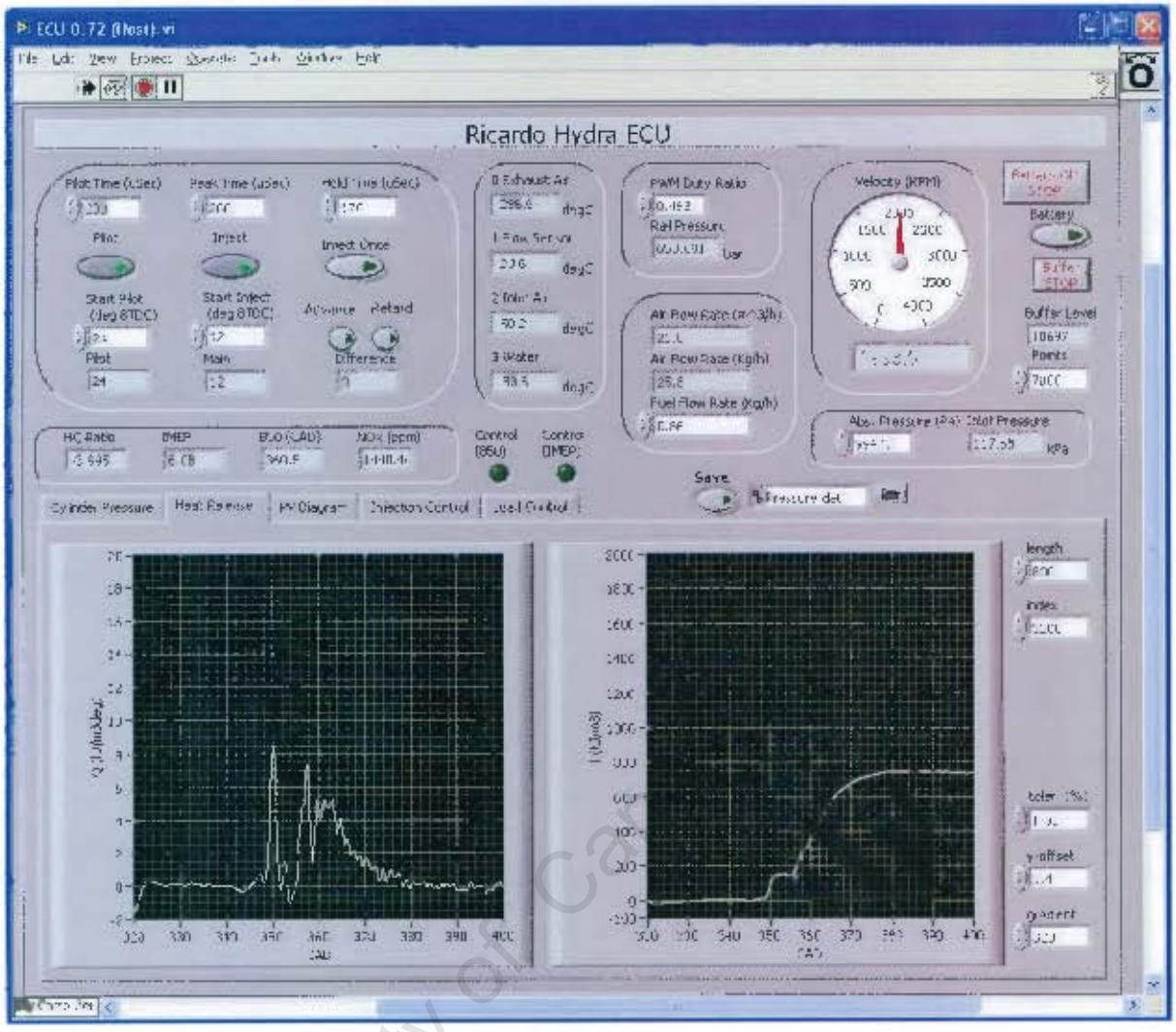

Figure 4-3: ECU screenshot

The FPGA program runs on the data acquisition card which does all the control and data capture. This control includes the thermocouple multiplexer channel selection, rail pressure relief valve, shaft encoder and injector solenoid driver (See Appendix A for selected flowcharts of these programs). The pressure signal is captured every 0.1 CAD and transferred through a direct memory access (DMA) buffer to the PC. The remaining signals are acquired and stored as often as possible since they are not time critical.

University of Ca

4.1.4. Engine Actuators

In essence the only engine outputs this ECU had were the injector and the rail pressure control valve. The rail pressure relief valve (Bosch 0 281 002 493) was driven using the 12 V battery and switching it using a MOSFET to obtain the desired rail pressure (circuit diagram contained in Appendix D).

The injector driver has a more complex driver circuit. In order to have precise metering of the fuel during injection, the injector (Bosch 0 445 110 030) needs to be opened and closed as quickly as possible. Typically the opening time is approximately 30 μs; this cannot be achieved by using the 12 V battery supply. The solution was to apply 95 V to the injector solenoid until the injector reached the required peak current of 15 A. A 150 Watt DC-DC converter was used to boost the 12 V to 95 V which was stored in a 100 μF capacitor. This capacitor can be fully charged in 6 ms by the DC-DC converter, and was chosen to ensure enough energy is stored, between injections, to supply boost voltage for pilot and main injection events each cycle.

Once the injector was opened it was held at this peak value for 200 μs, thereafter dropped to a lower holding current level of 12 A for the remainder of the injection event; this was done to reduce power consumption and therefore extend the battery life.

After injection closure there was a capacitor recharge period of around 300 μs where the injector could not be switched on. This is required so that the 100 μF capacitor could be charged up to 95 V again to ensure reliable opening for the next injection event. This injection waveform is depicted graphically in Figure 4-4 below.

University of Cape Town

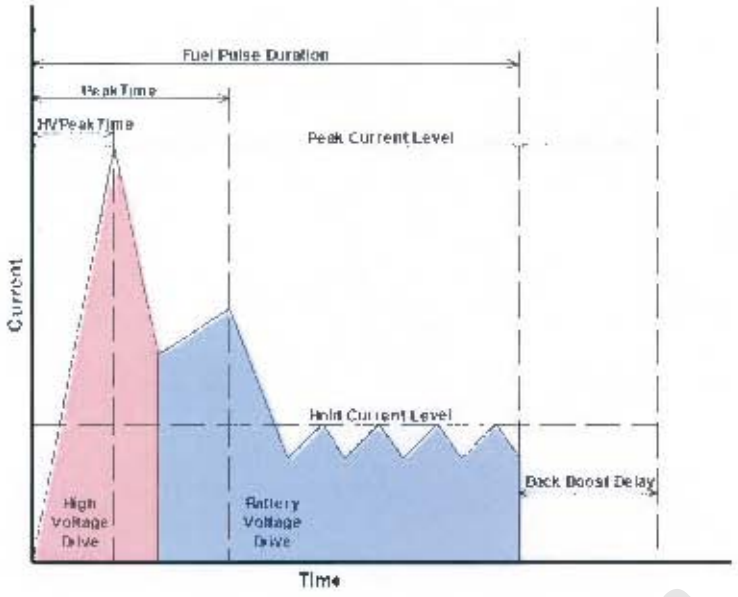

Figure 4-4: Injector current profile [16]

A half-bridge driver chip was used to drive the high- and low-side MOSFETS to control the above mention current waveform. Additionally a low-side current shunt was used to measure the injector current for the current control. This control method was to hold the current between two current levels which creates the saw tooth wave seen above.

There were a couple of off-the-shelf injector driver chips (e.g. LM1949) that could have done this but were not suitable. They did have a similar current control method, as mentioned above, but were primarily for petrol injectors. The problem with that was the peak to hold ratio was hard wired into the chip at 4 to 1. Additionally, there was no pickup-current phase, only the peak-current phase was evident. Because of these reasons the driver circuitry was designed specifically for this project.

Another issue that had to be overcome during injection closure was the back EMF generated when the solenoid is switched off. This high voltage will damage the MOSFET if nothing is done about it. There are various methods to cater for this problem; among others the methods include snubber circuits, fly-back diodes or zener diodes. The optimal solution found in this project was to place a 50 V zener diode across the MOSFET. This creates a ground path, through the low-side current shunt, for the back EMF to bypass the MOSFET. This is a beneficial

University of Cape Town

arrangement as the injector current is still known when the injector is switched off, and can therefore be controlled more accurately. A simplified circuit diagram is shown below in Figure 4-5. For the full detailed circuit diagram refer to Appendix D.

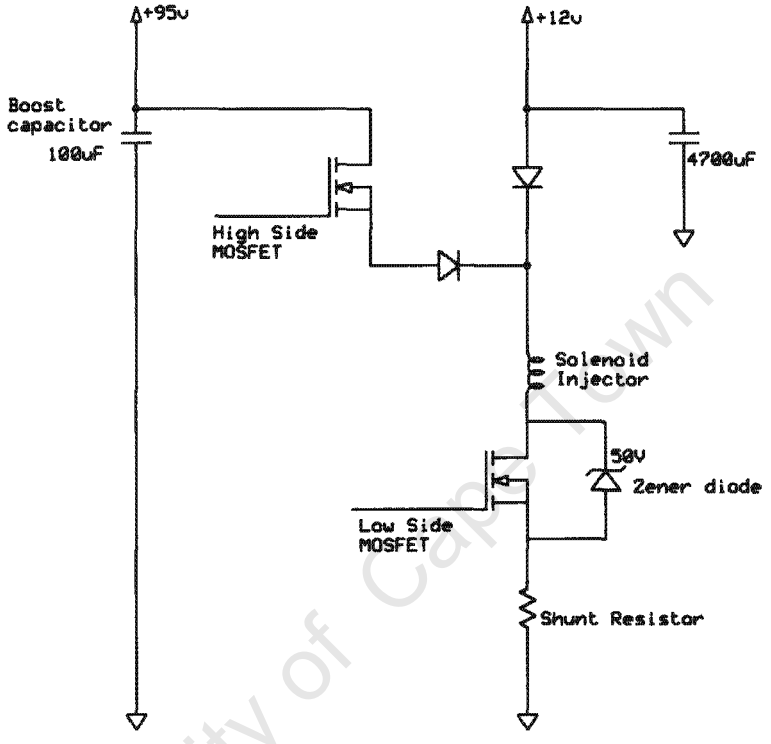

Figure 4-5: Simplified injector driver circuit

University of Cape Town

To summarise how this injection driver works, the MOSFET switching sequence will be stepped through:-

- *Opening phase*: High- and low-side ON.
  The injector is powered from the 95 V source through a protection diode (ultra-fast recovery type) and is blocked from flowing to the 12 V rail by another protection diode

- *Pickup-current phase*: High-side OFF and low-side ON.
  The injector is now powered from the 12 V source

- *Holding-current phase*: High-side OFF and low-side PULSED.

The injector current is held at the holding current level by pulsing the low-side MOSFET. The current feedback comes from the voltage drop across the shunt resistor

- *Switch off*: High-side OFF and low-side OFF.
  Both MOSFETs are switched off and the back EMF that is generated by the injector solenoid flows through the zener diode to ground.

The actual current waveform that was generated from the designed injector driver is shown in Figure 4-6 below.

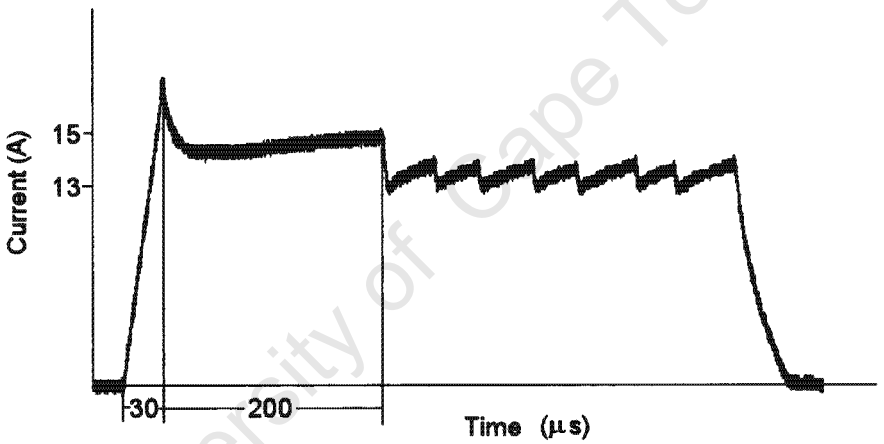

Figure 4-6: Actual injector current waveform

University of Cape Town

4.2. Control Strategy Hypothesis

The increase in engine sensors that are required by current closed-loop control strategies opens up new opportunities for novel control strategies. As this control strategy is aimed at optimising emissions when varying fuel blends of GTL and EN590 are used, there needs to be one fuel property that can be measured to indicate a change. After analysis of literature and the fuel properties table in Appendix C it was decided that one of the crucial measurable differences between the fuels was the H/C ratio. If a sensor existed that could directly measure this property, the fuel type detection would be greatly simplified - the literature review reports a sensor like this which is in a development stage. However, this property could be calculated by measuring the aspirated air-mass flow, gravimetric fuel-flow rate and the oxygen content in the exhaust in the form of lambda – this will be explained in greater detail later.

Real World Implementation

As this control strategy is a hypothesis and is aimed at becoming one of the many functions performed by an ECU, these aforementioned variables would need to be measured. Currently no gravimetric fuel flow sensors are fitted to production cars which present a problem in calculating the H/C ratio. A solution to this might include fitting a density meter in the fuel line, or alternatively to measure pressure at the bottom of the fuel tank when at a known volume to calculate the density. Combine this with the volumetric flow rate, inferred from the injection duration or fuel flow sensor, to calculate the gravimetric flow. A relative flow value is all that is necessary, rather than an absolute value.

Wide-band lambda sensors are currently becoming standard equipment on late model diesel cars. With the addition of NO_x accumulator type exhaust after-treatment systems and lambda closed-loop control, these will become standard if the stringent emission levels are to be met.

Hot-film air-mass meters have been fitted to all types of engines for some time now and will give reliable air-mass flow measurements.

University of Cape Town

With these three sensors in place the H/C ratio can be calculated and the following control strategy hypothesis implemented.

A better method would involve measuring the CO_2 concentration in the exhaust. With the additional knowledge of ambient O_2, N_2 and exhaust O_2 (from the lambda sensor) concentrations, the H/C ratio can be calculated from an atom balance. This method would be virtually instantaneous and more accurate than measuring gravimetric flow rates.

Hypothesis

If EN590 diesel runs at a set operating point, it will have an associated B50 point (see Figure 4-10 later) and a smoke limitation based on the AFR. Control of the B50 point, as opposed to the SOC point, was chosen because the combustion event can be phased more reliably when tracking the mid-point of the cumulative heat release; it is particularly advantageous when balancing different cylinders with each other. Additionally, this control parameter was found to be more sensitive to small changes in ignition delay [10].

When another fuel is used with a different H/C ratio and/or cetane number, the injection duration must be adjusted to give the same load output (as was produced by the reference fuel for a known set point); this must be achieved at the same B50 point and within the smoke limit of EN590.

After the controller has adjusted the injection settings to yield the same load and B50 point, the H/C ratio is calculated in the aforementioned manner (explained in more detail in Theory of Operation below). This H/C ratio is used by a supervisory controller as an indicator of the pollutant formation potential of the fuel, and can optimise the combustion accordingly.

This procedure would typically be run once after the driver has refuelled, as this is the only time that the fuel blend would be changed. It would also have to be done at the first opportunity when the engine is running at a steady state for a few seconds.

The example that was used to demonstrate this control strategy was to improve the NO_x and Soot emissions. There are many other parameters that could have been

University of Cape Town

chosen; i.e. Noise or BSFC. And often these parameters have conflicting requirements. which is where a high level supervisory controller would prioritise them.

As is known with NO_x and Soot, there is a trade-off. Additionally, as mentioned in the Literature Review, there is a linear relationship between H/C ratio and Soot/PM. This in turn implies that there are different NO_x – Soot trade-off curves based on the fuel's H/C ratio, which can therefore be traversed along to minimise the emissions. The optimum point would depend on what exhaust gas after-treatment devices are fitted - the cheaper option, compared to fitting expensive NO_x reducing catalysts, would be to minimise the NO_x and use a particulate trap. Alternatively, a gain on both emission fronts would involve moving towards the origin of the axes. Various fuel injection system parameters could be used. either individually, or in combination. to optimise the combustion process. for example injection timing or exhaust gas re-circulation (EGR). In this project injection timing was used as the control parameter. It is known that a very similar trade-off curve can be generated using EGR. With an injection timing control parameter there are timing limits on either end of these curves that the controller would not be allowed to exceed. The timing advance would be limited by the maximum allowable cylinder pressure that the engine was designed for. On the other end. the timing retardation would be limited by unburned hydrocarbons or BSFC, for example. This concept can be seen graphically below.

University of Cape Town

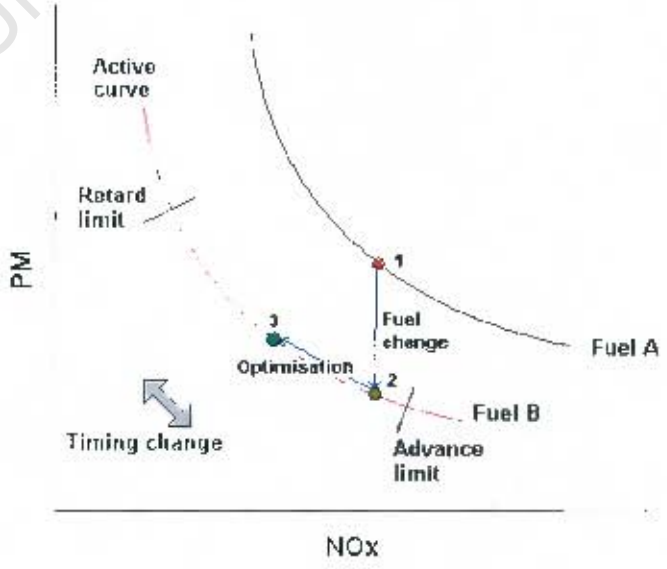

Figure 4-7: NOx - PM Trade-off curves

Theory of Operation

The B50 and load controllers that were implemented were simple Proportional & Integral (PI) controllers. If the control diagram (Figure 4-8 below) is followed the control process can be seen.

A set point is defined at the start and compared to a measured value. The resulting error is fed into the PI controller to yield a SOI value. The injector controller uses this and injects at the appropriate time, which after the ignition delay produces the combustion event.

A pressure transducer measures and sends the cylinder pressure trace via the FGPA card to the host computer for combustion analysis. Engine load, or indicated mean effective pressure (IMEP – explained below), and B50 are calculated and sent to their control summing points to calculate the error for the next cycle.

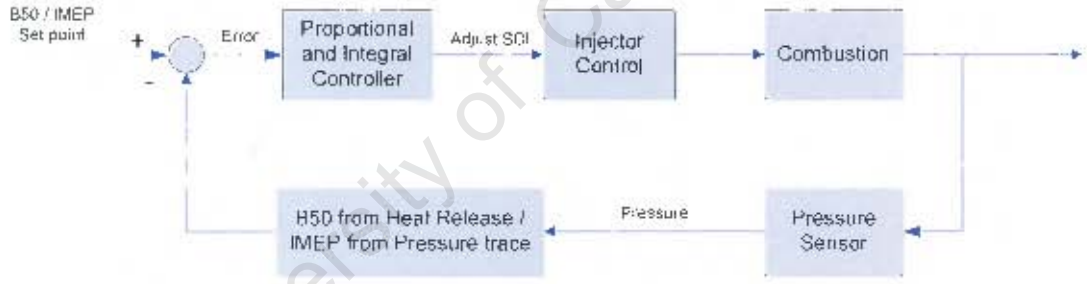

Figure 4-8: Control flow chart

The PI control constants were tuned using the Ziegler-Nichols method which yielded the following control constants.

Table 4-1: Control constants

	IMEP	B50
Proportional	40	-0.5
Integral	75	0.01

IMEP is calculated online by integrating the PV (Pressure vs. Volume) diagram over each engine cycle to get work, and dividing by the displaced volume.

University of Cape Town

$$IMEP = \frac{\oint p\,dV}{V_d}$$

Equation 4-1

B50 is the point at which 50% of the fuel's heat is released. This is extracted from the cumulative heat release diagram (Figure 4-10), which is the sum of all the instantaneous heat release calculations (Figure 4-9).

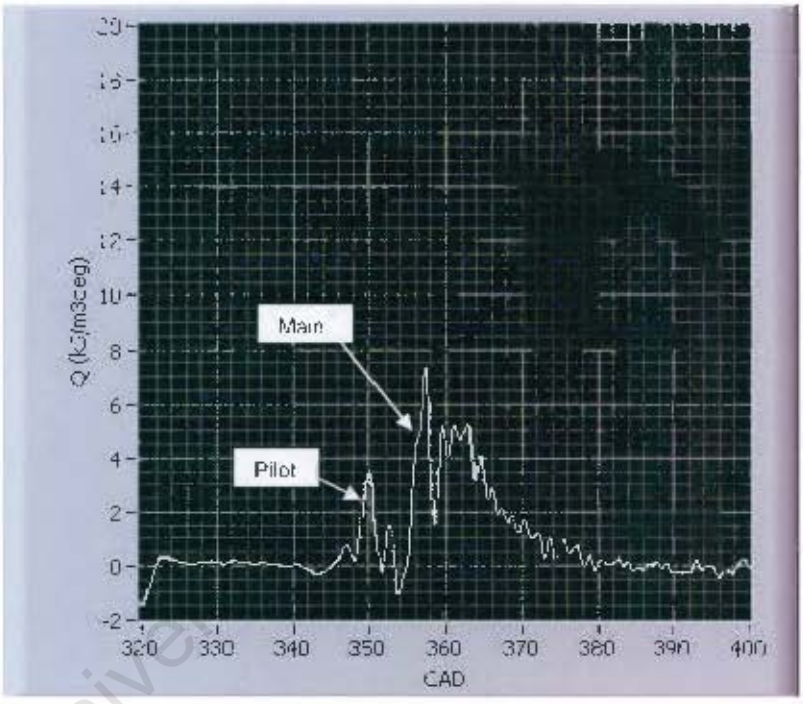

Figure 4-9: Instantaneous combustion heat release

Univ

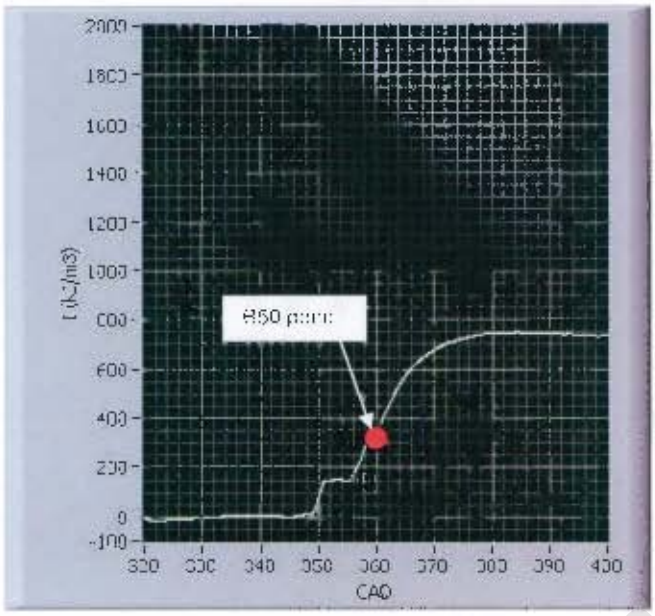

Figure 4-10: Cumulative combustion heat release

The instantaneous heat release is calculated using the following formula [1].

$$\frac{dQ_n}{dt} = \frac{\gamma}{\gamma - 1} p \frac{dV}{dt} + \frac{1}{\gamma - 1} V \frac{dp}{dt}$$

Equation 4-2

γ of 1.35 was used in the above formula.

H/C ratio is calculated using a carbon balance derived formula, as shown below. The full derivation is found in Appendix B.

$$H/C\ Ratio = \frac{(0.338 \frac{\dot{m}_{air}}{\dot{m}_{fuel}\lambda} - 4)}{(1 \quad 0.029 \frac{\dot{m}_{air}}{\dot{m}_{fuel}\lambda})}$$

Equation 4-3

University of Cape Town

5. Validation of Control Algorithm

In order to validate the control algorithm several different fuels were used with varying H/C ratios and Cetane numbers, and run at the same engine operating point with and without the control. Additionally, the tests were run with and without pilot injections. Emission data, fuel consumption and power output were recorded to highlight the benefits of the control system.

The engine that was used for the validation, and the way in which it was setup, is described below. Following that, the test fuels, engine operating point and validation procedure are shown.

University of Cape Town

5.1. Engine Setup

A single cylinder Ricardo Hydra research engine was used for this project. It was configured in the direct injection diesel mode using a high pressure common rail. The injector is solenoid actuated and has a 4-hole nozzle (Bosch 7712) which is located diagonally to the side of the combustion chamber. The cylinder head has one inlet and one exhaust valve. The table below lists the specifications of this engine:

Table 5-1: Specifications of the Ricardo Hydra Engine

Cylinders		1
Bore	mm	80.26
Stroke	mm	88.90
Con Rod	mm	158.01
Swept Volume	cc	450
Compression ratio	-	16:1
Max Engine Speed	rpm	4500
Max Power	kW	8
Exhaust Valve Opening		58° BBDC
Inlet Valve Closing		42° ABDC
Fuel injection system	-	Common rail - DI

The engine's output shaft is coupled to a dynamometer which is a DC machine; this can be set to load absorption or motoring. To measure this torque a load cell is fitted to the dynamometer. The test cell is shown below.

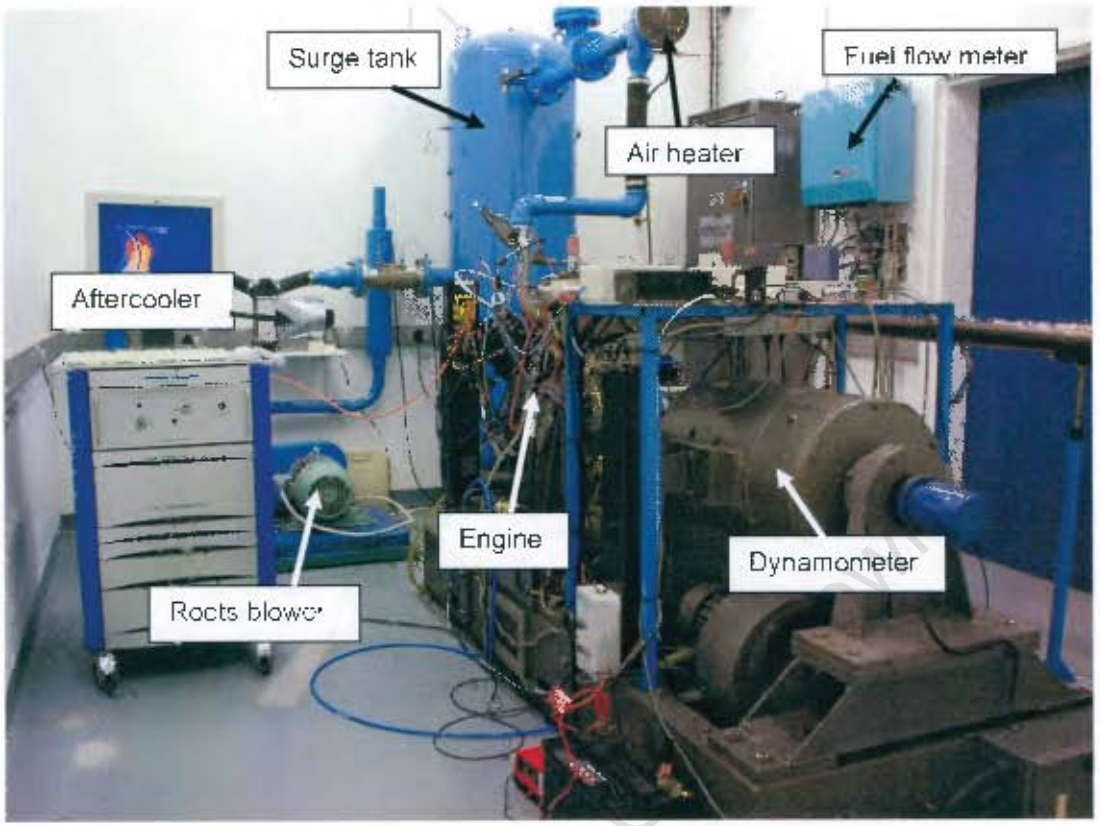

Figure 5-1: Hydra Engine Test Cell

A roots blower is fitted to the intake manifold to simulate supercharging by compressing the air to a set level. This air is ducted through an aftercooler and a laminar air flow meter; thereafter, it's fed into an accumulator tank to reduce the pressure pulsations which cause inaccuracies in the air flow reading.

In order to control inlet manifold temperature an air heater with temperature control is fitted after the accumulator tank. Ambient air is controlled by the test cell air conditioning.

A gravimetric fuel-flow meter (AVL 730) is fitted to the fuel line to measure fuel flow rate by measuring the change in mass of the fuel reservoir. The fuel temperature is also controlled by routing it through a water cooled heat exchanger

The engine speed and crank angle measurement are done by means of an AVL 364 light pulse crank angle encoder which is set to a resolution 0.1 crank angle degrees.

Exhaust emissions are measured in the exhaust pipe using a smoke meter (AVL 415) and a NO_x sensor (Horiba MEXA 720NO_x). The smoke meter measurements were converted from FSN (Filter Smoke Number) units to soot concentration. Additionally, a lambda sensor (Horiba MEXA 110λ) is fitted to measure oxygen concentration in the exhaust gases.

The cylinder pressure measurements are made using an AVL QH32C Quartz Pressure Transducer and a Kistler type 5015 charge amplifier.

University of Cape Town

5.2. Test Fuels

A matrix was constructed for the volumetric blending ratios of the test fuels, as shown below in Table 5-2. The H/C ratio of the blends was calculated using the gravimetric blending ratio.

Table 5-2: Test fuel matrix

Fuel no.	% Blend of EN590	% Blend of GTL	Density (kg/l)	Lower heating value (MJ/kg)	Effective H/C ratio
1	100	0	0.8297	42.75	1.87
2	75	25	0.8147	43.03	1.93
3	50	50	0.7998	43.30	1.99
4	25	75	0.7848	43.56	2.05
5	0	100	0.7698	43.81	2.11

The engine operating point was fixed for Fuel no. 1 at 2000 rpm. With these settings the engine, control disabled, was run with the remaining fuels and any changes observed. Thereafter, the control system was enabled and the engine tests repeated. The point that was chosen for the validation was as follows.

Table 5-3: Engine operating point

Rail Pressure	650 bar
Boost pressure (gauge)	200 mbar
Speed	2000 rpm
Load	6 bar IMEP
SOI Pilot (Control OFF)	24° BTDC
SOI Main (Control OFF)	12° BTDC
Inlet-air temperature	50 °C
B50	TDC

Additionally, an injection timing sweep was done for each fuel to ascertain the NO_x-Soot trade-off curve and where the operating point was on this curve.

University of Cape Town

6. Results and Discussion

This section discusses how well the design solution integrated together, and sees how effective the control system was. Firstly, the effect of the control system on the injection timing will be reported. Thereafter, the emission results for all of the fuels will be presented; these will include the relationship between the fuel's H/C ratio and NO_x/Soot concentration. Finally, the accuracy of the fuel H/C ratio detection will be shown.

For the full test results and pressure traces please refer to Appendix F.

6.1. Control System

The control system is essentially changing the injection settings to achieve a desired combustion result. Figure 6-1 shows the resulting pressure trace from a pilot and main injection sequence. This gives a feel for the ignition- and injection-delays that the control system compensates for by tracking the B50 point (at TDC in this case).

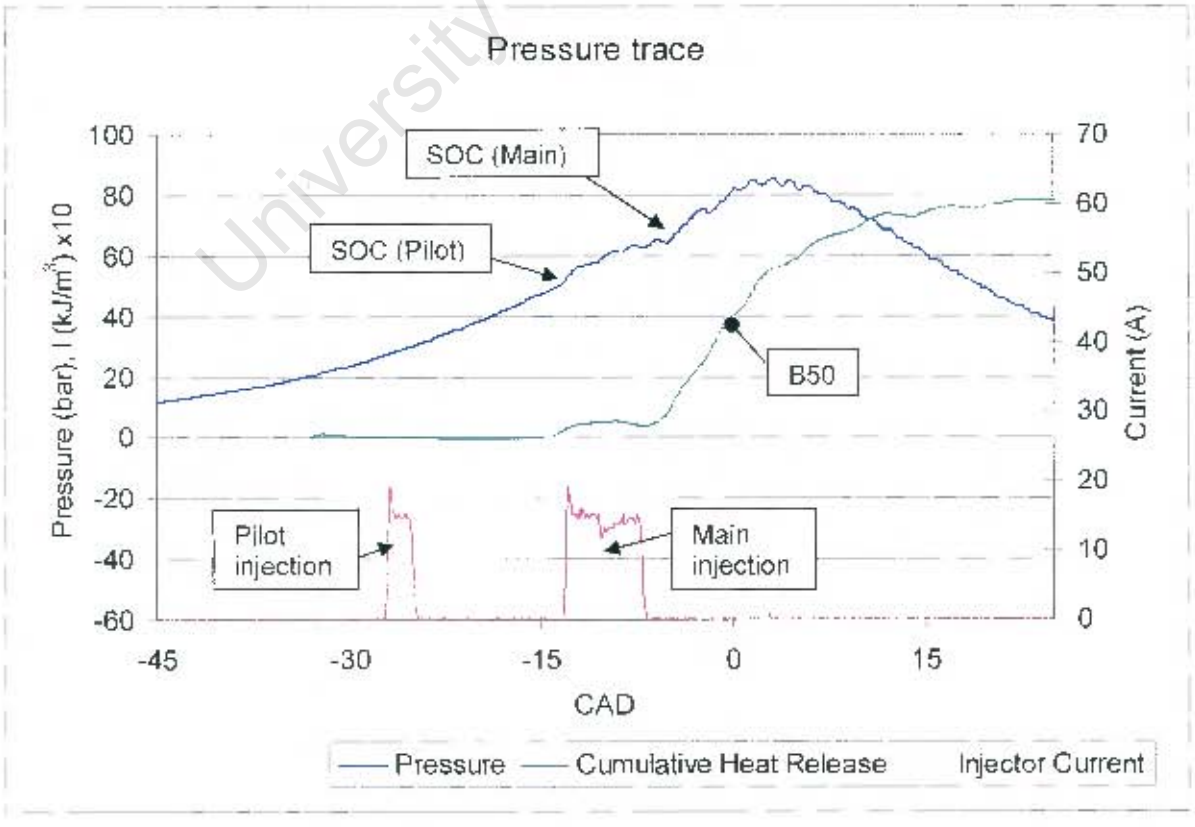

Figure 6-1: Pressure trace with injector current

University of Cape Town

IMEP and B50 controller performance

Controller performance was analysed by creating a step change of the controller setpoint and capturing the response. Firstly, the results were shown for the B50 controller, then for the IMEP controller.

The B50 change is shown on the left in the Injection Control graph (in Figure 6-2). The setpoint was changed from 363 CAD to 360 CAD. On the right is the Injection Timing graph, which shows how the controller changed the injection timing to achieve the new setpoint.

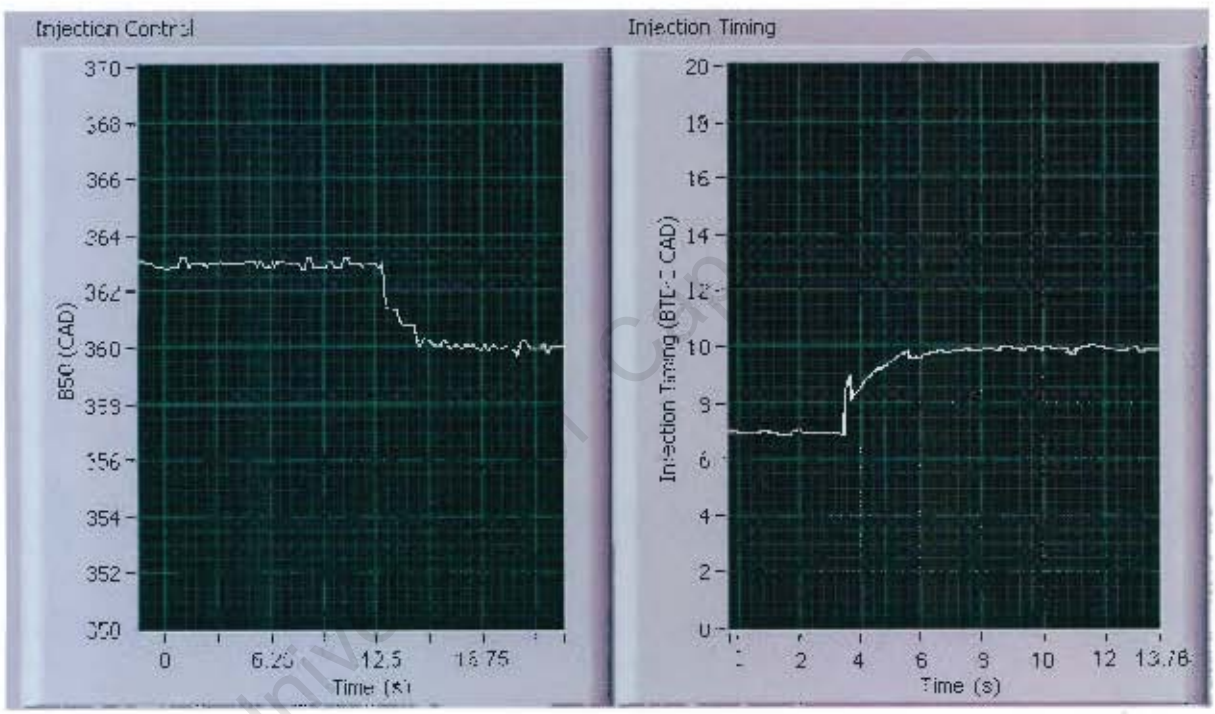

Figure 6-2: Step change response for B50 controller

The IMEP change is shown on the left in the Load graph (in Figure 6-3, injection duration is based on the injector current).The setpoint was changed from 5 bar to 6 bar. On the right is the Duration Control graph, which shows how the controller changed the injection duration to achieve the new IMEP setpoint.

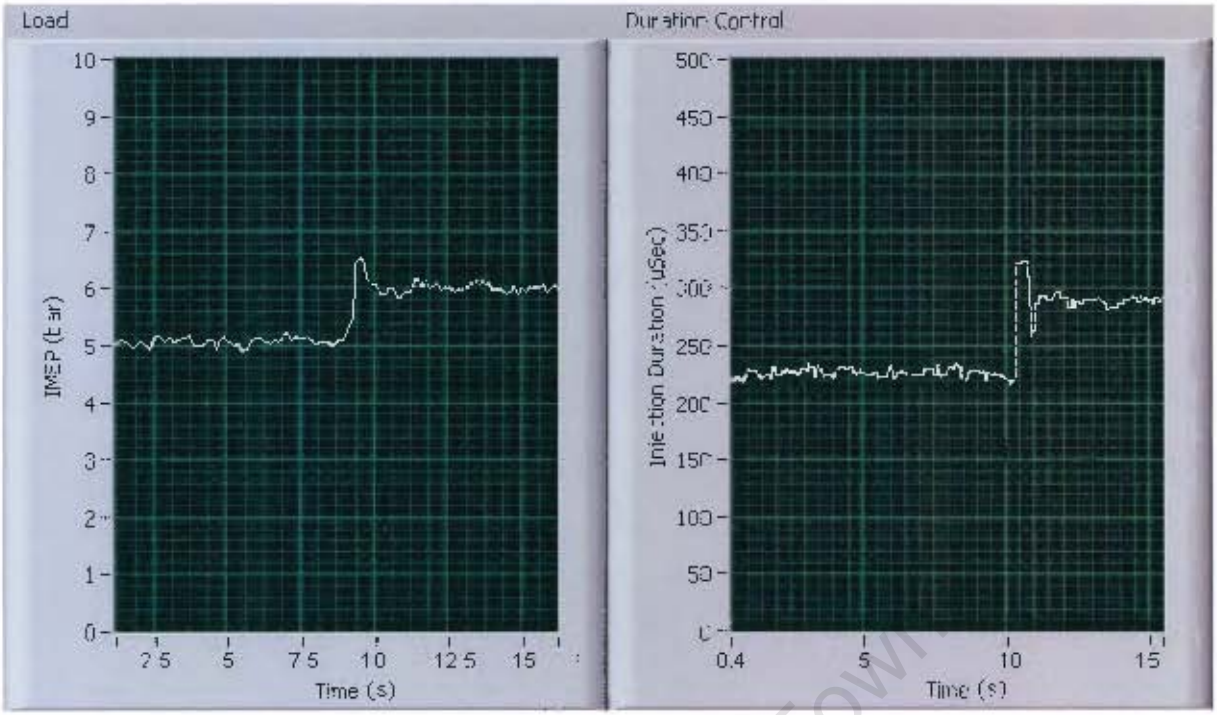

Figure 6-3: Step change response for IMEP controller

Discussion

The step test was done to demonstrate the stability and response time of the controllers. It can be seen that a satisfactory level of control was achieved by both controllers.

Fuel flow effects

The validation of the controller was done on all the fuels and the results were tabulated below. Table 6-1 shows how the injection settings (pilot injection off) were changed by the controller to compensate for any change in the IMEP and B50 point of each fuel. By controlling this point the fuel's energy content, injection delay and ignition delay are all compensated for – yielding the same B50 point and same torque for any fuel at a given operating point.

It can be seen below that the fuel flow without pilot injections agrees with conventional wisdom of a reducing gravimetric fuel flow, with increasing lower heating value (LHV).

University of Cape Town

Table 6-1: Injection timing effect from control system without pilot injections

	Control				
	Off		On		
Fuel Blend	Injection BTDC (CAD)	Main Injection Duration (µs)	Injection BTDC (CAD)	Main Injection Duration (µs)	Fuel flow (kg/h)
EN590	15.6	486	15.6	486	0.88
25%GTL + 75%EN590	15.6	484	15.6	484	0.86
50%GTL + 50%EN590	15.6	485	15.1	484	0.85
75%GTL + 25%EN590	15.6	485	16	485	0.84
GTL	15.6	485	15.9	484	0.84

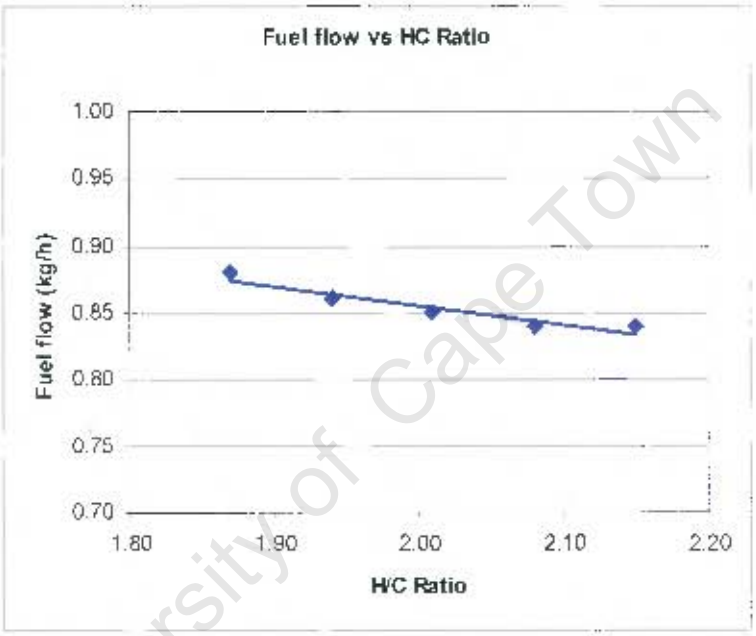

Figure 6-4: Fuel flow vs. H/C ratio (without Pilot)

University of Cape Town

To confirm what has been shown above, the expected change in gravimetric fuel flow rate (kg/h) can be calculated using the change in the inverse of gravimetric lower heating value (these units would now be kg/MJ). This compares the gravimetric flow rate for the same amount of energy being put into the engine, but this is only viable if the fuel conversion efficiency of all the fuels is constant. It was assumed that, to a first approximation, this would be the case, since the load and combustion phasing (as described by the B50 point) were equalised for each fuel.

Table 6-2 below makes a comparison between neat GTL and EN590 to see if the results correlate with the above-mentioned relationship to gravimetric lower heating value.

Table 6-2: Comparison of measured flow differences with calculated ones

	GTL	EN590	% change
Measured			
Fuel flow rate (kg/h)	0.84	0.88	**4.5**
Calculated			
LHV (MJ/kg)	43.81	42.75	
1 / LHV (kg/MJ)	0.0228	0.0234	**2.5**

It can be seen, when going from GTL to EN590, that there is a measured increase in gravimetric flow of 4.5% and the theoretical calculation suggests a 2.5% increase.

Pilot injections were turned on to see if this expected flow reduction held, and the results are shown in Table 6-3.

Table 6-3: Injection timing effect from control system with pilot injections

	Control				
	Off		On		
Fuel Blend	Injection BTDC (CAD)	Main Injection Duration (µs)	Injection BTDC (CAD)	Main Injection Duration (µs)	Fuel flow (kg/h)
EN590	12.7	392	12.7	392	0.87
25%GTL + 75%EN590	12	386	12.3	392	0.88
50%GTL + 50%EN590	12	391	12.7	390	0.88
75%GTL + 25%EN590	12	387	12.7	390	0.85
GTL	12	390	12.8	392	0.88

What is interesting to note is that there is little to no difference in the injection duration and fuel flow, despite there being differences in gravimetric lower heating value – as shown with no pilot injections above.

University of Cape Town

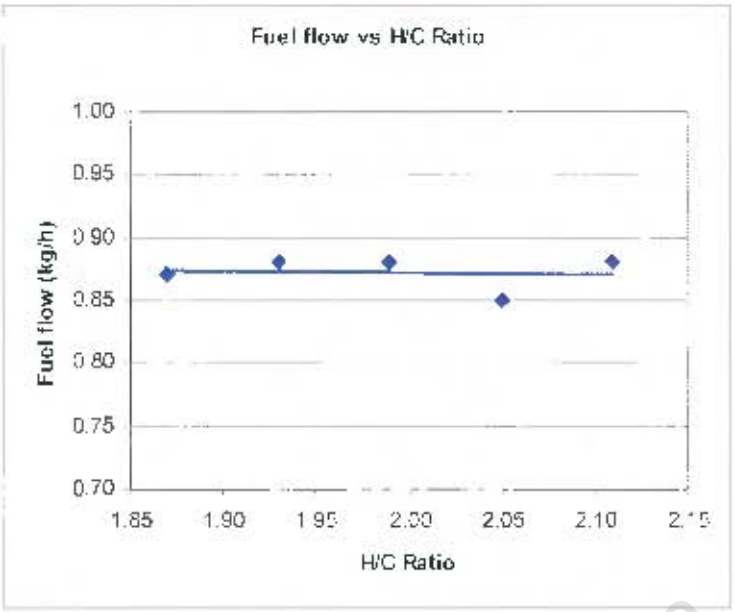

Figure 6-5: Fuel flow vs. H/C ratio (with Pilot)

University of Cape Town

Discussion

As the fuel conversion efficiency in the pilot-injection-off case was constant (GTL 24.48 % and EN590 24.45 %), the difference between the 4.5% measured increase in gravimetric flow and the 2.5% theoretical calculation increase would be attributed to experimental inaccuracies.

When using pilot injections it can be seen from Table 6-3 that there appears to be an insensitivity of the fuel flow to the injection duration, despite a difference in volumetric heating value. A possible reason for this insensitivity could be attributed to how the fuel flows during the short duration pilot injections. Recent unpublished research conducted at the Sasol Advanced Fuels Laboratory has showed evidence of inertia effects, due to the difference in fuel density, affecting the time taken for fuel flow to stabilise; thus, implying that a lower density fuel will start flowing earlier, and for longer during pilot injections when the injector needle barely lifts.

From Figure 6-5 it can be seen that the assumption of constant fuel conversion efficiency did not entirely hold for the pilot injections case, which could explain this insensitivity to lower heating value. Fuel conversion efficiency varied from 23.6 % to 24.1 % with GTL and EN590 respectively. Therefore, the fuel flow results for this pilot-injection-on case cannot be compared directly.

6.2. Emissions

Soot and NO_x emissions

As stated in the literature review there is an approximately linear relationship between H/C ratio and PM/soot concentration. The validation process of the controller (pilot injections on) was completed using all five test fuels, and the soot emissions were plotted against the H/C ratio (seen Figure 6-6). The linear relationship was confirmed and similar trends were observed for the pilot injection off case.

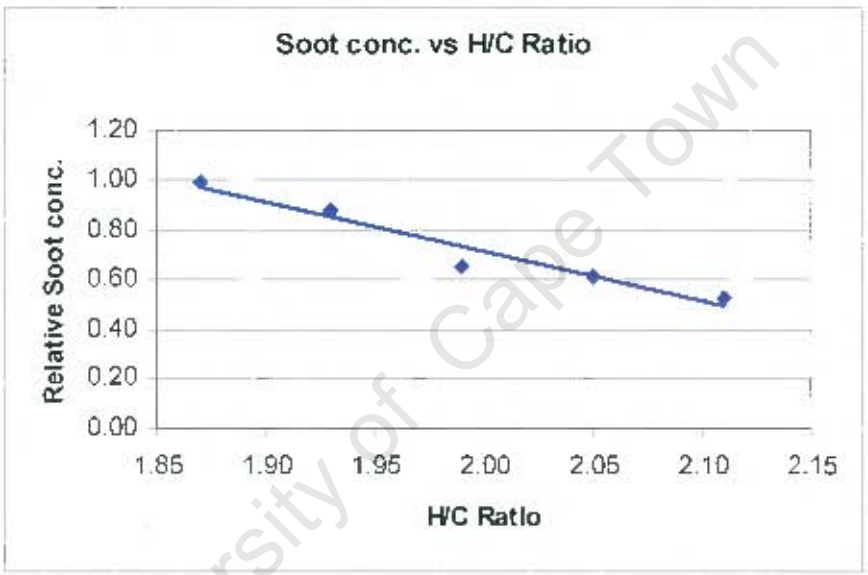

Figure 6-6: Plot of H/C ratio vs. Soot emissions

The difference between the NO_x emissions and H/C ratio was largely unchanged. See figure 6-7 below.

University of Cape Town

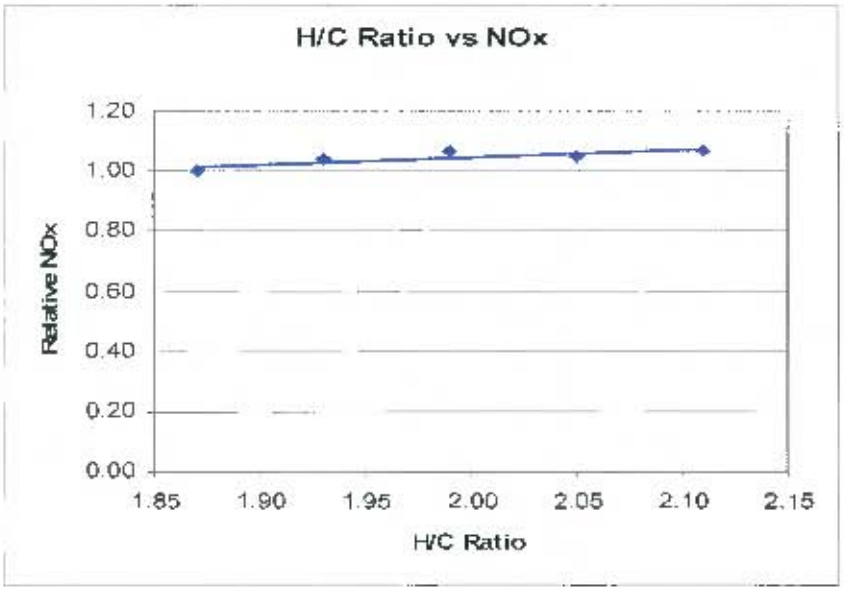

Figure 6-7: Plot of NO_x emissions vs. H/C ratio

University of Cape Town

Discussion

A shorter ignition delay, shown as a shorter start-of-combustion (SOC) seen in Figure 6-8 below for GTL, implies that less fuel is burned during the uncontrolled premixed combustion phase – responsible for high pressure rise rates - thus reducing the peak pressures and temperatures. Moreover, the heating value per stoichiometric air-fuel mixture becomes lower for a higher H/C ratio fuel; thus, reducing the adiabatic flame temperature.

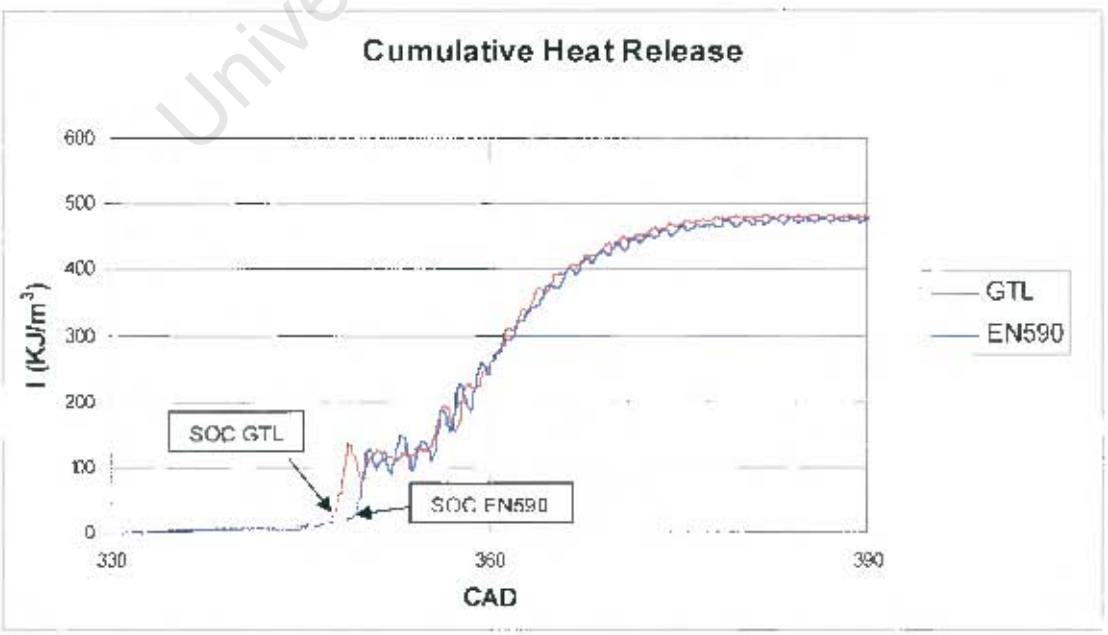

Figure 6-8: Heat release comparison

Therefore, it was expected with the lower temperatures generated by GTL that this effect would be shown as a NO_x reduction. This suggests that there is some secondary mechanism that is reducing the combustion temperatures of the EN590 to that of the GTL; thus, yielding similar NO_x emissions (as shown previously in Figure 6-7).

One mechanism that could explain this phenomenon is radiative heat transfer caused by soot particules. The radiative heat transfer contributes approximately 20 to 35 percent of the total heat transfer in diesel engines [1]. Therefore, it is speculated that the lowered combustion temperature of EN590 is attributed to a higher flame radiation heat loss caused by its higher combustion soot level (almost double that of GTL – shown previously in Figure 6-6).

NO_x-Soot trade-off curves

NO_x-Soot trade-off curves (pilot injection on) were generated from the timing sweep that was done during the controller validation. Here (Figure 6-9) all fuels were plotted on the same graph with the operating point shown as a red marker.

These are the curves that would be stored in the ECU in order for it to determine the virtual emissions for each fuel during operation, and optimise the injection timing to achieve desired emissions.

University of Cape Town

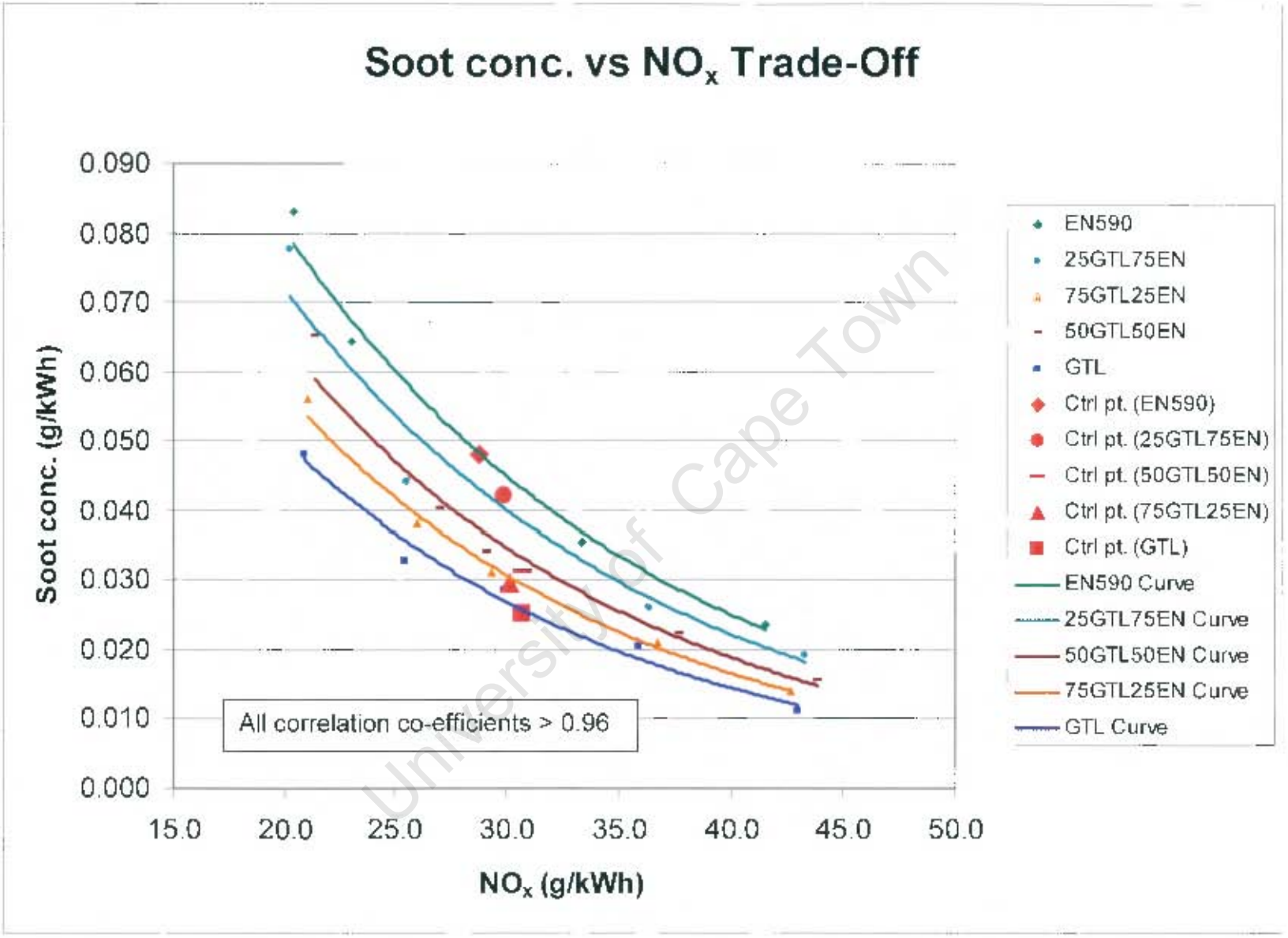

University of Cape Town

Figure 6-9: Soot-NO_x trade-off curves (pilot on)

To demonstrate the potential reduction in emissions, a case was used of changing the fuel from EN590 to GTL. Figure 6-10 shows the fuel change effect where the EN590 control point (red diamond in Figure 6-9) was moved to the GTL control point (red square in Figure 6-9). After optimisation (Figure 6-11) the GTL control point was moved to where a direct line, from the EN590 control point to the origin, intersects the GTL trade-off curve. This gave a neutral gain in emissions, but the control strategy could have been to optimise a specific emission to suit the exhaust gas aftertreatment system of a vehicle.

The difference between these two graphs was the effect of the control strategy.

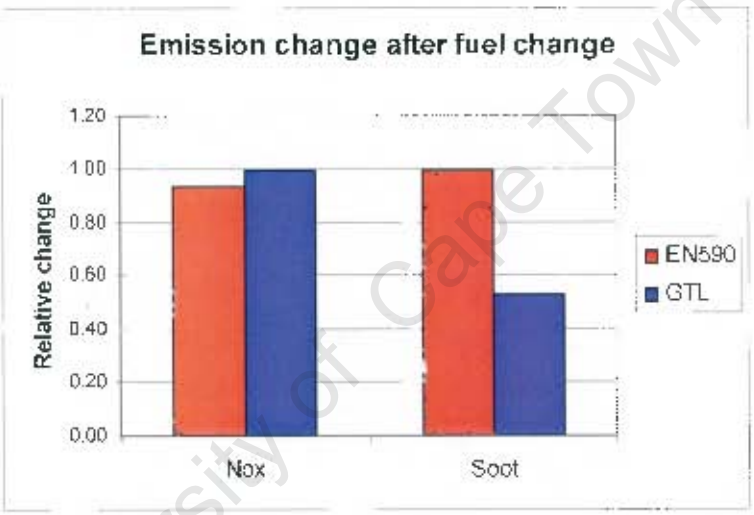

Figure 6-10: Emission change after fuel change

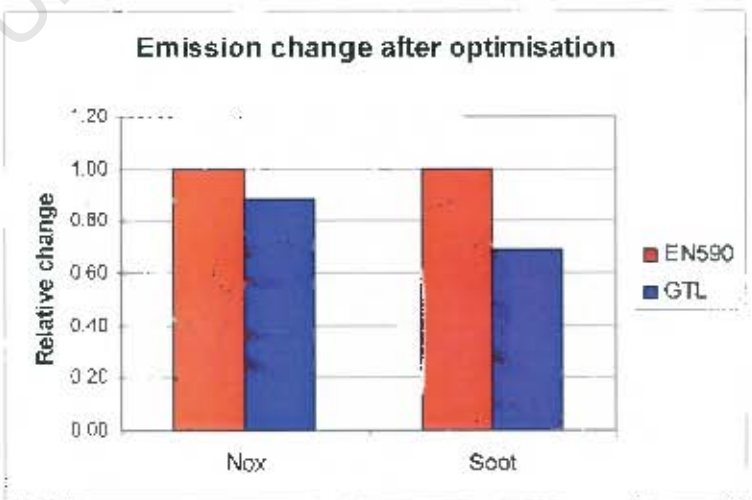

Figure 6-11: Emission change after optimisation

University of Cape Town

6.3. H/C Ratio Detection

At each controlled point for a fuel, the H/C ratio was calculated using measured values with the formula (Equation 4-3) in Section 4.2. These measured values are compared with the actual values below in Figure 6-12 for the pilot-injection-on case.

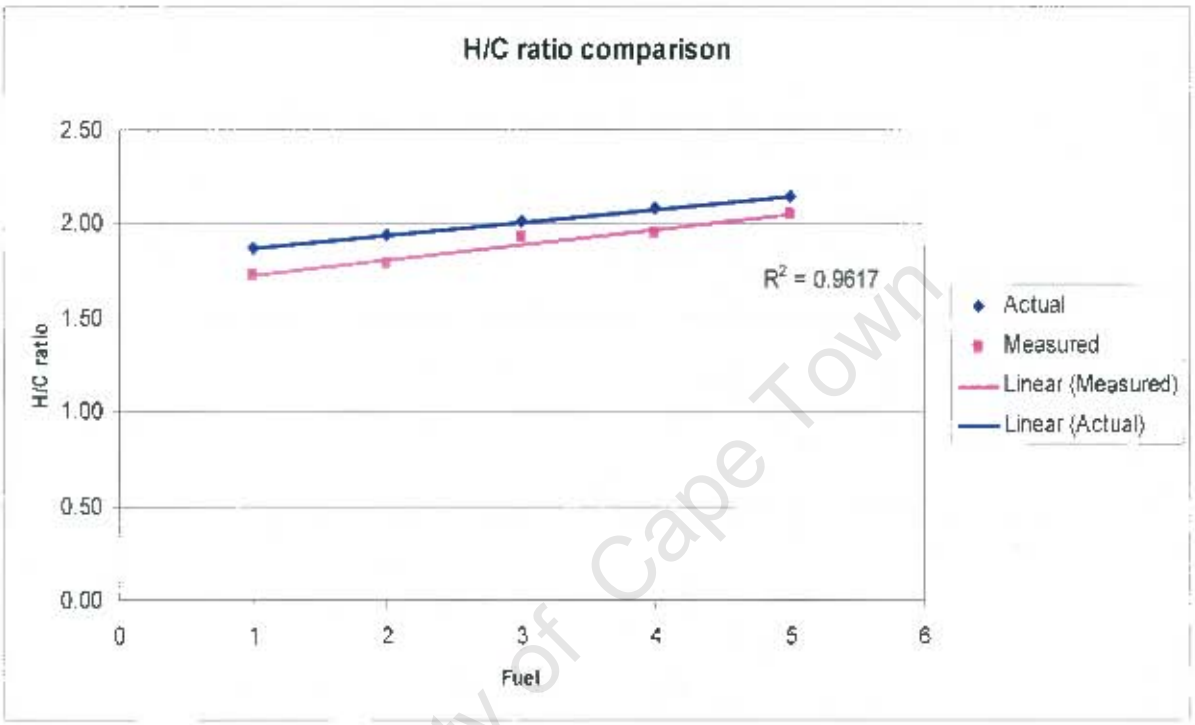

Figure 6-12: Comparison between calculated and measured H/C ratios with pilot injections

Pilot injections were turned off and another comparison was made. See Figure 6-13 below.

University of Cape Town

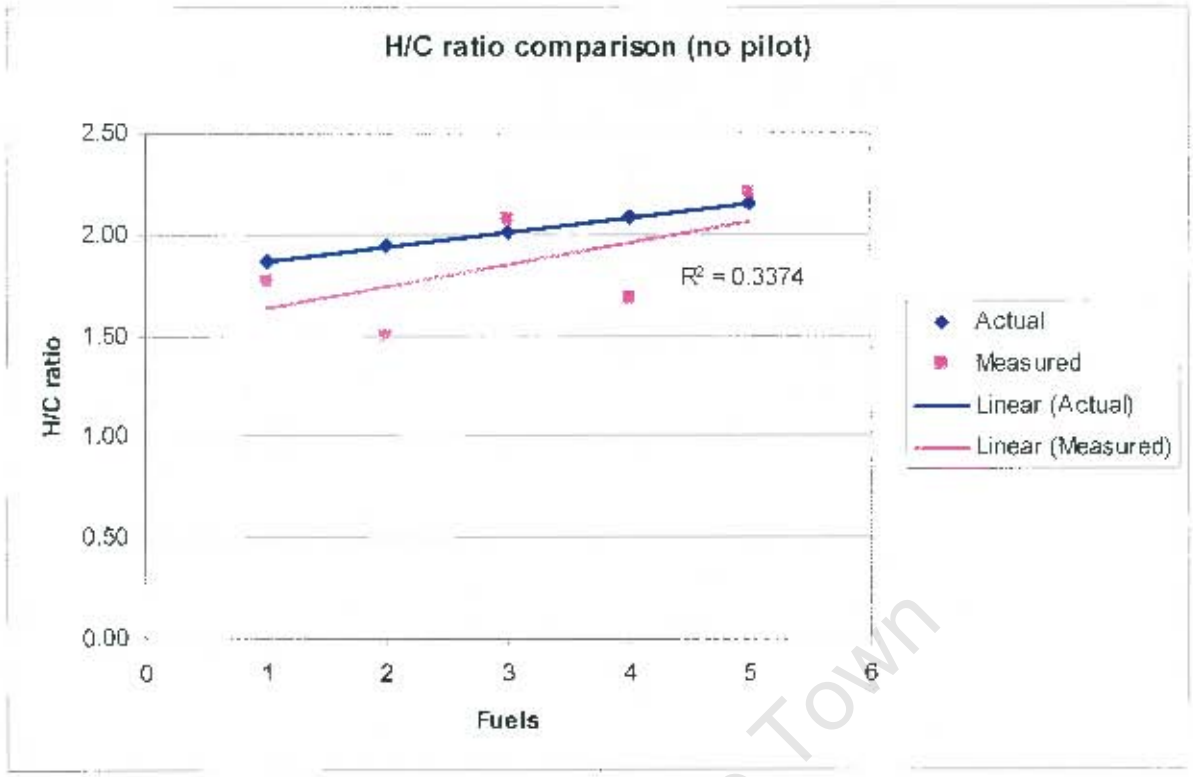

Figure 6-13: Comparison between calculated and measured H/C ratios without pilot injections

University of Cape Town

Discussion

A good correlation was achieved when pilot injections were on. The offset in this pilot-injection-on case could be due to a systematic measurement error, which could be corrected by a correction factor which was developed later in this section.

In the no-pilot-injection case the change in air density, due to fluctuation in atmospheric pressure on different test days, (which is used to calculate the air flow and then H/C ratio) could explain the poor correlation in this case. This point is highlighted in Figure 6-14 by showing how the air density change is directionally the same as the H/C ratio change.

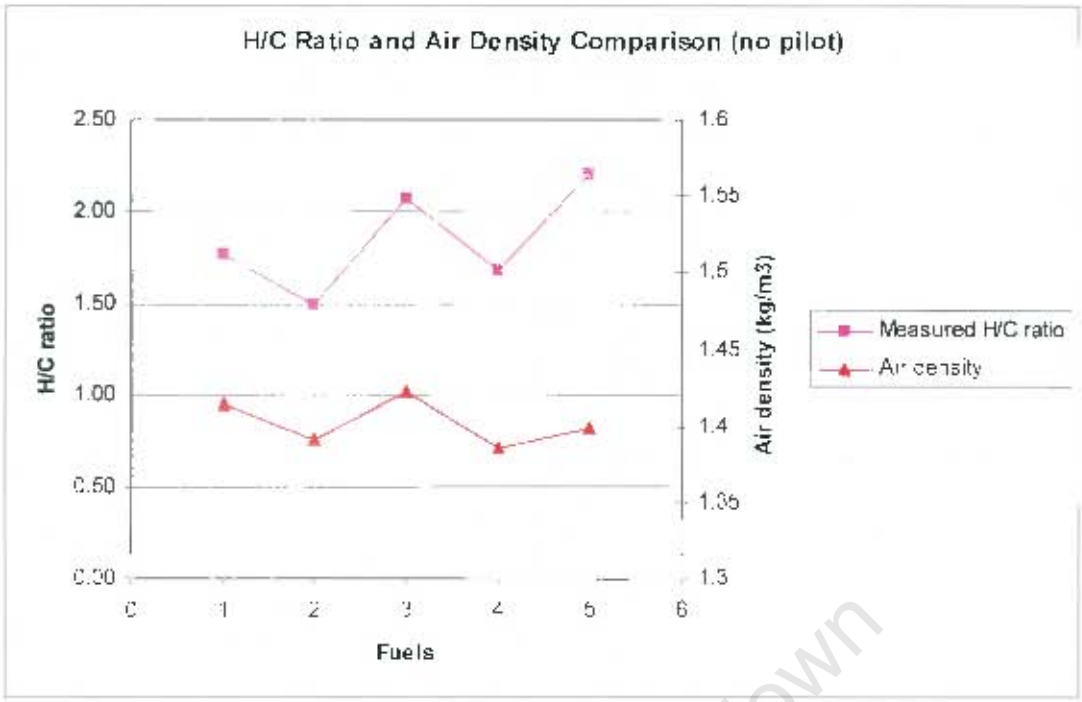

Figure 6-14: Air density and H/C ratio comparison

An empirical correction factor for density change and the systematic offset was developed. This correction was based on the fraction error of the measured air density with what the inlet manifold air density would be at standard conditions (i.e. 15 ^{O}C and 101.325kPa + boost pressure). The rest of the formula was developed by numerically solving the constants to get the best fit with the empirical data.

$$H/C_{corrected} = \left[\left[15.06\left(\frac{\rho_{airstd} - \rho_{measured}}{\rho_{airstd}}\right)\right]^{0.48} + 0.53\right] \times H/C_{measured} + 0.96 \qquad \text{Equation 6-1}$$

As this is an empirical correction factor it should be used with caution. The systematic offset could vary with different sensors, and the air density could vary with changing humidity levels or other ambient conditions. Also, improving the accuracy of the data acquisition could improve the H/C ratio prediction capability. That aside, the correction factor was applied to both sets of results shown above and the new results are shown below in Figure 6-15 to 6-16.

University of Cape Town

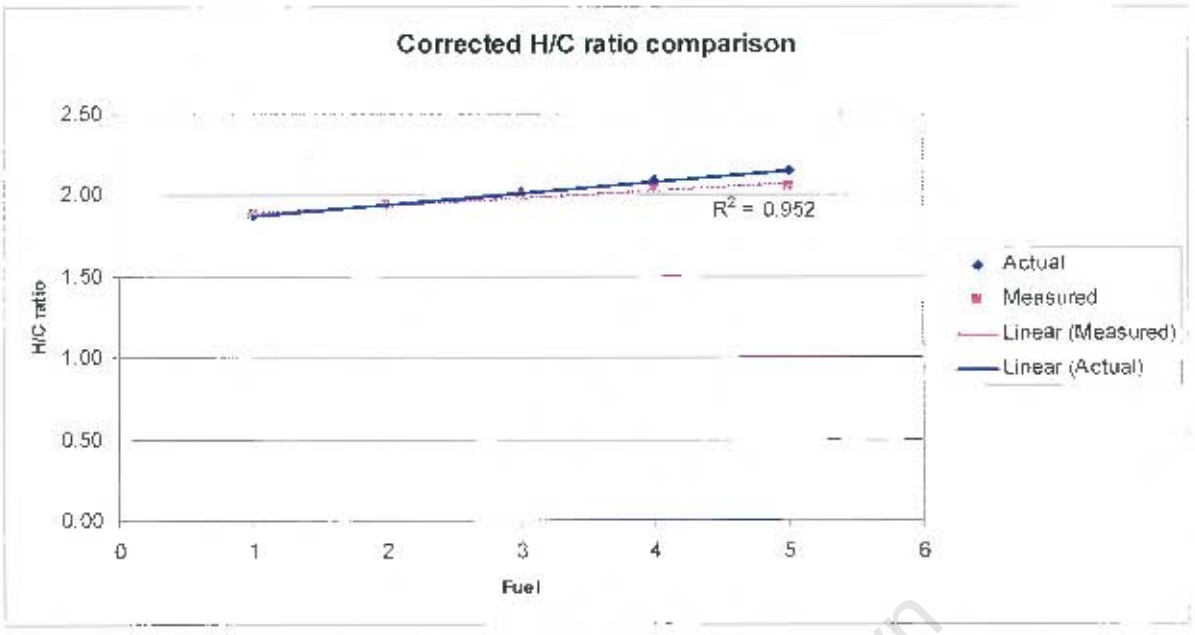

Figure 6-15: Corrected H/C ratios (Pilot injection on)

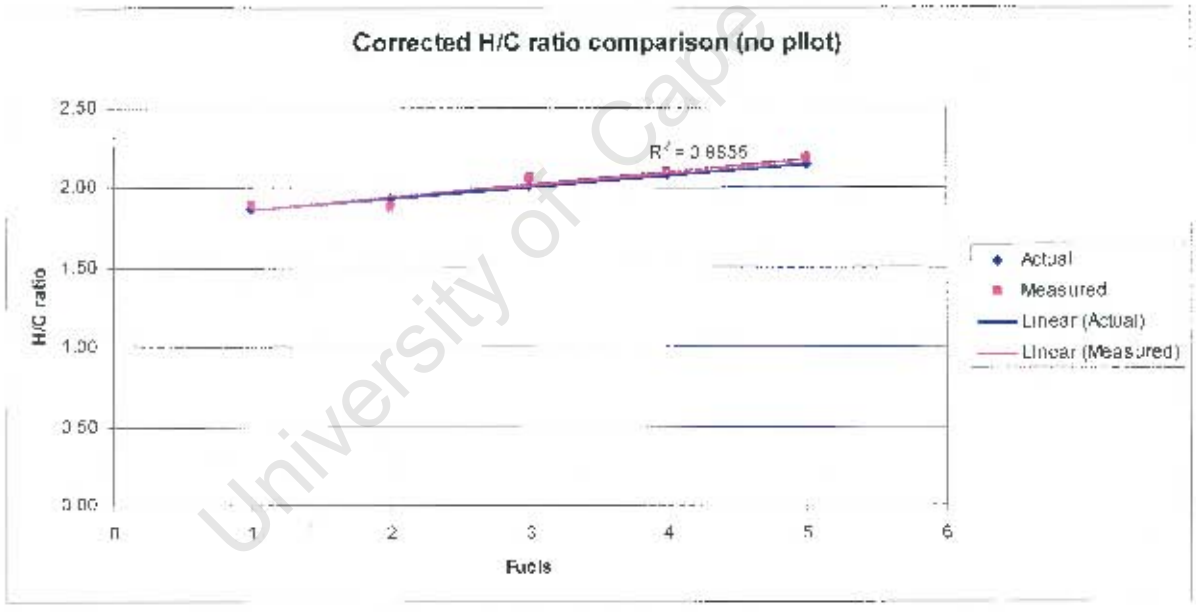

Figure 6-16: Corrected H/C ratios (Pilot injection off)

The comparisons are demonstrated more clearly in Figures 6-17 and 6-18 by plotting the calculated vs. actual H/C ratios.

University of Cape Town

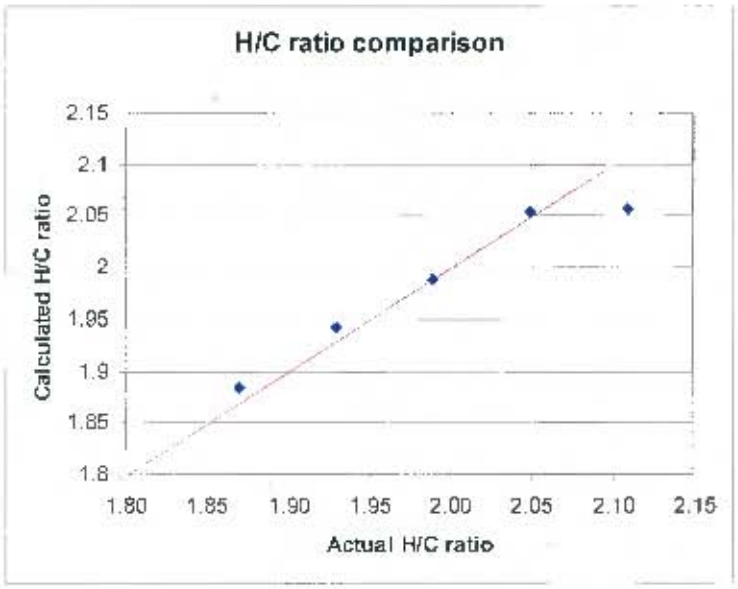

Figure 6-17: H/C ratio comparison (Pilot-injection-on)

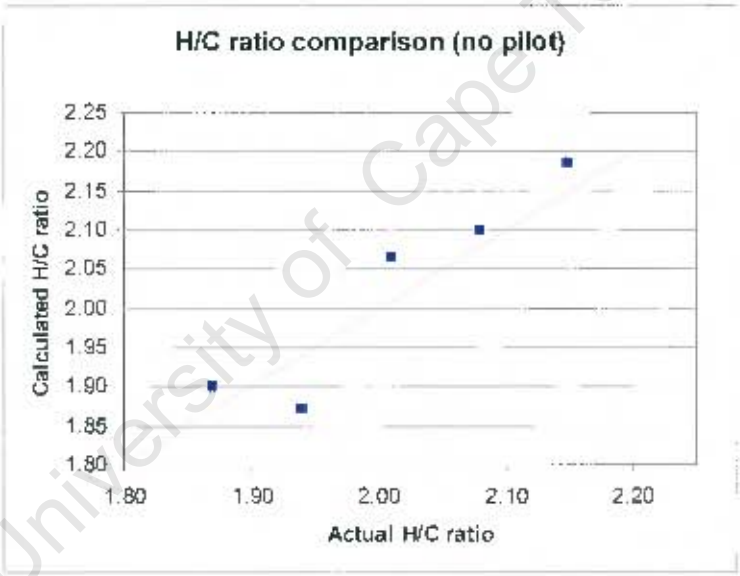

Figure 6-18: H/C ratio comparison (Pilot-injection-off)

University of Cape Town

It can be seen for the pilot-injection-on case that the H/C ratios are corrected, and now predict the actual values to a good degree of accuracy.

The correction factor also improved the pilot-injection-off case to a good degree of accuracy, with the exception of one point.

7. Conclusions

Based on the preceding results and discussion the following conclusions have been drawn.

- The ECU was fully functional and fulfilled all its requirements

- Satisfactory control over the B50 point as well as the load was achieved. This control technique compensated for any differences in fuel energy content, injection delay and ignition delay

- Different Soot - NO_x trade-off curves were clearly identified based on the fuel's H/C ratio. These distinct curves have the potential to be traversed, with knowledge of the H/C ratio and the end limits, to significantly optimise emissions performance in favour of either NO_x or soot

- Furthermore, the fuel's H/C ratio had a clear linear relationship with soot concentration – reducing soot with increasing H/C ratio. An insignificant change between the NO_x emissions and the H/C ratio was noticed, despite the difference in cetane numbers. It is speculated that this is caused by the increased flame radiation heat loss for EN590 combustion, due to its higher soot levels

- The H/C ratio detection followed the trend of the fuel's actual H/C ratio, but to an unsatisfactory level without correction. An empirical correction factor was developed which improved the correlation by compensating for changes in the ambient conditions and correcting a systematic measurement error in the lambda measurement

- This document serves as a proof-of-concept for a high level supervisory controller to identify a fuel's H/C ratio and thereafter, to make the necessary injection setting changes in order to actively reduce emissions. Going from EN590 to GTL a 12% and a 31% reduction in NO_x and Soot emission respectively was achieved

University of Cape Town

8. Recommendations / Future Work

Based on the conclusions, results and discussion the following recommendations have been made and further work suggested:

- This proof-of-concept for a high level supervisory controller could be developed further to see if there is a future in production engines for it. This would involve refining the H/C ratio detection and developing an inexpensive gravimetric fuel flow measurement technique

- The results showed an apparent insensitivity in the fuel flow rate to injection duration. Further studies into the differences in flow rate for fuels with varying density and bulk modulus, in common rail fuel injections systems, would need to be made to explain this. A comparison should be made between main injections with and without pilot injections

- An investigation into why the NO_x emissions were unchanged despite the difference in cetane number and H/C ratio should be made

University of Cape Town

9. References

[1] *Heywood, J., Internal Combustion Engine Fundamentals, McGraw-Hill Book Company, 1988, pp. 69, 510, 636, 683.*

[2] *Natarajan, M., Frame, E.A., Naegeli, D.W., Asmus, T.W., Clark, W., Garbak, J.A., Gonzalez, M.A., Liney, E., Piel, W.J. and Wallace III, J.P., "Oxygenates for Advanced Petroleum-Based Fuels: Part 1 - Screening and Selection Methodology for the Oxygenates", SAE Technical Paper No. 2001-01-3631, 2001.*

[3] *Schaberg, P., Myburgh, I.S., Botha, J.J., Roets, P.N., Viljoen, C.L., Dancuart, L.P. and Starr, M.E., "Diesel Exhaust Emissions Using Sasol Slurry Phase Distillate Fuels", SAE Technical Paper 972898, 1997.*

[4] *Leet, J., "Potential Application of Fischer-Tropsch Fuels", Proceedings on Gas-to-Liquids Processing Bringing Clean Fuels to Market, Intertech Conferences, 1998.*

[5] *Sirman, M., Owens, E., Whitney, K., "Emissions Comparison of Alternative Fuels in an Advanced Automotive Diesel Engine", Southwest Research Institute Report for DOE and US Army TARDEC, Interim Report TFLRF No. 338, 1998.*

[6] *Martin, B., Aakko, P., Beckman, D., Giacomo, N.D., and Giavazzi, F., "Influence of Future Fuel Formulations on Diesel Engine Emissions- A Joint European Study", SAE Technical Paper 972966, 1997.*

[7] *Norton, P., Vertin, K., Bailey, B., Clark, N., Lyons, D., Goguen, S., Eberhardt, J., "Emissions from Trucks using Fischer-Tropsch Diesel Fuel", SAE Technical Paper 982526, 1998.*

University of Cape Town

[8] *May, P., Vertin, K., Ren, S. and Gui, X., Myburgh, I. and Schaberg, P., "Development of Truck Engine Technologies for Use with Fischer-Tropsch Fuels", SAE Technical Paper 2001-01-3520, 2001*

[9] *Schaberg, P., Botha, J., Schnel, M., Herrmann, H., Keppeler, S. and Friess, W., "HSDI Diesel Engine Optimisation for GTL Diesel Fuel", SAE Technical Paper 2007-01-0027, 2007.*

[10] *Beasley, M., Cornwell, R., Fussey, P, King, R, Noble, A., Salamon, T. and Truscott, A., Ricardo UK Ltd, "Reducing Diesel Emissions Dispersion by Coordinated Combustion Feedback Control", SAE Technical Paper 2006-01-0186, 2006.*

[11] *General Motors Corporation, "Cadillac to Debut GM's Powerful New V-6 Clean Diesel", viewed 15 August 2007, <http://www.gm.com/explore/fuel_economy/news/2007/adv_engines/cadillac-engine-030707.jsp>, 6 March 2007.*

[12] *Fitzpatrick, M., "A new design of optical in-cylinder pressure sensor for automotive applications", SAE Technical Paper 2000-01-0539, 2000.*

[13] *Moriwaki, J., Murai, H., Kameshima, A., DENSO corp., "Glow plug with combustion pressure sensor", SAE Technical Paper 2003-01-0707, 2003.*

[14] *Yates, A. and Rabe, T., "The Effect of Diesel Density, Injection Technology and External Variables on the Acceleration Performance of Modern Passenger Cars", SAE Technical Paper 2007-01-0063, 2007.*

[15] *Robert Bosch GmbH, Diesel-Engine Management, 3rd Edition, 2004.*

[16] *Drivven, Inc., DI Driver Module Kit User's Manual, Revision C, 2006.*

[17] *Schaberg, P., Sasol Technology, Schnell, M., Sasol Chevron, Keppeler, S., DaimlerChrysler AG, "Technologies : Challenging Gas Fields – Changing Markets", Energy Frontiers International Conference, 2006.*

University of Cape Town

[17] *SP3H, "On-Board System for the Analysis of Fuel Molecular Structure for Optimizing Combustion Processes", viewed 28 August 2007, <http://www.greencarcongress.com/2007/08/on-board-system.html>, 16 August 2007.*

[18] *Bowman, C.T., "Kinetics of Pollutant Formation and Destruction in Combustion", Prog. Energy Combust. Sci., vol. 1, 1975, pp. 33-45.*

[19] *Röpke, S., Schweimer, G.W. and Strauss, T.S., "NOx Formation in Diesel Engines for Various Fuels and Intake Gases", Volkswagen AG, SAE Technical Paper 950213, 1995.*

[20] *Schaberg, P., Botha, J., Schnel, M., Herrmann, H., Pelz, N. and Maly, R., "Emissions Performance of GTL Diesel Fuel and Blends with Optimised Engine Callibrations", SAE Technical Paper 2005-01-2187, 2005.*

University of Cape Town

Appendix A: ECU Design

The project was broken down into two phases, namely the development of the ECU system and the implementation of control algorithms into the ECU. They are broken down further as follows:

Specifications

The high level specifications will require that the ECU have the following:

- Normal diesel engine ECU features

The ECU will have to fulfil the standard operation of using look-up tables to retrieve injection times. This will be the base system in which the following specification will be built upon.

- Production standard injector driver

The injector driver must be capable of applying full current to the solenoid after 30-50 μs, as is the current ability of production ECU's. Additionally, a peak then hold current waveform is required. Finally, the system must be capable of having injection events as close as 250 μs.

- Pilot and main injection events

In order to mimic the modern ECU's ability of attaining the ideal injection characteristics using a common rail injection system, pilot and main injection events are required. These injection characteristics are explained in the Theoretical background section.

- Control algorithm support

This specification, required for part two of this project, is for the ECU to have the ability to integrate some novel control algorithm into the standard operation of the ECU.

University of Cape Town

- PC based

Since this ECU will be used for fuels research it is important to have a user friendly PC interface to setup the ECU and its various control algorithms. This will ensure accelerated development of new control strategies which will give insight into how the most can be extracted from a certain fuel.

- Fail safe

The ECU should have the necessary procedures built-in in order to detect a malfunction and provide a suitable "limp home" mode.

- Programmed in LabVIEW

It is preferable that the ECU be coded in a visual programming package called LabVIEW. Due to the ease of using this package, it would facilitate easier follow-on MSc projects.

- Control load and injection timing to a desired set point

To improve the combustion phasing, injection timing control needs to be implemented. Additionally, Load control will be required to correct for any differences in a fuel's energy content or density.

University of Cape Town

Data Acquisition Board

In order to ascertain how many inputs/outputs are required of the data acquisition board, the various sensor requirements and driver outputs need to be identified. Figure 4-2 shows this. The requirements are tabulated below: in Table A-1.

Table A-1: Data acquisition board requirements

Inputs		Outputs	
Digital (Clocked)	Analogue	Digital	Analogue
Crankshaft-CDM	Temperature	Rail-pressure control valve	
Crankshaft-Trig	Intake-air pressure	Injector solenoid high-side	
Camshaft-Phase	Rail pressure	Injector solenoid low-side	
	Cylinder pressure	Multiplexer Control A	
	Lambda	Multiplexer Control B	
	Flow sensor pressure difference	Safety Relay	
	Flow sensor absolute pressure		
Inject Trigger Out	RPM from Indesit	Inject Trigger In	
Pilot Trigger Out		Pilot Trigger In	

Totalling up the above table, 5 digital inputs, 8 digital outputs, and 8 analogue inputs will be required.

University of Cape Town

The actual channel assignments that were used in the data acquisition card are shown below in Table A-2.

Table A-2: Channel assignment

Analogue	
Channel	**Description**
0	Cylinder Pressure
1	Inlet Pressure
2	Temperature
3	Injector Current
4	RPM from Indesit
5	Rail Pressure
6	Lambda
7	Flow Sensor

Digital	
Channel	**Description**
0	CDM
1	TRIG
2	High Side MOSFET
3	
4	
5	
6	Inject Trigger Out
7	Inject Trigger In
8	Pilot Trigger Out
9	MUX A
10	MUX B
11	Safety Relay
12	Proximity Pump
13	Pressure Relief
14	Low Side MOSFET
15	Pilot Trigger In

Channel 6,7 are bridged together as well as 8,15
Channel 3,4,5 are not working

University of Cape Town

Software

This section describes the software that was written with the use of flow charts and signal waveforms. Only the more complex routines were shown.

Shaft Encoder

The flowchart below shows the algorithm designed for the AVL shaft encoder.

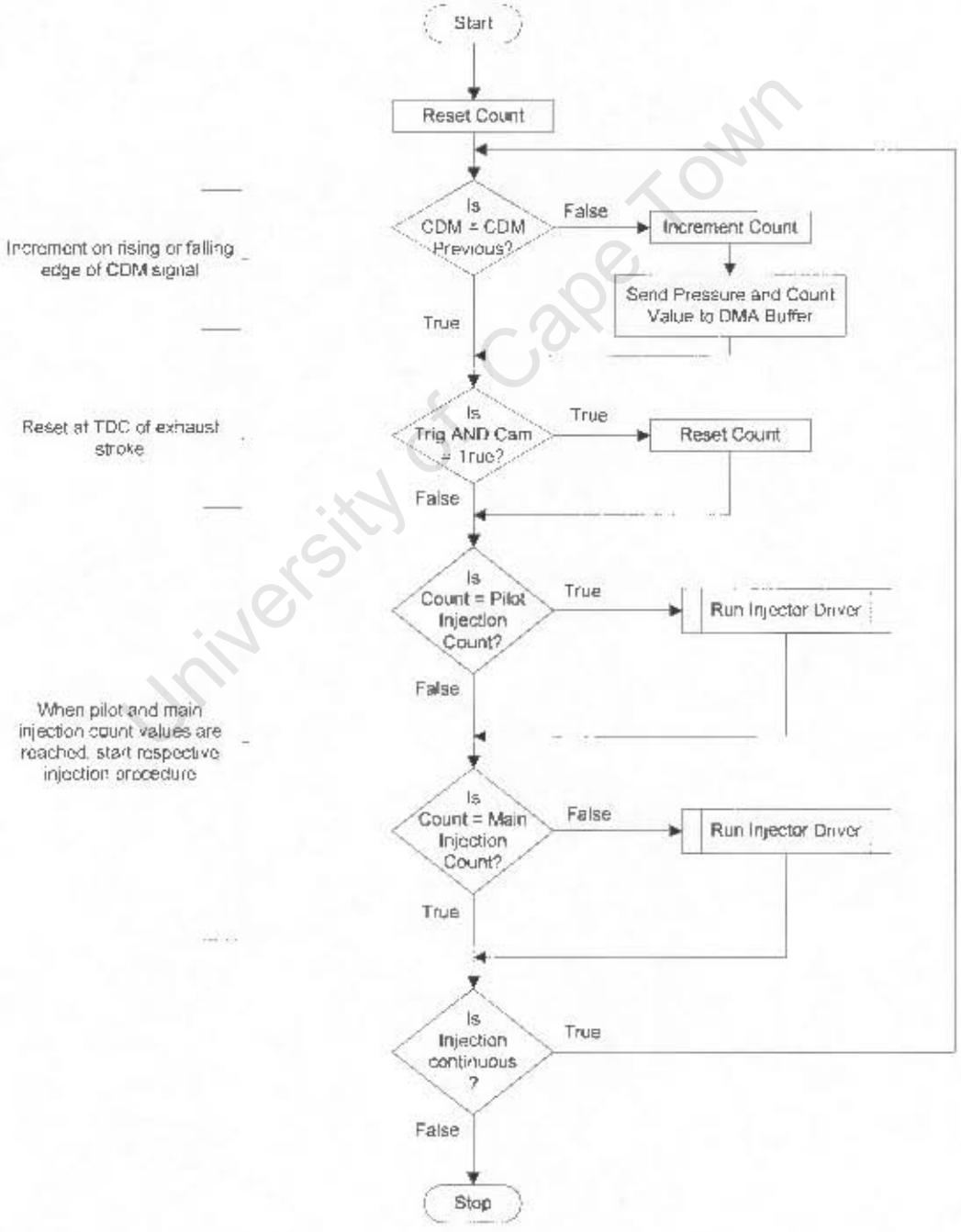

Figure A-1: Flowchart of shaft encoder

University of Cape Town

To see how the counter is reset at TDC of the exhaust stroke, the various signal waveforms were plotted against time. See figure A-2 below.

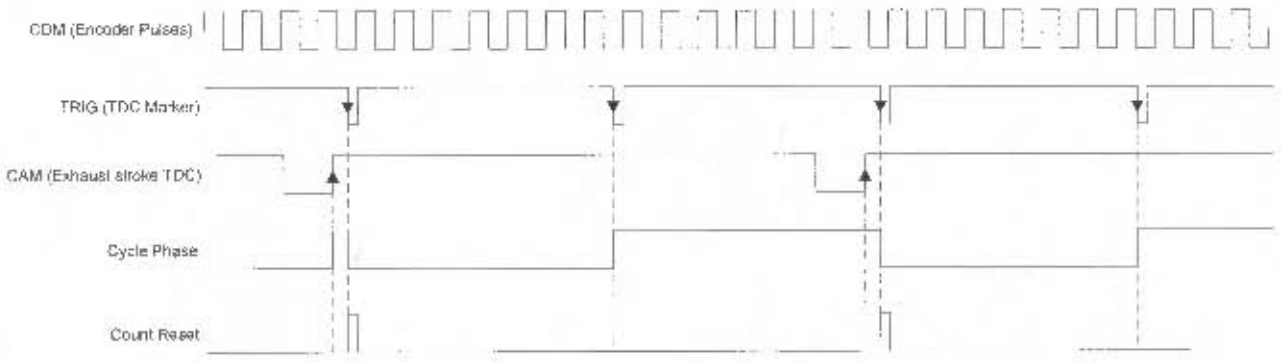

Figure A-2: Shaft encoder waveforms

As the *CAM* signal is not a true TDC, the *TRIG* signal was used. This involved some more logic to detect but provided more accurate triggering.

The rising edge of the *CAM* signal sets the *Cycle Phase* signal high, whether it is low (as in the initialisation) or high (during normal running). Additionally every *TRIG* falling edge will invert the *Cycle Phase* signal.

With that logic in place *Count* is only reset when there is a falling edge on *TRIG* and *Cycle Phase* is true.

University of Cape Town

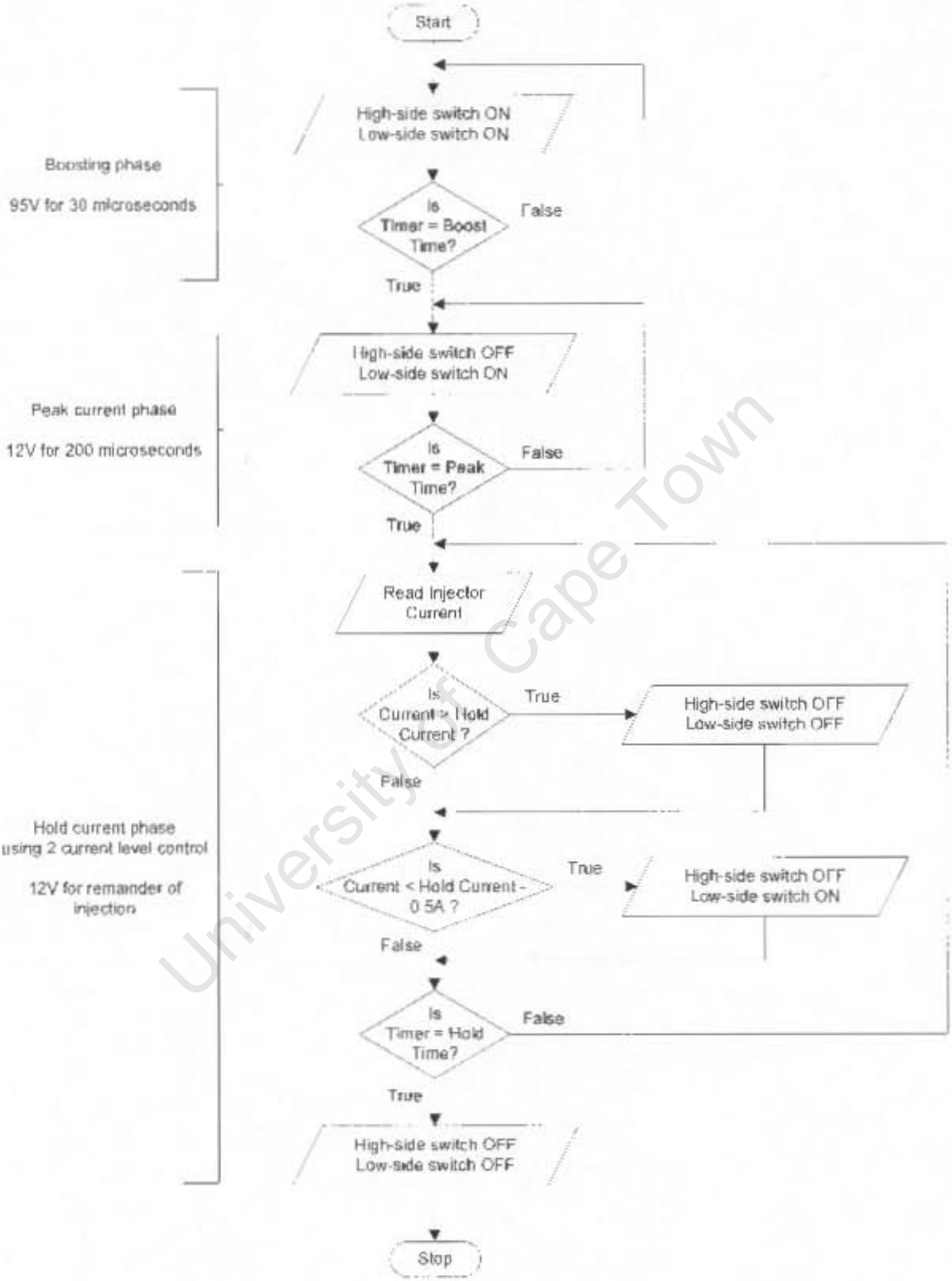

Figure A-3: Flow chart of injector driver

University of Cape Town

Appendix B: Combustion Analysis Formula

H/C Ratio Derivation

If we consider the complete combustion (stoichiometric) of a general hydrocarbon with air we have the following [1],

$$C_a H_b + (a + \frac{b}{4})(O_2 + 3.773N_2) = aCO_2 + \frac{b}{2} H_2O + 3.773(a + \frac{b}{4})N_2 \qquad \text{(B-1)}$$

The above equation can be rearranged in terms of the stoichiometric AFR, using a substitution for the H/C ratio, *y*, equal to *b/a* [1].

$$AFR_{stoichiometric} = \frac{(1 + y/4)(32 + 3.773 \times 28.16)}{12.011 + 1.008y} \qquad \text{(B-2)}$$

Additionally we have,

$$\lambda = \frac{AFR}{AFR_{stoichiometric}} \qquad \text{(B-3)} \quad , \quad \text{and} \quad AFR = \frac{\dot{m}_{air}}{\dot{m}_{fuel}} \qquad \text{(B-4)}$$

Rearranging B-2 in terms of *y* and substituting in B-3 and B-4, we get the following.

$$H/C\ Ratio = y = \frac{(0.338 \frac{\dot{m}_{air}}{\dot{m}_{fuel}\lambda} - 4)}{(1 - 0.029 \frac{\dot{m}_{air}}{\dot{m}_{fuel}\lambda})} \qquad \text{(B-5)}$$

University of Cape Town

Appendix C: Test Fuel Properties

The following table shows important property differences between the two fuels that were used for the tests.

Table C-3: Fuel properties

Property	Units	EN590	GTL
Density @ 20°C	kg/l	0.8297	0.7698
Cetane Number		54.8	>74
Total sulphur	mg/kg	<10	<1
ASTM D86 Distillation			
10%	°C	212	208
50%	°C	276	269
95%	°C	350	363
Final boiling point	°C	371	369
Flash point	°C	60	63
Viscosity @ 40°C	cSt	2.73	2.46
CFPP	°C	-8	-19
Total aromatics	% m/m	27.9	0.14
Carbon content	% m/m	86.2	85
Hydrogen content	% m/m	13.8	15
H/C ratio (molar)		1.87	2.11
Lower heating value	MJ/kg	42.75	43.81
Volumetric lower heating value	MJ/l	33.72	35.47

University of Cape Town

Appendix D: Circuit Diagrams

University of Cape Town

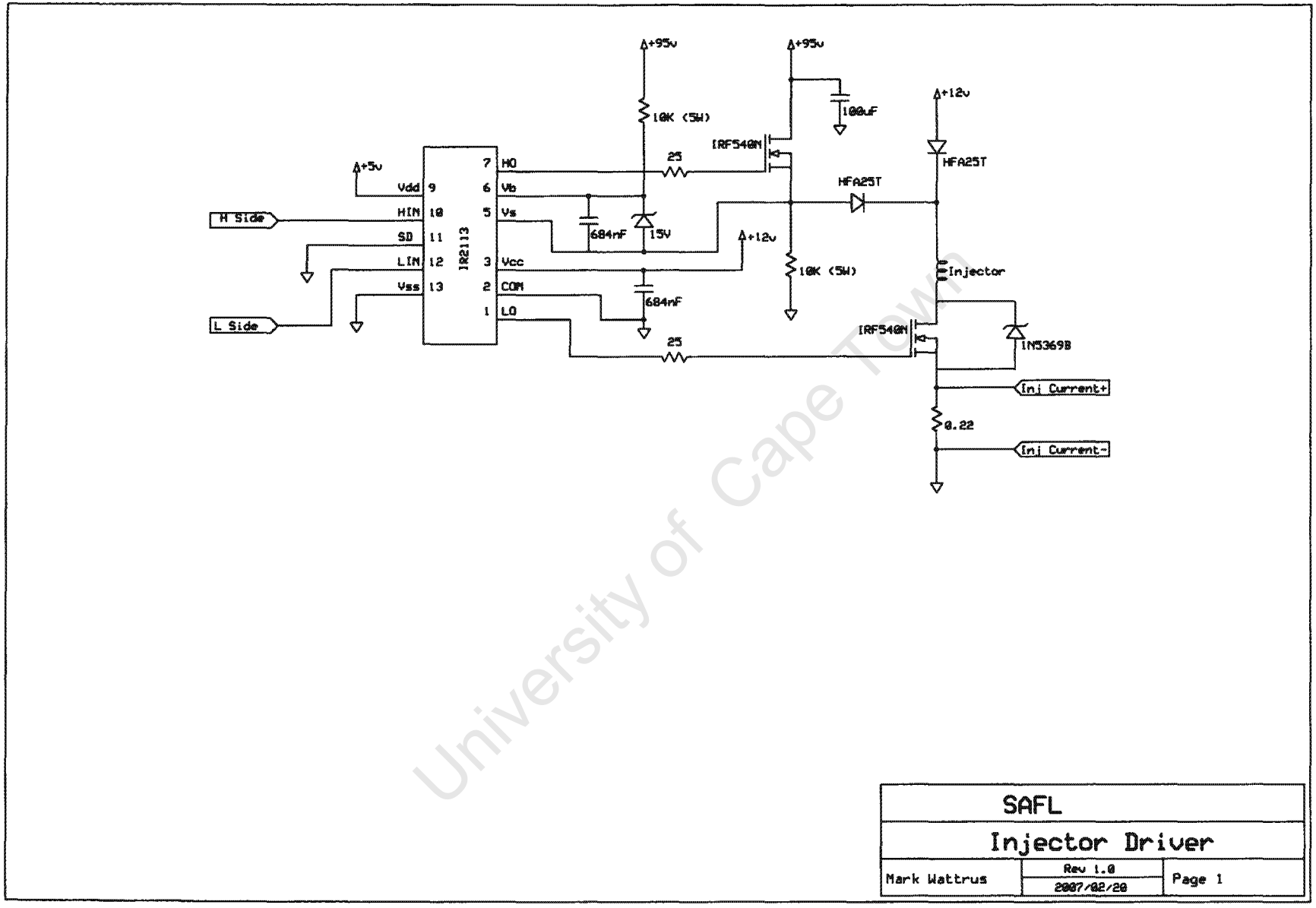

University of Cape Town

Figure D-4: Injector driver circuit

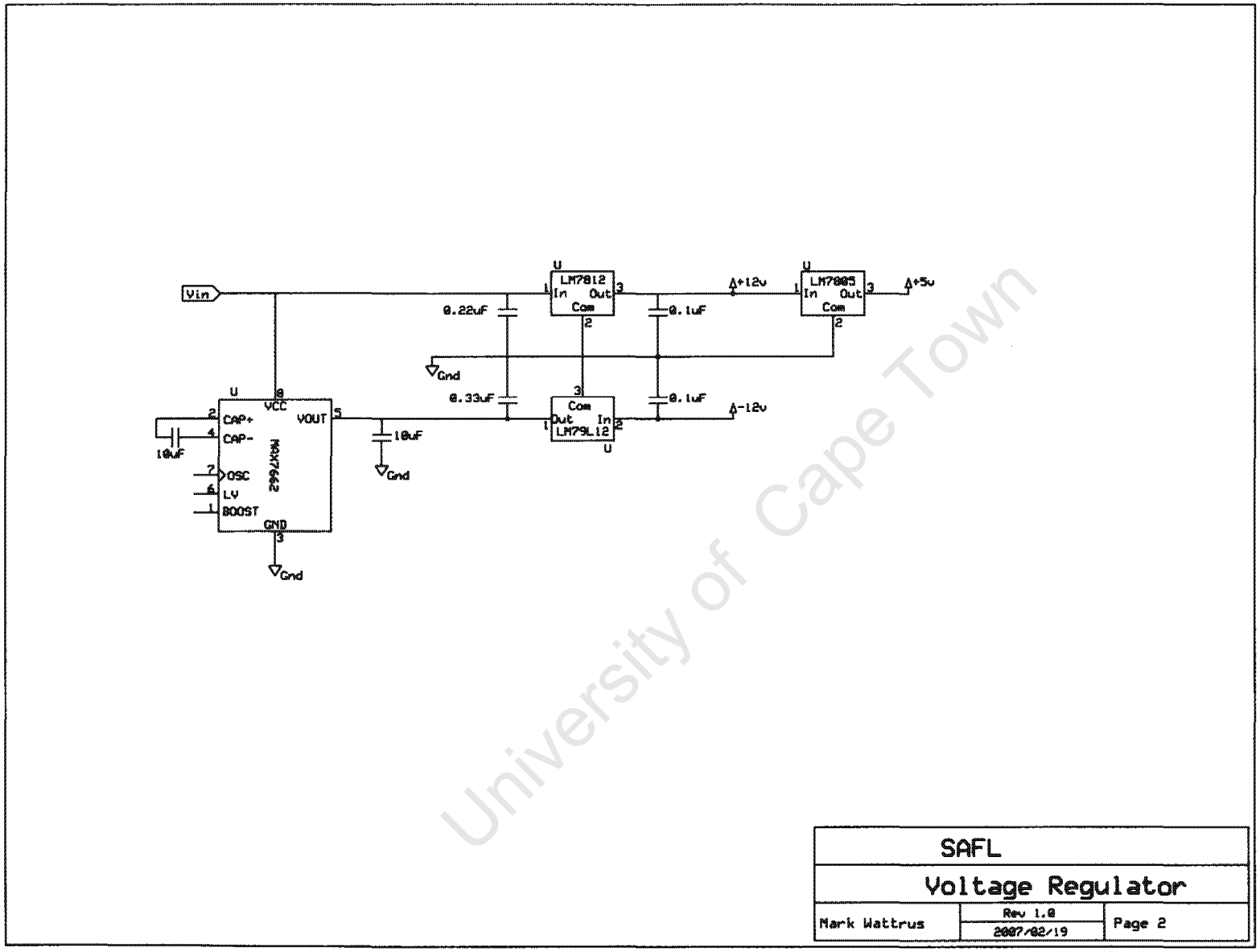

University of Cape Town

Figure D-5: Voltage regulator circuit

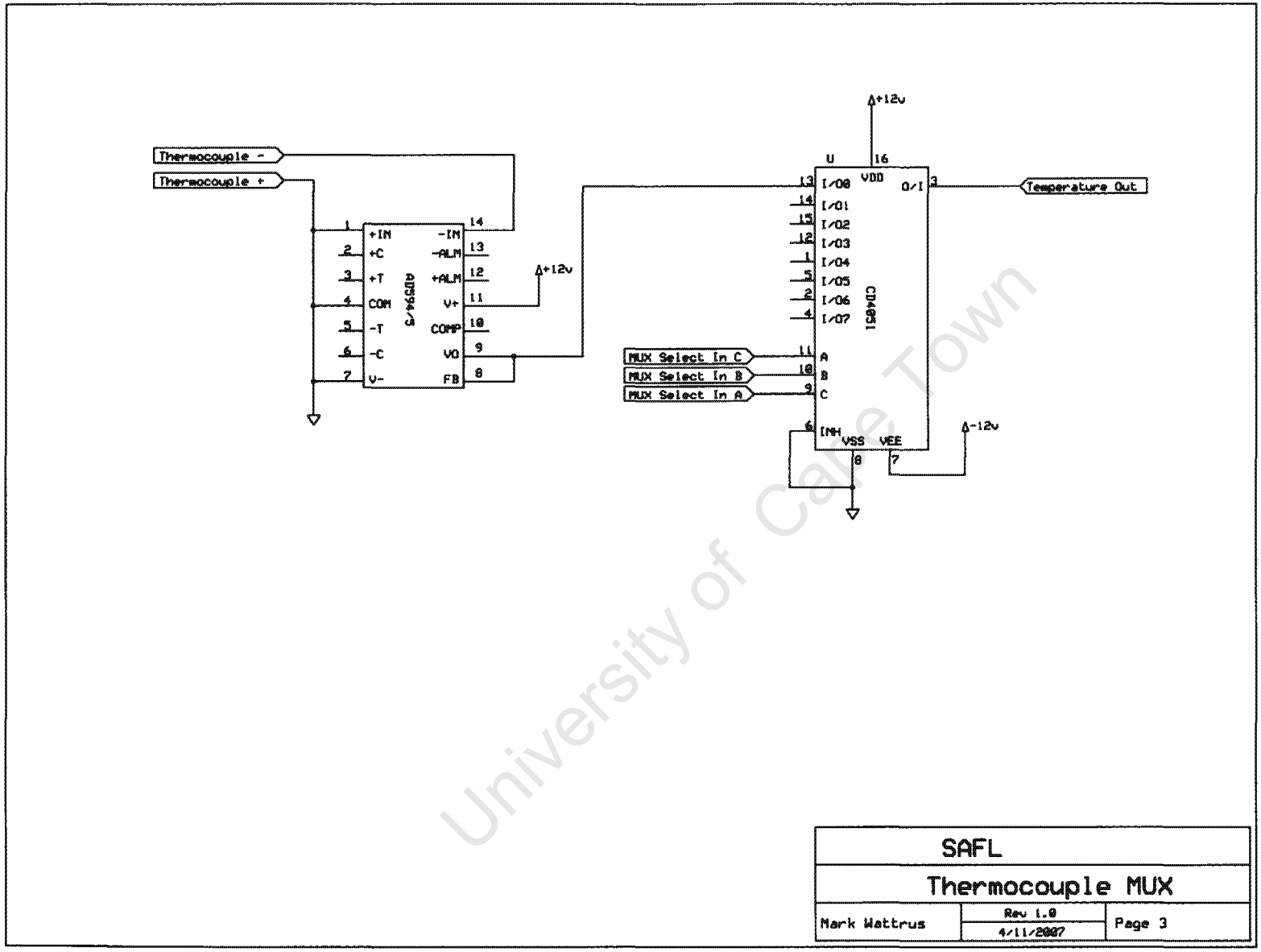

University of Cape Town

Figure D-6: Thermocouple multiplexer circuit

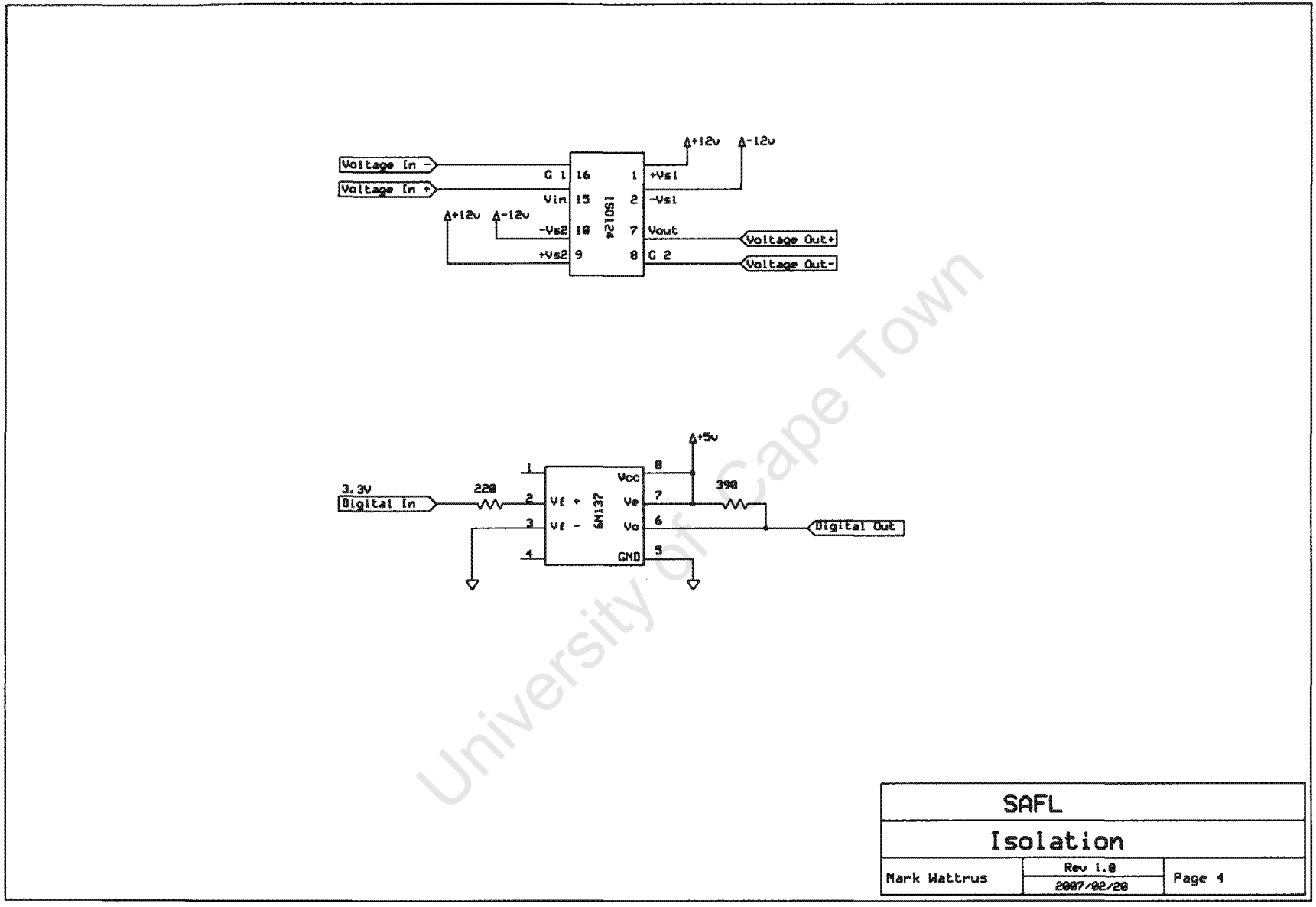

University of Cape Town

Figure D-7: Isolation circuit

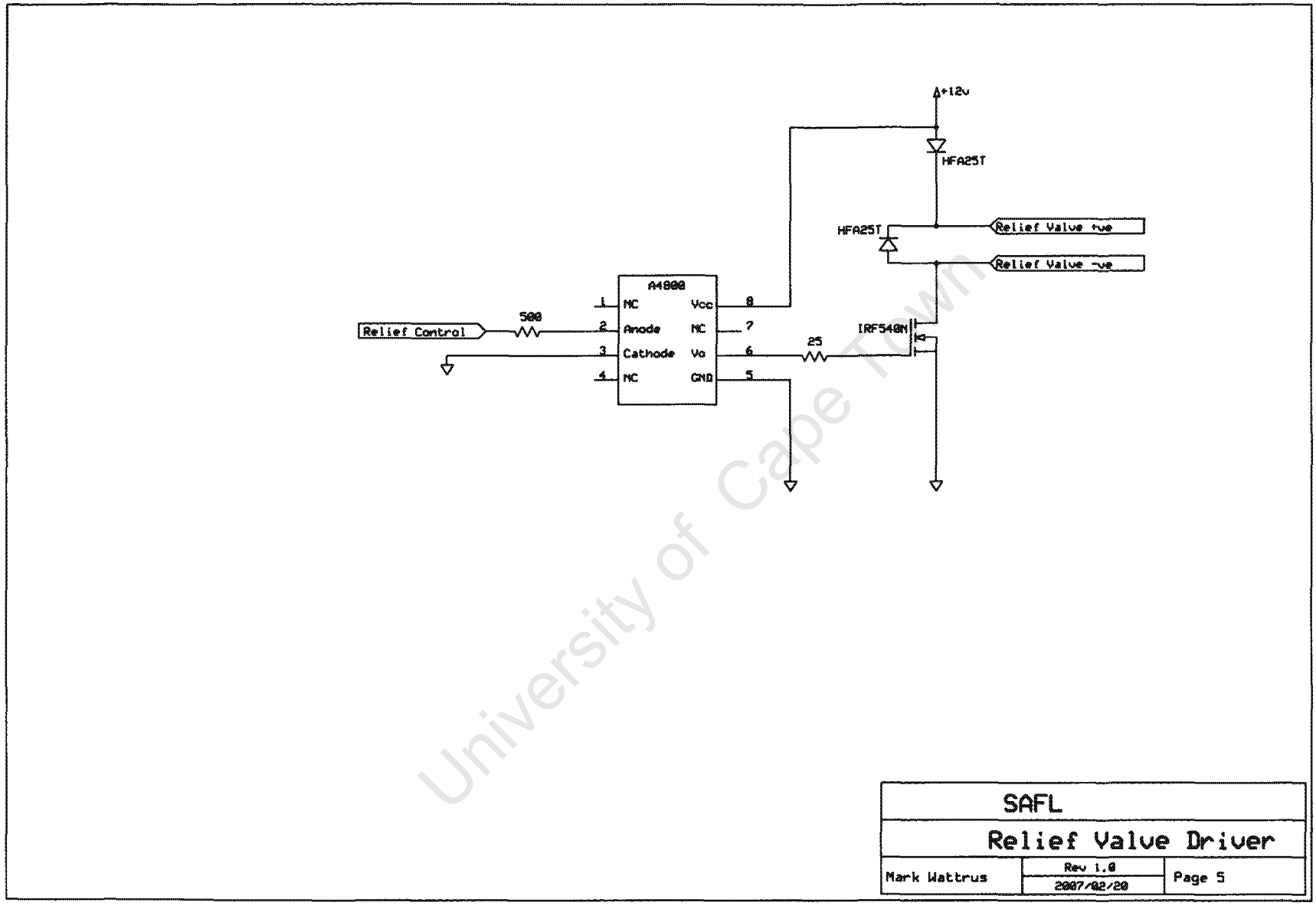

University of Cape Town

Figure D-8: Relief valve driver circuit

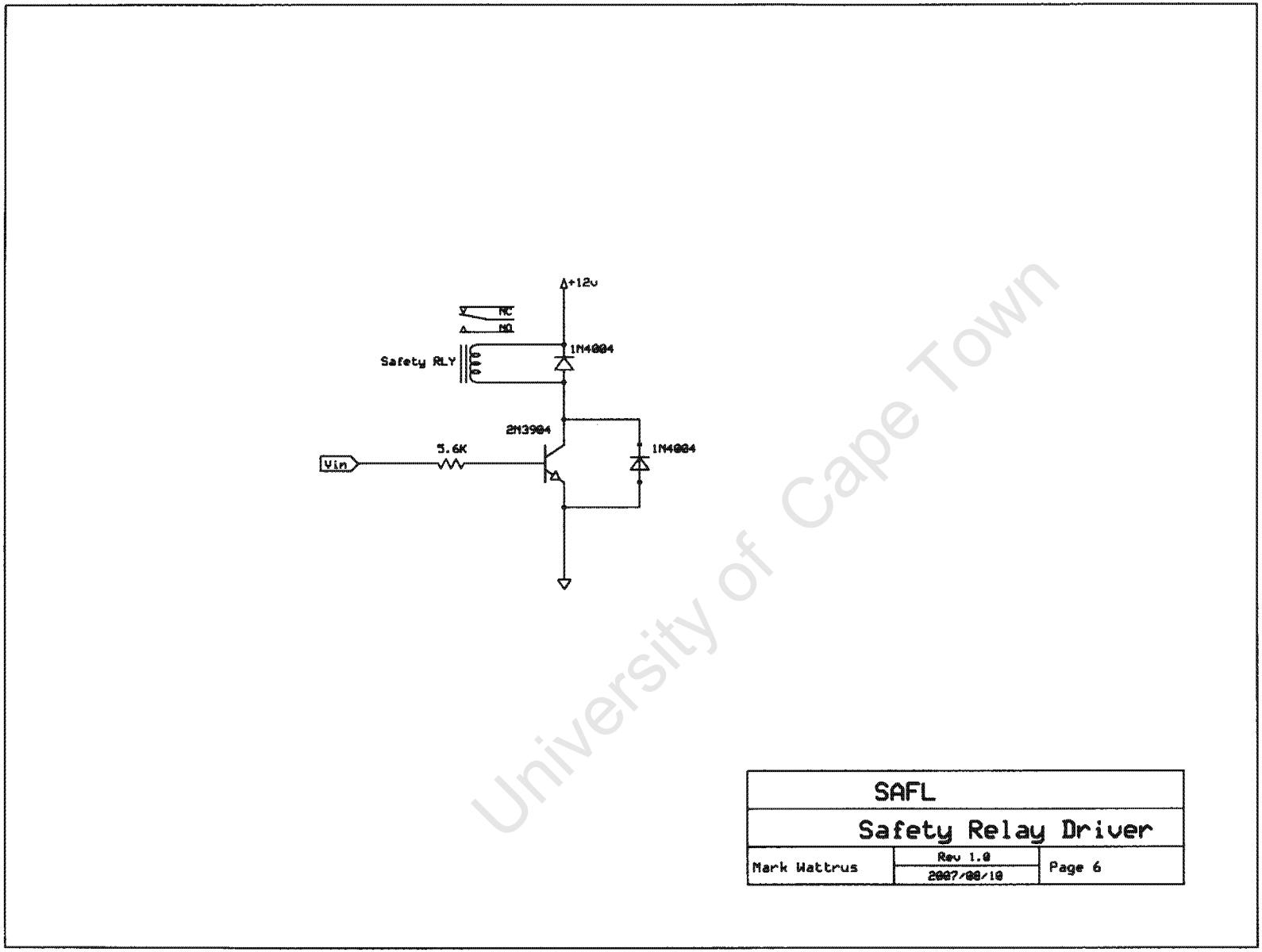

University of Cape Town

Figure D-9: Safety Relay Driver

Appendix E: Bosch Actuator/Sensor Information

Rail Pressure Relief Valve (Bosch 0 281 002 493)

Pin Layout

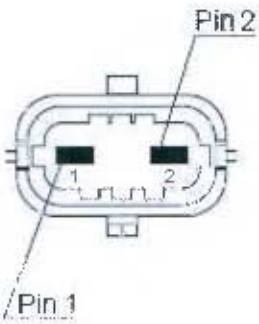

1 - Ground

2 - 12V

Rail Pressure Sensor (Bosch 0 281 002 260)

Pin Layout

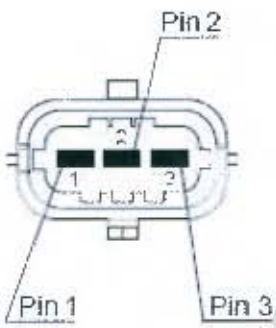

1 - Ground

2 - Signal

3 - 12V

University of Cape Town

Measuring Circuit

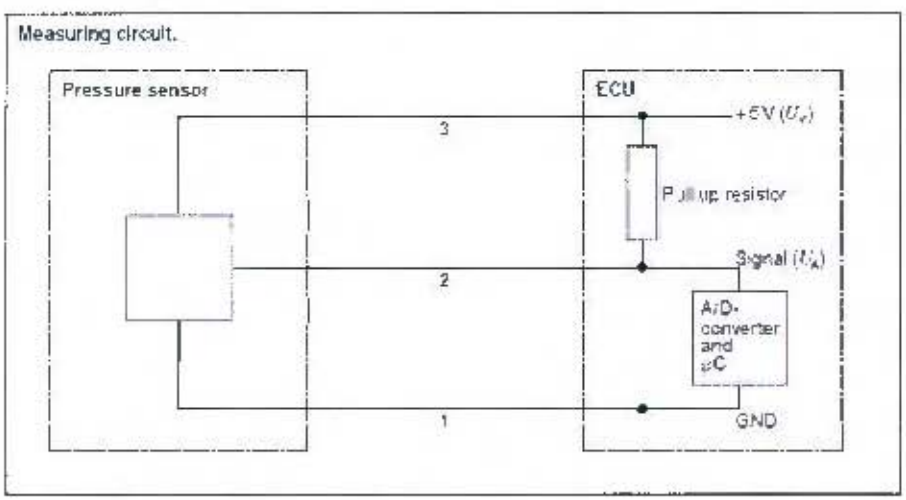

Output Signal

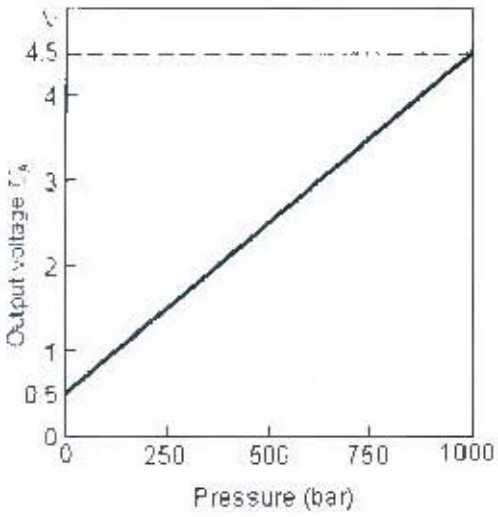

*Pressure (bar) = (U_A – 0.5)*1000/4*

Pump-shaft Proximity Sensor (Bosch 0 281 002 406)

Pin Layout

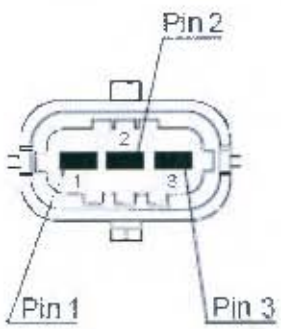

1 - Ground
2 - Signal (0V or 5V)
3 - 12V

Measuring Circuit

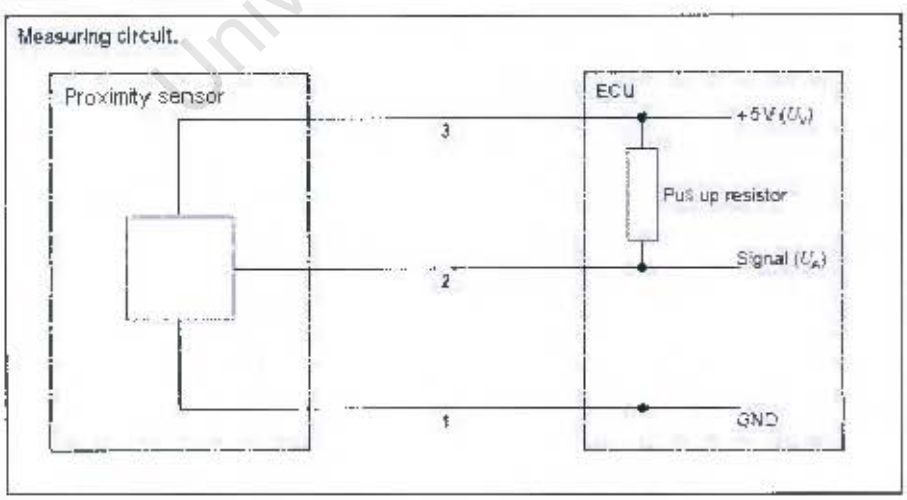

Output Signal

Gap - LOW

Metal in proximity - HIGH

University of Cape Town

Appendix F: Test Results

Refer to the front of this report if unclear on any of the acronyms in this section.

University of Cape Town

Table F-4: EN590 Test results

Operating point	Speed (min⁻¹)	Torque (Nm)	Fuel Flow (kg/h)	Air Flow (kg/h)	Exhaust Flow (kg/h)	P inlet (mbar)	T inlet (°C)	T exh (°C)	P Rail (bar)	P Baro (mbar)	Rel. Hum. (%)	Abs. Hum. (g/kg air)	T RH (°C)	Start of Main deg	Duration Main micros	Start of Pilot deg	Duration Pilot micros	B50
1	2000	11.95	0.83	31.670	32.550	LFM1F	50	300	551	1013.00	58.3	8.57	26	16.7	401	23.7	200	-4.3
2	2000	11.95	0.83	31.670	32.550	LFM1F	50	295	551	1013.00	58.3	8.57	26	14.7	397	20.7	200	-2
3	2000	11.90	0.87	31.748	32.618	LFM1F	50	296	551	1013.00	58.3	8.57	26	15.7	399	21.7	200	0
4	2000	11.85	0.86	31.670	32.530	LFM1F	50	296	551	1013.00	58.3	8.57	26	16.7	399	22.7	200	2.1
5	2000	11.75	0.85	31.708	32.568	LFM1F	50	300	551	1013.00	58.3	8.57	26	18.7	398	20.7	200	5
Check	2000	11.85	0.87	31.701	32.571	LFM1F	50	296	551	1013.00	58.3	8.57	25	15.7	399	24.7	200	0.2

Operating point	Speed (min⁻¹)	NOX (ppm)	O2 (%)	Lambda	FSN	Soot Conc. (g/m3)
1	2000	2096	13.1	2.461	0.18	0.00824
2	2000	1880	13.2	2.465	0.26	0.00835
3	2000	1445	13.5	2.472	0.34	0.00847
4	2000	1153	13.75	2.477	0.44	0.00854
5	2000	1015	13.5	2.494	0.54	0.00851
Check	2000	1435	13.3	2.485	0.35	0.00849

Operating point	Speed (min⁻¹)	Torque (Nm)	P kW	LFM Δp (mm H2O)	LFM Δp (Pa)	LFM P (mbar)	LFM T (°C)	Density (kg/m3)	Air Flow (kg/h)
1	2000	11.95	2.50238	42.1	413.034	200	26	1.412	31.670
2	2000	11.95	2.50238	42.1	413.034	200	26	1.412	31.670
3	2000	11.9	2.49323	42.2	413.912	200	26	1.412	31.748
4	2000	11.85	2.48519	42.1	413.034	200	26	1.412	31.670
5	2000	11.75	2.46619	42.15	413.523	200	26	1.412	31.708
Check	2000	11.85	2.48519	42	412.056	200	25	1.417	31.701

Operating point	NOX (g/h)	K h,d
1	101.84	0.9594
2	93.37	0.9594
3	77.80	0.9561
4	67.15	0.9589
5	60.34	0.9587
Check	77.60	0.9027

Operating point	NOX (g/kWh)	Soot Conc. (g/kWh)
1	41.5	0.024
2	38.3	0.036
3	28.6	0.048
4	23.0	0.054
5	20.5	0.033
6	28.3	0.050

HC Ratio	Lambda Calc
1.872	2.5038
1.861	2.500
1.730	2.543
1.802	2.566
1.834	2.600
1.804	2.530

Combustion analysis filename				
Date:	19/08/2007	12 IPM		
Fuel:	EN 590 Sulphur Free			
AFR	14.3			

Bore	0.09128	m
Stroke	0.0839	m
V	0.0004898	m3
Calibration Coefficient	0.0001470	

University of Cape Town

University of Cape Town

Table F-6: 25% GTL + 75% EN590 test results

Operating point	Speed	Torque	Fuel Flow	Air Flow	Exhaust Flow	P inlet	T inlet	T exh	P Rail	P Baro	Rel. Hum.	Abs. Hum.	T RH	Start of Main	Duration Main	Start of Pilot	Duration Pilot	B50	Control
	(min⁻¹)	(Nm)	(kg/h)	(kg/h)	(kg/h)	(mbar)	(°C)	(°C)	(bar)	(mbar)	(%)	(g/kg air)	(°C)	deg	micros	deg	micros		
1	2000	12.1[illegible]	[illegible].30	31.44[illegible]	[illegible]	[illegible]MP	50	306	65[illegible]	995[illegible]	77.[illegible]	11.54	24	16.3	[illegible]40	[illegible]	2[illegible]0	-4.6	On-1
2	2[illegible]0	12.1[illegible]	[illegible].9	31.49[illegible]	[illegible].[illegible]05	IFMP	50	300	650	995.[illegible]	77.[illegible]	11.54	25	14.[illegible]	[illegible].98	26.3	2.30	-2.1	On+2
3.2	2000	12.1[illegible]	[illegible].38	31.44[illegible]	[illegible].326	[illegible]MP	50	301	650	995.[illegible]	77.[illegible]	11.54	[illegible]4	12.3	[illegible]32	[illegible]	2[illegible]0	0	On
3.1	2[illegible]0	[illegible]2.0[illegible]	[illegible]6[illegible]	[illegible]1.47	[illegible].[illegible]57	[illegible]MP	50	299	650	995.[illegible]	77.5	11.54	[illegible]3	[illegible]2	[illegible]86	[illegible]4	[illegible]30	2.5	Off
4	2000	12.0[illegible]	[illegible].87	31.32[illegible]	[illegible].508	LFMP	50	297	[illegible]50	99[illegible].[illegible]	77.5	11.54	[illegible]5	[illegible].3	[illegible]89	[illegible].[illegible]	[illegible]60	[illegible].5	On-3
5	[illegible].00	11.9[illegible]	[illegible].86	[illegible]5.[illegible]	[illegible].[illegible]93	IFMP	50	[illegible]97	650	995.[illegible]	77.5	11.54	[illegible]6	[illegible].3	[illegible]84	[illegible].[illegible]3	[illegible]00	4.8	On-4
Check	[illegible].30	12.0[illegible]	[illegible].88	31.5[illegible].3	[illegible].2413	LFM P	50	30[illegible]	650	995.[illegible]	77.5	[illegible]1.54	[illegible]6	1.[illegible].3	390	24.3	[illegible].80	0.2	On

Operating point	Speed	NOX	O2	Lambda	FSN	Soot Conc.
	(min⁻¹)	(ppm)	(%)			(g/m3)
1	[illegible]00	[illegible]90[illegible]	[illegible]2.80	2.4[illegible]6	0.15	0.0[illegible]9
2	[illegible]300	1775	12.90	[illegible]4.5	0.20	0.0[illegible]5
3.2	[illegible]300	[illegible]45.[illegible]	[illegible]3.04	[illegible]4.35	0.31	0.00[illegible]3
3.1	[illegible]300	[illegible]42[illegible]	13.1	2.4[illegible]8	0.31	0.0[illegible]3
4	[illegible]300	[illegible]225	13.2	[illegible]4.25	0.[illegible]2	0.0[illegible]4
5	[illegible]300	[illegible]07[illegible]	13.35	2.4[illegible]5	0.52	0.0[illegible]7
Check	[illegible]300	1370	13.15	[illegible].4[illegible]5	0.31	0.[illegible].[illegible]

Operating point	Speed	Torque	P	LFM Δp	LFM Δp	LFM P	LFM T	Density	Air Flow
	(min⁻¹)	(Nm)	kW	(mm H2O)	(Pa)	(mbar)	(°C)	(kg/m3)	(kg/h)
1	[illegible]200	12.[illegible]5	[illegible].544[illegible]	42.[illegible]	[illegible]11.814	[illegible]00	24	[illegible].402	[illegible]1.440
2	[illegible].[illegible]00	12.15	[illegible].5447	42.[illegible]	[illegible]12.8[illegible]	200	25	[illegible].398	[illegible]1.415
3.2	[illegible]300	[illegible]2.1	[illegible].5342	42.[illegible]	[illegible]11.8[illegible]	[illegible]00	24	[illegible].402	[illegible]1.445
3.1	[illegible]300	[illegible].	[illegible]4[illegible].3	42.[illegible]	[illegible]0.956[illegible]	200	25	[illegible].402	[illegible]1.477
4	[illegible]400	[illegible]2	[illegible].5[illegible]3	42.[illegible]	[illegible]5.74[illegible]	[illegible]00	25	[illegible].398	[illegible]1.638
5	[illegible]500	[illegible]1.35	[illegible].50[illegible]	42.[illegible]	[illegible]5.74[illegible]	[illegible]00	25	[illegible].393	[illegible].[illegible]2[illegible]
Check	[illegible]600	[illegible]2	[illegible].45[illegible]	42.5	[illegible]5.74[illegible]	200	[illegible]5	[illegible].393	[illegible].153[illegible]

Operating point	NOX	K h,d
	(g/h)	
[illegible]	[illegible]3.2064	1.0[illegible]56
2	[illegible].[illegible]400	1.0[illegible]50
3.2	75.8900	1.0[illegible]39
[illegible].1	[illegible]4.[illegible]74[illegible]	1.0[illegible]28
4	[illegible]4.2420	1.0[illegible]52
5	[illegible].[illegible]754[illegible]	1.0[illegible]3
[illegible]	[illegible]1.[illegible]568[illegible]	1.0[illegible]15

Operating point	NOX	Soot Conc.
	(g/kWh)	(g/kWh)
[illegible]	4.[illegible]	[illegible].[illegible]09
2	36.3	0.[illegible]28
3.2	29.9	0.[illegible]42
3.1	29.7	0.[illegible]42
4	25.6	[illegible].[illegible]44
5	20.[illegible]	[illegible].[illegible]79
[illegible]	28.4	[illegible].[illegible]43

HC Ratio	Lambda Calc
1.56[illegible]	2.4[illegible]8
1.62[illegible]	2.44[illegible]
1.7[illegible]	2.47[illegible]
1.86[illegible]	2.4[illegible]5
1.891	2.[illegible]17
2.06[illegible]	2.5[illegible]7
1.782	2.430

Combustion analysis filename

Date	07/08/2007 [illegible]:20 AM
Fuel	[illegible]% GTL 75%
	25% GTL
AFD	11.45

Bore	0.0[illegible].26	m
Stroke	0.0[illegible].39	m
V	[illegible].000[illegible]4377	m3
Calibration Coefficient		0.00[illegible]0147[illegible]

University of Cape Town

Table F-7: 50% GTL + 50% EN590 test results

Operating point	Speed	Torque	Fuel Flow	Air Flow	Exhaust Flow	P inlet	T inlet	T exh	P Rail	P Baro	Rel Hum.	Abs Hum.	T RH	Start of Main	Duration Main	Start of Pilot	Duration Pilot	B50	Control
	[min^{-1}]	(Nm)	(kg/h)	(kg/h)	(kg/h)	(mbar)	(°C)	(°C)	(bar)	(mbar)	(%)	(g/kg air)	(°C)	deg	micros	deg	micros		
1	2000	11.97	0.39	31.783	32.553	LFMP	50	290	650	1016.77	81.8	11.93	24	12.7	398	28.7	200	-5	On-4
2	2000	12.05	0.39	31.793	32.573	LFMP	50	298	650	1016.77	81.8	11.93	24	12.7	395	28.7	200	-2.5	On-3
3.2	2000	11.90	0.38	31.859	32.730	LFMP	50	295	650	1016.77	81.8	11.93	24	12.7	390	24.7	200	0	On
3.1	2000	11.95	0.38	31.954	32.739	LFMP	50	294	650	1016.77	81.8	11.93	24	12.7	391	24	200	0.8	Off
4	2000	11.85	0.36	31.928	32.688	LFMP	50	293	650	1016.77	81.8	11.93	25	10.7	388	22.7	200	2	On-1
5	2000	11.82	0.36	31.904	32.654	LFMP	50	297	650	1016.77	81.8	11.93	25	8.7	388	20.7	200	4.5	On-4
Check	2000	11.95	0.38	31.904	32.784	LFMP	50	295	650	1016.77	81.8	11.93	25	12.7	391	24.7	200	0	On

Operating point	Speed	NOX	O2	Lambda	FSN	Soot Conc.
	(min^{-1})	(ppm)	(%)			(g/m3)
1	2000	2055	13.35	2.41	0.12	0.0015
2	2000	1785	13.15	2.44	0.17	0.0023
3.2	2000	1470	13.35	2.404	0.23	0.0031
3.1	2000	1355	13.35	2.407	0.25	0.0034
4	2000	1265	13.4	2.397	0.29	0.0041
5	2000	990	13.45	2.369	0.44	0.0064
Check	2000	1425	13.3	2.41	0.23	0.0031

Operating point	Speed	Torque	P	LFM Δp	LFM Δp	LFM P	LFM T	Density	Air Flow
	(min^{-1})	(Nm)	kW	(mm H2O)	(Pa)	(mbar)	(C)	(kg/m3)	(kg/h)
1	2000	11.97	2.507	419	109.900	200	24	1.427	31.763
2	2000	12.05	2.523	418	408.900	200	24	1.427	31.793
3.2	2000	11.9	2.4923	418	409.278	200	24	1.427	31.859
3.1	2000	11.95	2.5003	419	409.878	200	24	1.427	31.954
4	2000	11.85	2.4814	42	410.506	200	25	1.423	31.928
5	2000	11.82	2.4768	421	411.334	200	25	1.423	31.904
Check	2000	11.95	2.5038	421	411.334	200	25	1.423	31.904

Operating point	NOX	K h,d
	(g/h)	
1	110.8145	1.0160
2	95.10134	1.0182
3.2	76.83170	1.0205
3.1	72.88148	1.0265
4	67.01639	1.0228
5	52.09147	1.0229
	75.43052	1.0125

Operating point	NOX	Soot Conc.
	(g/kWh)	(g/kWh)
1	4.3.0	0.0595
2	37.7	0.0912
3.2	30.7	0.1231
3.1	29.1	0.1364
4	27.0	0.1640
5	21.4	0.1995
6	30.3	0.1351

Operating point	HC Ratio	Lambda Calc
1	1.653	2.427
2	1.726	2.454
3.2	1.935	2.462
3.1	1.922	2.470
4	2.235	2.544
5	2.521	2.630
6	1.96	2.432

Combustion analysis filename			
		Bore	0.08026
Date:	07/08/2007 9:00:49 AM	Stroke	0.1889
Fuel:	50% EN590	V	0.00038[illegible]
	50% GTL		
AFR	14.56	Calibration Constant	1000.4796

University of Cape Town

Pilot-injection-on results

Table F-4: EN590 Test results

Operating point	Speed	Torque	Fuel Flow	Air Flow	Exhaust Flow	P inlet	T inlet	T exh	P Rail	P Baro	Rel. Hum.	Abs. Hum.	T RH	Start of Main	Duration Main	Start of Pilot	Duration Pilot	B50
	(min $^{-1}$)	(Nm)	(kg/h)	(kg/h)	(kg/h)	(mbar)	(°C)	(°C)	(bar)	(mbar)	(%)	(g/kg air)	(°C)	deg	micros	deg	micros	
1	2000	11.95	0.88	31670	32.550	LFM P	50	300	650	1011.9	58.3	8.57	26	16.7	401	28.7	200	-4.8
2	2000	11.95	0.88	31670	32.550	LFM P	50	299	650	1011.9	58.3	8.57	26	14.7	397	26.7	200	-2
3	2000	11.95	0.87	31748	32.616	LFM P	50	296	650	1011.9	58.3	8.57	26	12.7	393	24.7	200	0
4	2000	11.85	0.85	31670	32.530	LFM P	50	298	650	1011.9	58.3	8.57	26	10.7	389	22.7	200	2.7
5	2000	11.75	0.86	31736	32.598	LFM P	50	295	650	1011.9	58.3	8.57	26	8.7	385	20.7	200	5
Check	2000	11.95	0.87	31.70	32.571	LFM P	50	296	650	1011.9	58.3	8.57	25	12.7	393	24.7	200	0.2

Operating point	Speed	NOX	O2	Lambda	FSN	Soot Conc.
	(min $^{-1}$)	(ppm)	(%)			(g/m3)
1	2000	2055	13.1	2.451	0.16	0.0024
2	2000	1880	13.2	2.458	0.26	0.0035
3	2000	1845	13.25	2.472	0.34	0.0047
4	2000	1852	13.45	2.477	0.41	0.0064
5	2000	1918	13.5	2.494	0.54	0.0087
Check	2000	1435	13.3	2.485	0.35	0.0049

Operatin q point	Speed	Torque	P	LFM _p	LFM _p	LFM P	LFM T	Density	Air Flow
	(min $^{-1}$)	(Nm)	kW	(mm H2O)	(Pa)	(mbar)	(°C)	(kg/m3)	(kg/h)
1	2000	11.95	2.5028	42.1	412.904	200	26	1.412	31670
2	2000	11.95	2.5028	42.1	412.904	200	26	1.412	31670
3	2000	11.9	2.4933	42.2	413.892	200	26	1.412	31746
4	2000	11.85	2.4819	42.1	412.904	200	26	1.412	31670
5	2000	11.75	2.4609	42.15	413.398	200	26	1.412	31708
Check	2000	11.85	2.4819	42	411.856	200	26	1.412	31701

Operating point	NOX	K h,d
	(g/h)	
1	101.96	0.04594
2	93.37	0.05014
3	91.65	0.05041
4	57.15	0.05539
5	50.24	0.05897
Check	71.50	0.05027

Operating point	NOX	Soot Conc.
	(g/kWh)	(g/kWh)
1	4.15	0.024
2	3.83	0.035
3	3.78	0.049
4	2.30	0.064
5	2.05	0.083
6	2.98	0.050

HC Ratio	Lambda Calc
1.877	2.508
1.881	2.518
1.870	2.540
1.902	2.566
1.864	2.509
1.864	2.509

Combustion analysis filename		
Date:	16/08/2007	0 30PPM
Fuel:	EN590 Sulphur Free	
AFR	14.35	

Bore	0.02026	m
Stroke	0.0889	m
V	0.000 14498	m3
Calibration Coefficient		0.0030147 06

University of Cape Town

Table F-9: EN590 Test results (no pilot)

Operating point	Speed	Torque	Fuel Flow	Air Flow	Exhaust Flow	P inlet	T inlet	T exh	P Rail	P Baro	Rel. Hum.	Abs. Hum	T RH	Start of Main	Duration Main	Start of Pilot	Duration Pilot	B50
	(min⁻¹)	(Nm)	(kg/h)	(kg/h)	(kg/h)	(mbar)	(°C)	(°C)	(bar)	(mbar)	(%)	(g/kg air)	(°C)	deg	micros	deg	micros	
1	2000	1[illegible]19	[illegible]	31.745	32.636	LFMP	[illegible]	[illegible]42	650	1009.9	55.2	8.06	[illegible]24	13.6	490			-5
2	2000	12.20	0.89	31.763	[illegible]	LFMP	[illegible]0	237	650	1009.4	55.2	8.06	[illegible]24	17.6	493			-2.1
3	2000	12.20	0.88	31.614	32.754	LFMP	50	246	650	1009.9	55.2	8.06	[illegible]4	15.6	486			0
4	2000	1[illegible]19	0.87	31.843	32.713	LFMP	[illegible]0	[illegible]31	650	1009.9	55.2	8.06	[illegible]24	13.6	481			2
5	2000	12.00	0.86	31.81[illegible]	32.671	LFMP	50	230	650	1009.9	55.2	8.06	24	11.6	478			4
Check	2000	1[illegible]19	[illegible]88	31682	32.642	LFMP	50	[illegible]44	650	1009.9	55.2	8.06	[illegible]24	15.6	485			0

Operating point	Speed	NOX	O2	Lambda	FSN	Soot Conc.
	(min⁻¹)	(ppm)	(%)			(g/m3)
1	2000	2390	[illegible]3.[illegible]	2.165	0.05	0.0036
2	2000	2030	13.18	2.146	0.07	0.0039
3	2000	1730	13.35	2.131	0.1	0.0013
4	2000	1504	13.5	2.135	0.18	0.0024
5	2000	1139	13.4	2.15	0.26	0.0035
Check	2000	664	[illegible]3.[illegible]	2.125	3.09	0.011

Operating point	Speed	Torque	P	LFM Δp	LFM Δp	LFM P	LFM T	Density	Air Flow
	(min⁻¹)	(Nm)	kW	(mm H2O)	(Pa)	(mbar)	(C)	(kg/m3)	(kg/h)
1	2000	12.1	2.534[illegible]	42.2	413.[illegible]	200	26.0	1.412	31.74[illegible]
2	2000	12.2	2.55[illegible]	42.3	413.791	200	26	1.[illegible]	31.763
3	2000	12.2	2.505[illegible]	42.3	413.791	200	26	1.[illegible]5	31.614
4	2000	[illegible]	2.534[illegible]	41.4	414.765	200	26	1.[illegible]0	31.843
5	2000	[illegible]	2.51[illegible]	42.5	415.741	200	27	1.405	31.811
Check	2000	1[illegible]15	2.54[illegible]	42.5	415.741	200	27	1.405	31.[illegible]

Operating point	NOX	K h,d
	(g/h)	
1	110.7[illegible]	0.9579
2	100.51	0.9579
3	85.[illegible]	0.9577
4	67.69	0.9575
5	56.76	0.9573
Check	[illegible]2.[illegible]	0.9578

Operating point	NOX	Soot Conc.
	(g/kWh)	(g/kWh)
1	46.[illegible]	[illegible].008
2	29.[illegible]	0.009
3	33.4	0.01[illegible]
4	28.[illegible]	0.024
5	22.[illegible]	0.036
6	[illegible].[illegible]	0.0[illegible]

HC Ratio	Lambda Calc
3.535	2.486
1.616	2.4[illegible]
1.763	2.5[illegible]4
1.915	2.561
2.050	2.579
1.781	2.507

Combustion analysis filename		
Date:	04/08/2017	12:30:[illegible]M
Fuel:	EN590 Sulphur Free	

Bore	0.0[illegible]26	m
Stroke	0.[illegible]0889	m
Y	0.0[illegible]04498	m
Calibration Coefficient		0.000[illegible]14796

University of Cape Town

Table F-5: GTL test results

Operating point	Speed	Torque	Fuel Flow	Air Flow	Exhaust Flow	P inlet	T inlet	T exh	P Rail	P Baro	Rel. Hum.	Abs. Hum.	T RH	Start of Main	Duration Main	Start of Pilot	Duration Pilot	B50	Control
	(min^{-1})	(Nm)	(kg/h)	(kg/h)	(kg/h)	(mbar)	(°C)	(°C)	(bar)	(mbar)	(%)	(g/ kg air)	(°C)	deg	micros	deg	micros		
1	2000	12.20	0.90	31.789	32.689	LFMP	50	303	550	1011.9	55.2	8.04	27	14.3	4[illegible]	[illegible]	[illegible]0	-4.5	C1-4
2	2000	12.20	0.89	31.864	32.754	LFMP	50	302	550	1011.9	55.2	8.04	27	14.3	39.2	25.8	200	--	C1-2
3.2	2000	12.05	0.88	32.046	32.926	LFMP	50	297	550	1011.9	55.2	8.04	28	13.7	39.2	24.8	200	0	On
3.1	2000	12.50	0.88	31.971	32.851	LFMP	50	295	550	1011.9	55.2	8.04	28	12	39.2	24	200	0.5	On
4	2000	12.90	0.87	32.014	32.884	LFMP	50	295	550	1011.9	55.2	8.04	27	11.5	37.7	23.8	200	2.5	On-2
5	2000	12.00	0.88	32.069	32.949	LFMP	50	300	550	1011.9	55.2	8.04	27	9.8	33.4	23.8	200	5	On-4
Check	2000	12.00	0.87	31.758	32.628	LFMP	50	300	550	1011.9	55.2	8.04	28	12.3	39.2	24.8	200	0.5	On

Operating point	Speed	NOX	O2	Lambda	FSN	Soot Conc.
	(min^{-1})	(ppm)	(%)			(g/m3)
1	2000	1220	11	2.17	0.05	0.0011
2	2000	860	10.1	2.72	0.15	0.0021
3.2	2000	1060	10.3	2.42	0.10	0.0025
3.1	2000	1490	12.4	2.35	0.21	0.0028
4	2000	1282	12.5	2.34	0.24	0.0032
5	2000	957	12.5	2.32	0.34	0.0047
Check	2000	1550	13.2	2.37	0.19	0.0025

Operating point	Speed	Torque	P	LEM Δp	LEM Δp	LEM P	LEM T	Density	Air Flow
	(min^{-1})	(Nm)	kW	(mm H2O)	(Pa)	(mbar)	(°C)	(kg/m3)	(kg/h)
1	2000	12.2	2.5552	42.4	414.769	200	27	1.408	31.789
2	2000	12.2	2.5552	42.5	416.747	201	27	1.405	31.864
3.2	2000	12.05	2.5237	42.6	417.725	200	26	1.412	32.046
3.1	2000	11.9	2.4714	42.5	416.747	200	26	1.412	31.971
4	2000	11.9	2.4923	42.7	417.704	200	27	1.402	32.014
5	2000	12	2.5133	42.8	418.682	200	27	1.408	32.089
Check	2000	12	2.5133	42.5	416.747	200	28	1.405	31.758

Operating point	NOX	K h,d
	(g/h)	
1	10.98011	0.3479
2	9.72339	0.3475
3.2	7.70695	0.3504
3.1	7.30147	0.3505
4	8.34143	0.3467
5	9.24376	0.3469
	25.82139	0.3435

Operating point	NOX	Soot Conc.
	(g/kWh)	(g/kWh)
1	4.31	0.011
2	35.9	0.021
3.2	30.7	0.025
3.1	29.9	0.029
4	26.4	0.033
5	20.9	0.049
6	30.2	0.025

HC Ratio	Lambda Calc
1.977	2.371
1.959	2.403
2.051	2.414
2.012	2.436
2.157	2.470
2.112	2.447
2.100	2.450

Combustion analysis filename	
Date:	14/08/2007 7:17 PM
Fuel:	EN590 Sulphur Free
AFR	14.9

Bore	0.09326	m
Stroke	0.0[illegible]89	m
V	0.000[illegible]49/7	m3
Calibration Coefficient	2.000[illegible]4706	

University of Cape Town

Table F-6: 25% GTL + 75% EN590 test results

Operating point	Speed	Torque	Fuel Flow	Air Flow	Exhaust Flow	P inlet	T inlet	T exh	P Rail	P Baro	Rel. Hum.	Abs. Hum.	T RH	Start of Main	Duration Main	Start of Pilot	Duration Pilot	B50	Control
	(min⁻¹)	(Nm)	(kg/h)	(kg/h)	(kg/h)	(mbar)	(°C)	(°C)	(bar)	(mbar)	(%)	(g/kg air)	(°C)	deg	micros	deg	micros		
1	2000	125.5	0.93	31446	32345	LFM F	50	305	650	995.1	77.5	11.84	24	16.3	395	28.3	200	4.5	On+1
2	2000	125.5	0.79	31415	32306	LFM F	50	303	650	995.1	77.5	11.84	25	14.3	398	26.3	200	2.1	On+2
3.2	2000	125.0	0.68	31446	32326	LFM F	50	301	650	995.1	77.5	11.84	24	12.3	392	24.3	200	0	On
3.1	2000	125.0	0.83	31477	32357	LFM F	50	299	650	995.1	77.5	11.84	23	12	395	24	200	4.5	On
4	2000	125.0	0.97	31508	32388	LFM F	50	297	650	995.1	77.5	11.84	26	10.3	389	22.3	200	2.5	On-2
5	2000	125.0	0.86	31533	32390	LFM F	50	297	650	995.1	77.5	11.84	26	8.3	384	21.4	200	4.5	On-4
Check	2000	125.0	0.69	31533	32417	LFM F	50	297	650	995.1	77.5	11.84	26	10.3	390	24.3	200	2.2	On

Operating point	Speed	NOX	O2	Lambda	FSN	Soot Conc.
	(min⁻¹)	(ppm)	(%)			(g/m3)
1	2000	2186	12.70	2.436	0.15	0.0019
2	2000	1975	12.90	2.415	0.20	0.0026
3.2	2000	1450	13.04	2.436	0.31	0.0042
3.1	2000	1430	13.1	2.438	0.31	0.0043
4	2000	1245	13.2	2.425	0.32	0.0044
5	2000	975	13.35	2.405	0.52	0.0077
Check	2000	1.79	13.15	2.415	0.31	0.0043

Operating point	Speed	Torque	P	LFM Δp	LFM ρ	LFM P	LFM T	Density	Air Flow
	(min⁻¹)	(Nm)	kW	(mm H2O)	(Pa)	(mbar)	(°C)	(kg/m3)	(kg/h)
1	2000	12.1	25.447	42.1	412.934	200	25	1.402	31.446
2	2000	12.1	25.447	41.9	410.972	200	25	1.398	31.415
3.2	2000	12.1	25.342	42.1	412.934	200	24	1.402	31.446
3.1	2000	12	25.133	42	411.954	200	23	1.407	31.477
4	2000	12	25.133	41.5	407.032	200	25	1.393	31.508
5	2000	11.95	25.028	41.5	407.032	200	24	1.393	31.533
Check	2000	12	25.133	41.5	407.032	200	25	1.393	31.533

Operating point	NOX	K h,d
	(g/h)	
1	68.2934	1.186
2	62.483	1.160
3.2	45.990	1.189
3.1	74.674	1.1228
4	64.2427	1.152
5	50.7543	1.010
	71.3562	1.011

Operating point	NOX	Soot Conc.
	(g/kWh)	(g/kWh)
1	4.3	0.119
2	3.9	0.026
3.2	2.9	0.042
3.1	4.7	0.042
4	4.1	0.044
5	3.2	0.048
6	4.5	0.043

HC Ratio	Lambda Calc
1.560	2.415
1.632	2.415
1.796	2.473
1.669	2.473
1.89	2.517
2.007	2.517
1.782	2.483

Combustion analysis filename	
Date:	06/02/2007 16:20AM
Fuel:	75% EN 590
	25% GTL
AFR	14.45

Bore	0.13026	m
Stroke	0.1889	m
V	0.0244977	m3
Calibration Coefficient	0.0051796	

University of Cape Town

Table F-7: 50% GTL + 50% EN590 test results

Operating point	Speed	Torque	Fuel Flow	Air Flow	Exhaust Flow	P inlet	T inlet	T exh	P Rail	P Baro	Rel Hum.	Abs. Hum.	T RH	Start of Main	Duration Main	Start of Pilot	Duration Pilot	B50	Control
	(min^{-1})	(Nm)	(kg/h)	(kg/h)	(kg/h)	(mbar)	(°C)	(°C)	(bar)	(mbar)	(%)	(g/kg air)	(°C)	deg	micros	deg	micros		
1	2000	11.97	0.83	31.785	32.613	LFMP	50	299	65.1	1016.77	81.3	11.30	24	16.7	390	28.7	200	-5	On+4
2	2000	12.15	0.84	31.782	32.673	LFMP	50	295	65.0	1016.77	81.3	11.30	24	14.7	395	26.7	200	-2.5	On+2
3.2	2000	11.90	0.83	31.859	32.739	LFMP	50	295	65.1	1016.77	81.3	11.93	24	12.7	390	24.7	200	0	On
3.1	2000	11.85	0.83	31.859	32.739	LFMP	50	294	65.1	1016.77	81.3	11.93	24	12	390	24.7	200	0.9	Off
4	2000	11.85	0.83	31.828	32.688	LFMP	50	290	65.0	1016.77	81.3	11.93	25	10.7	380	22.7	200	2	On 3
5	2000	11.82	0.83	31.804	32.654	LFMP	50	291	65.0	1016.77	81.3	11.93	25	8.7	385	20.7	200	4.5	On 4
Check	2000	11.95	0.83	31.804	32.784	LFMP	50	295	65.0	1016.77	81.3	11.93	25	12.7	390	24.7	200	0	On

Operating point	Speed	NOX	O2	Lambda	FSN	Soot Conc.
	(min^{-1})	(ppm)	(%)			(g/m3)
1	2000	2368	13.95	2.411	0.03	0.0316
2	2000	1735	13.85	2.418	0.01	0.00422
3.2	2000	1435	13.95	2.404	0.02	0.0331
3.1	2000	1385	13.95	2.407	0.02	0.0334
4	2000	1263	13.4	2.447	0.04	0.0340
5	2000	1193	13.45	2.365	0.44	0.1064
Check	2000	1425	13.3	2.407	0.03	0.0331

Operating point	Speed	Torque	P	LFM Δp	LFM Δp	LFM P	LFM T	Density	Air Flow
	(min^{-1})	(Nm)	kW	(mm H2O)	(Pa)	(mbar)	(°C)	(kg/m3)	(kg/h)
1	2000	11.97	2.507	41.8	409.790	1.0	24	14.7	31.79
2	2000	12.05	2.523	41.8	409.790	1.0	24	14.7	31.79
3.2	2000	11.9	2.493	41.9	409.278	1.0	24	14.7	31.855
3.1	2000	11.85	2.482	41.9	409.278	1.0	24	14.7	31.855
4	2000	11.85	2.479	42	411.850	1.0	25	14.23	31.679
5	2000	11.82	2.476	42	411.834	1.0	25	14.23	31.804
Check	2000	11.95	2.502	42.1	411.834	1.0	25	14.23	31.804

Operating point	NOX	K h,d
	(g/h)	
1	110.5345	1.0261
2	85.1034	1.0202
3.2	70.0278	1.0265
3.1	72.6398	1.0265
4	67.0939	1.0229
5	58.3647	1.0229
	75.3062	1.0225

Operating point	NOX	Soot Conc.
	(g/kWh)	(g/kWh)
1	4.29	0.012
2	3.7	0.002
3.2	3.07	0.001
3.1	3.91	0.004
4	2.70	0.014
5	2.14	0.035
6	3.03	0.011

HC Ratio	Lambda Calc
1.875	2.417
1.705	2.454
1.905	2.460
1.902	2.488
2.235	2.544
2.514	2.590
1.963	2.492

Combustion analysis filename		
Date:	07/08/2007	9:10AM
Fuel	50% EN590	
	50% GTL	
AFR	14.55	

Bore	0.08026	m
Stroke	0.0889	m
V	0.000451977	m3
Discharge Coefficient		0.00614796

University of Cape Town

Table F-8: 75% GTL + 25% EN590 test results

Operating point	Speed	Torque	Fuel Flow	Air Flow	Exhaust Flow	P inlet	T inlet	T exh	P Rail	P Baro	Rel. Hum.	Abs. Hum.	T RH	Start of Main	Duration Main	Start of Pilot	Duration Pilot	B50	Control
	(min^{-1})	(Nm)	(kg/h)	(kg/h)	(kg/h)	(mbar)	(°C)	(°C)	(bar)	(mbar)	(%)	(g/ kg air)	(°C)	deg	micros	deg	micros		
1	2000	11.85	0.87	31.436	32.306	LFM P	50	304	650	1000.12	64.2	9.48	26	16.7	396	28.7	200	-5	On+4
2	2000	11.85	0.86	31.511	32.371	LFM P	50	301	650	1000.12	64.2	9.48	26	14.7	393	26.7	200	-2.3	On+2
3.2	2000	11.80	0.85	31.436	32.286	LFM P	50	300	650	1000.12	64.2	9.48	26	12.7	390	24.7	200	0	On
3.1	2000	11.75	0.85	31.392	32.242	LFM P	50	298	650	1000.12	64.2	9.48	26	12	387	24	200	0.8	Off
4	2000	11.95	0.85	31.660	32.510	LFM P	50	296	650	1000.12	64.2	9.48	26	10.7	386	22.7	200	2.5	On-2
5	2000	11.85	0.84	31.628	32.468	LFM P	50	295	650	1000.12	64.2	9.48	27	8.7	384	20.7	200	5	On-4
Check	2000	11.80	0.85	31.554	32.404	LFM P	50	297	650	1000.12	64.2	9.48	27	12.7	388	24.7	200	0	On

Operating point	Speed	NOX	O2	Lambda	FSN	Soot Conc.
	(min^{-1})	(ppm)	(%)			(g/m3)
1	2000	2115	12.90	2.423	0.11	0.0014
2	2000	1820	13.15	2.446	0.16	0.0021
3.2	2000	1491	13.2	2.452	0.22	0.0029
3.1	2000	1440	13.25	2.468	0.23	0.0031
4	2000	1282	13.11	2.475	0.28	0.0038
5	2000	1044	13.35	2.482	0.39	0.0055
Check	2000	1481	13.25	2.467	0.25	0.0034

Operating point	Speed	Torque	P	LFM Δp	LFM Δp	LFM P	LFM T	Density	Air Flow
	(min^{-1})	(Nm)	kW	(mm H2O)	(Pa)	(mbar)	(°C)	(kg/m3)	(kg/h)
1	2000	11.85	2.4819	42.2	412.812	200	26	1.399	31.436
2	2000	11.85	2.4819	42.3	413.791	200	26	1.399	31.511
3.2	2000	11.8	2.4714	42.2	412.812	200	26	1.399	31.436
3.1	2000	11.75	2.4609	42	410.856	200	25	1.403	31.392
4	2000	11.95	2.5028	42.5	415.747	200	26	1.399	31.660
5	2000	11.85	2.4819	42.6	416.725	200	27	1.394	31.628
Check	2000	11.8	2.4714	42.5	415.747	200	27	1.394	31.554

Operating point	NOX	K h,d
	(g/h)	
1	105.8287	0.9747
2	91.2295	0.9745
3.2	74.5321	0.9744
3.1	72.1590	0.9781
4	65.0244	0.9743
5	52.2644	0.9703
	74.0164	0.9706

Operating point	NOX	Soot Conc.
	(g/kWh)	(g/kWh)
1	42.6	0.014
2	36.8	0.021
3.2	30.2	0.030
3.1	29.2	0.031
4	26.0	0.038
5	21.1	0.056
6	29.9	0.034

HC Ratio	Lambda Calc
1.833	2.459
1.880	2.493
1.952	2.536
1.786	2.512
1.928	2.534
2.013	2.561
1.927	2.525

Combustion analysis filename		
Date:	08/08/2007	4:30PM
Fuel:	25% EN 590	
	75% GTL	
AFR	14.7	

Bore	0.08026	m
Stroke	0.0889	m
V	0.000044977	m3
Calibration Coefficient		0.00014796

University of Cape Town

Table F-10: GTL test results (no pilot)

Operating point	Speed (min⁻¹)	Torque (Nm)	Fuel Flow (kg/h)	Air Flow (kg/h)	Exhaust Flow (kg/h)	P inlet (mbar)	T inlet (°C)	T exh (°C)	P Rail (bar)	P Baro (mbar)	Rel. Hum (%)	Abs. Hum. (g/ kg air)	T RH (°C)	Start of Main deg	Duration Main micros	Start of Pilot deg	Duration Pilot micros	B50	Control
1	2000	12.0	3.85	31.693	32.543	LFM P	50	237	650	1003.4	55.2	8.36	25	19.9	494			5	On+4
2	2000	12.0	3.85	31.842	32.692	LFM P	50	232	650	1003.4	55.2	8.36	25	17.9	488			2.5	On+2
3.2	2000	11.97	3.84	31.767	32.607	LFM P	50	239	650	1003.4	55.2	8.36	25	15.9	484			0	On
3.1	2000	12.00	3.85	31.693	32.543	LFM P	50	239	650	1003.4	55.2	8.36	25	15.6	485			0.3	On
4	2000	11.90	3.84	31.842	32.692	LFM P	50	237	650	1003.4	55.2	8.36	25	13.9	479			2.2	On-2
5	2000	11.80	3.84	31.767	32.607	LFM P	50	233	650	1003.4	55.2	8.36	25	11.9	477			3.9	On-4
Check	2000	11.9	3.85	31.916	32.766	LFM P	50	234	650	1003.4	55.2	8.36	25	15.9	484			0.2	On

Operating point	Speed (min⁻¹)	NOX (ppm)	O2 (%)	Lambda	FSN	Soot Conc. (g/m3)
1	2000	2390	13.2	2.439	0.04	0.0005
2	2000	1170	11.25	2.436	0.05	0.0006
3.2	2000	1660	10.35	2.449	0.066	0.0008
3.1	2000	1610	10.3	2.443	0.07	0.0009
4	2000	1330	11.5	2.432	0.12	0.0015
5	2000	1085	12.4	2.438	0.13	0.0016
Check	2000	1615	10.3	2.442	0.07	0.0009

Operating point	Speed (min⁻¹)	Torque (Nm)	P (kW)	LFM Δp (mm H2O)	LFM Δp (Pa)	LFM P (mbar)	LFM T (°C)	Density (kg/m3)	Air Flow (kg/h)
1	2000	12.0	2.5342	42.5	416.747	200	23	1.400	31.693
2	2000	12	2.5133	42.7	417.704	200	23	1.400	31.842
3.2	2000	11.95	2.5028	42.6	416.725	200	23	1.400	31.767
3.1	2000	12	2.5133	42.5	416.747	200	23	1.400	31.693
4	2000	11.9	2.4923	42.7	417.704	200	23	1.400	31.842
5	2000	11.8	2.4714	42.6	416.725	200	23	1.400	31.767
Check	2000	11.9	2.4923	42.3	413.682	200	23	1.400	31.916

Operating point	NOX (g/h)	K h,d
1	47.8855	0.9537
2	47.5034	0.9524
3.2	82.0030	0.9534
3.1	79.2419	0.953
4	65.8432	0.9534
5	53.5533	0.9534
	80.1612	0.9524

Operating point	NOX (g/kWh)	Soot Conc. (g/kWh)
1	46.5	0.005
2	46.2	0.006
3.2	32.6	0.008
3.1	31.5	0.009
4	26.4	0.016
5	21.7	0.024
6	32.2	0.009

HC Ratio	Lambda Calc
2.115	2.532
2.101	2.514
2.209	2.536
2.093	2.536
2.310	2.544
2.139	2.513
2.161	2.510

Combustion analysis filename	
Date:	04/08/2007 3:19PM
Fuel:	GT. Sulphur Free

Bore	0.08026	m
Stroke	0.0889	m
V	0.00044377	m3
Calculation Coefficient		0.0014796

University of Cape Town

Table F-11: 25% GTL + 75% EN590 test results (no pilot)

Operating point	Speed (min⁻¹)	Torque (Nm)	Fuel Flow (kg/h)	Air Flow (kg/h)	Exhaust Flow (kg/h)	P inlet (mbar)	T inlet (°C)	T esh (°C)	P Rail (bar)	P Baro (mbar)	Rel Hum. (%)	Abs. Hum. (g/kg air)	T RH (°C)	Start of Main deg	Duration Main micros	Start of Pilot deg	Duration Pilot micros	B50	Control
1	2000	11.95	0.83	31.544	32.424	LFM P	50	29.2	850	994.12	77.5	11.55	27	-9.6	434			4.3	On-4
2	2000	12.00	0.87	31.578	32.446	LFM P	50	29.2	850	994.12	77.5	11.55	26	-10.6	433			-2	On-2
3.2	2000	11.90	0.83	31.501	32.361	LFM P	50	29.1	850	994.12	77.5	11.55	26	-15.6	434			0	**On**
3.1	2000	11.80	0.86	31.501	32.361	LFM P	50	29.1	850	994.12	77.5	11.55	26	-15.6	434			0	Off
4	2000	11.80	0.84	31.692	32.532	LFM P	50	28.7	850	994.12	77.5	11.55	27	-10.6	437			2.3	On-2
5	2000	11.85	0.83	31.618	32.446	LFM P	50	29.1	850	994.12	77.5	11.55	27	-11.6	435			-1	On-4
Check	2000	11.80	0.87	31.618	32.478	LFM P	50	29.1	850	994.12	77.5	11.55	27	-15.6	434			0	On

Operating point	Speed (min⁻¹)	NOX (ppm)	O2 (%)	Lambda	FSN	Soot Conc. (g/m3)
1	2000	2215	13.01	2.537	0.05	0.0006
2	2000	1958	13.14	2.538	0.07	0.0009
3.2	2000	1555	13.35	2.541	0.09	0.0015
3.1	2000	1536	13.35	2.541	0.09	0.0011
4	2000	1756	13.51	2.545	0.13	0.0018
5	2000	1634	13.42	2.547	0.09	0.0021
Check	2000	1642	13.35	2.525	0.08	0.0010

Operating point	Speed (min⁻¹)	Torque (Nm)	P kW	LFM Δp (mm H2O)	LFM Δp (Pa)	LFM P (mbar)	LFM T (°C)	Density (kg/m3)	Air Flow (kg/h)
1	2000	11.95	2.5029	42.7	417.704	200	27	1.387	31.544
2	2000	12	2.513	42.6	416.725	200	26	1.392	31.576
3.2	2000	11.9	2.4923	42.5	415.747	200	26	1.392	31.501
3.1	2000	11.9	2.4923	42.5	415.747	200	26	1.392	31.501
4	2000	11.8	2.4711	42.9	419.680	200	27	1.387	31.692
5	2000	11.85	2.4806	42.8	418.692	200	27	1.387	31.618
Check	2000	11.85	2.4816	42.8	418.692	200	27	1.387	31.618

Operating point	NOX (g/h)	K h,d
1	15.0103	1.0078
2	16.3015	1.0116
3.2	16.8895	1.0116
3.1	16.8895	1.0116
4	15.4193	1.0076
5	16.7152	1.0075
	16.1900	1.0077

Operating point	NOX (g/kWh)	Soot Conc. (g/kWh)
1	4.0	0.006
2	3.8	0.009
3.2	3.5	0.01
3.1	3.5	0.01
4	3.5	0.00
5	3.5	0.032
	3.5	0.00

HC Ratio	Lambda Calc
1.314	2.436
1.424	2.489
1.499	2.492
1.499	2.492
1.777	2.567
1.364	2.591
1.556	2.591

Combustion analysis filename		
Date	06/12/2007	12:00 PM
Fuel	75% EN590	
	25% GTL	

Bore	0.08026	m
Stroke	0.0889	m
V	0.000443677	m3
Calibration Coefficient	0.0014796	

University of Cape Town

Table F-12: 50% GTL + 50% EN590 test results (no pilot)

Operating point	Speed	Torque	Fuel Flow	Air Flow	Exhaust Flow	P inlet	T inlet	T exh	P Rail	P Baro	Rel Hum.	Abs. Hum	T RH	Start of Main	Duration Main	Start of Pilot	Duration Pilot	D50	Control
	(min^{-1})	(Nm)	(kg/h)	(kg/h)	(kg/h)	(mbar)	(°C)	(°C)	(bar)	(mbar)	(%)	(g/kg air)	(°C)	deg	micros	deg	micros		
1	[illegible]	[illegible]	0.85	31.90	32.761	LFM1P	5[illegible]	[illegible]	[illegible]	[illegible]	65.5	9.56	2[illegible]	[illegible]	[illegible]			-4.5	Cn+4
[illegible]	2000	11.77	0.85	31.87	32.720	LFM1P	5[illegible]	239	650	1016.6	65.6	9.56	2[illegible]	[illegible]	497			-2.[illegible]	[illegible]
3.1	[illegible]	[illegible]	0.85	31.95	32.796	LFM1P	5[illegible]	237	650	1016.6	65.[illegible]	9.56	2[illegible]	[illegible]	[illegible]			0.5	On
3.2	2000	11.77	0.85	31.90	32.751	LFM1P	5[illegible]	236	650	1016.6	65.6	9.56	2[illegible]	[illegible]	484			0	On
4	2000	11.77	0.84	31.845	32.686	LFM1P	5[illegible]	234	650	1016.6	65.[illegible]	9.55	2[illegible]	[illegible]	481			-2.[illegible]	[illegible]
[illegible]	2000	11.75	0.85	31.945	32.795	LFM1P	[illegible]	[illegible]	650	1016.6	65.6	9.56	2[illegible]	[illegible]	479			-4.5	Cn-4
Check	2000	11.75	0.85	32.021	[illegible]	LFM1P	5[illegible]	236	650	1016.6	65.6	9.56	2[illegible]	[illegible]	484			0	On

Operating point	Speed	NOX	O2	Lambda	FSN	Soot Conc	Operating point	Speed	Torque	P	LFM Δp	LFM Δp	LFM P	LFM T	Density	Air Flow
	(min^{-1})	(ppm)	(%)			(g/m3)		(min^{-1})	(Nm)	kW	(mm H2O)	(Pa)	(mbar)	(°C)	(kg/m3)	(kg/h)
[illegible]	2000	2193	13.35	2.485	0.4	0.0005	1	2000	11.75	2.4609	42.[illegible]	411.634	200	[illegible]	[illegible]	31.631
2	2000	1612	13.41	2.495	0.76	0.0009	2	2000	11.77	2.4661	42.[illegible]	412.812	200	2[illegible]	1418	31.670
3.1	2000	1565	13.65	2.485	0.8	0.0011	3.1	2000	11.65	2.4400	41.8	408.678	200	[illegible]	1427	31.576
3.2	2000	1439	13.55	2.484	0.1	0.0012	3.2	2000	11.7	2.4504	42.[illegible]	410.934	200	[illegible]	1423	31.601
4	2000	1258	13.75	2.492	0.8	0.0024	4	2000	11.7	2.4504	42.[illegible]	410.791	200	2[illegible]	1416	31.585
5	2000	1035	13.[illegible]	2.469	0.3	0.0057	5	2000	11.75	2.4609	42.[illegible]	412.791	200	[illegible]	1410	31.545
Check	2000	1456	13.[illegible]	2.481	0.9	0.001	Check	2000	11.7[illegible]	2.46[illegible]	42.[illegible]	411.769	200	[illegible]	1418	31.601

Operating point	NOX	K h,d	Operating point	NOX	Soot Conc.	HC Ratio	Lambda Calc
	(g/h)			(g/kWh)	(g/kWh)		
1	[illegible]	0.[illegible]	[illegible]	14.8	0.005	19.7	2.[illegible]
2	[illegible]	0.[illegible]	[illegible]	17.3	0.00[illegible]	20.3	2.561
3.1	73.5030	0.[illegible]	3.1	12.6	0.01[illegible]	20.7	2.550
3.2	75.8861	0.[illegible]	3.2	13.0	0.01[illegible]	20.79	2.553
4	61.8887	0.[illegible]	4	15.3	0.024	21.52	2.[illegible]
5	51.0409	0.[illegible]	5	20.7	0.0[illegible]	2.508	2.618
Check	74.6021	0.[illegible]	6	30.4	0.0[illegible]	2.448	2.563

Combustion analysis filename		
Date	[illegible]7/05/2007 [illegible]:[illegible]PM	
Fuel	50% EN590	
	50% GTL	

Bore	0.08126	m
Stroke	0.0[illegible]39	m
V	0.000044077	m3
Ca Brake Constant	0.000114796	

University of Cape Town

Table F-13: 75% GTL + 25% EN590 test results (no pilot)

Operating point	Speed	Torque	Fuel Flow	Air Flow	Exhaust Flow	P inlet	T inlet	T exh	P Rail	P Baro	Rel. Hum	Abs. Hum	T RH	Start of Main	Duration Main	Start of Pilot	Duration Pilot	B50	Control
	(min⁻¹)	(Nm)	(kg/h)	(kg/h)	(kg/h)	(mbar)	(°C)	(°C)	(bar)	(mbar)	(%)	(g/kg air)	(°C)	deg	micros	deg	micros		
1	[illegible]	11.95	3.88	31.427	32.287	LFMF	50	288	650	994.12	77.5	[illegible]	26	20	431			4.2	On+4
2	2001	11.90	3.85	31.427	32.277	LFMF	50	294	650	994.12	77.5	11.55	26	18	483			-2.1	On+2
3.1	2001	11.90	3.84	31.398	32.238	LFMF	50	290	650	994.12	77.5	11.55	27	16	483			0	On
3.1	2001	11.85	3.84	31.427	32.267	LFMF	50	290	650	994.12	77.5	11.55	26	15.6	483			0.3	Off
4	2001	11.70	3.81	31.427	32.257	LFMF	50	286	650	994.12	77.5	11.55	26	13.8	483			1.8	On-2
5	2001	11.60	0.81	31.398	32.208	LFMF	50	285	650	994.12	77.5	11.55	27	11.8	483			4.1	On-4
Check	2001	11.7	3.84	31.427	32.267	LFMF	50	290	650	994.12	77.5	11.55	26	16	483			0	On

Operating point	Speed	NOX	O2	Lambda	FSN	Soot Conc.
	(min⁻¹)	(ppm)	(%)			(g/m3)
1	2000	2385	13.1	2.438	0.04	0.0070
2	2010	2018	13.2	2.525	0.05	0.0086
3.2	2000	1655	13.3	2.544	0.07	0.0109
3.1	2013	1581	13.33	2.551	0.07	0.0110
4	2000	1343	13.5	2.584	0.10	0.0167
5	2000	1112	13.6	2.627	0.11	0.0188
Check	2000	1[illegible]	13.55	2.621	0.08	0.0140

Operating point	Speed	Torque	P	LFM Δp	LFM Δp	LFM P	LFM T	Density	Air Flow
	(min⁻¹)	(Nm)	kW	(mm H2O)	(Pa)	(mbar)	(°C)	(kg/m3)	(kg/h)
1	2000	11.95	2.50[illegible]	42.4	414.783	[illegible]	26	1.370	31.427
2	2010	11.9	2.493	42.4	414.[illegible]	[illegible]	26	1.372	31.427
3.2	2000	11.8	2.474	42.5	415.747	[illegible]	27	1.367	31.398
3.1	2000	11.85	2.484	42.4	414.[illegible]	[illegible]	26	1.372	31.427
4	2000	11.7	2.454	42.4	414.[illegible]	[illegible]	26	1.372	31.427
5	2000	11.6	2.4[illegible]	42.5	415.747	[illegible]	27	1.367	31.398
Check	2000	11.7	2.454	42.4	414.[illegible]	[illegible]	26	1.372	31.427

Operating point	NOX	K h,d
	(g/h)	
1	123.7998	1.0018
2	104.5996	1.0016
3.2	85.4201	1.0015
3.1	80.2127	1.0016
4	69.9510	1.0016
5	57.2215	1.0025
	64.3916	1.0016

Operating point	NOX	Soot Conc.
	(g/kWh)	(g/kWh)
1	4.25	0.005
2	4.20	0.008
3.2	3.46	0.009
3.1	3.31	0.010
4	3.35	0.017
5	3.36	0.029
6	3.44	0.01[illegible]

HC Ratio	Lambda Calc
1841	2.426
1350	2.515
1563	2.542
1784	2.545
1835	2.576
2184	2.937
1784	2.545

Combustion analysis filename		
Date:	05/08/2007 [illegible] PM	
Fuel	75% EN590	
	75% GTL	

Bore	0.0830	m
Stroke	0.0883	m
V	0.00044377	m3
Compression Coefficient	3.00014796	

University of Cape Town

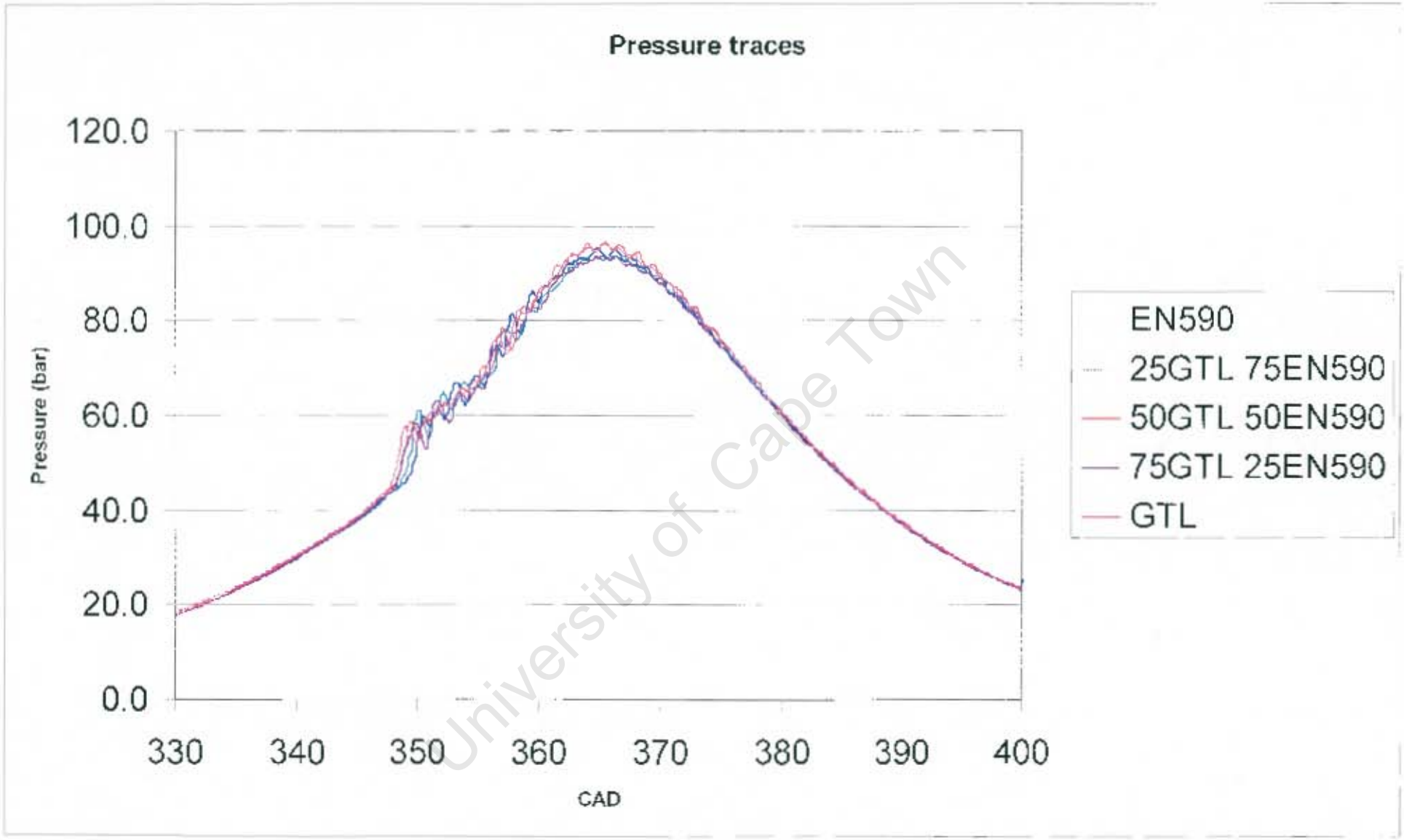

University of Cape Town

Figure F-10: Pressure traces for all test fuels with pilot injections

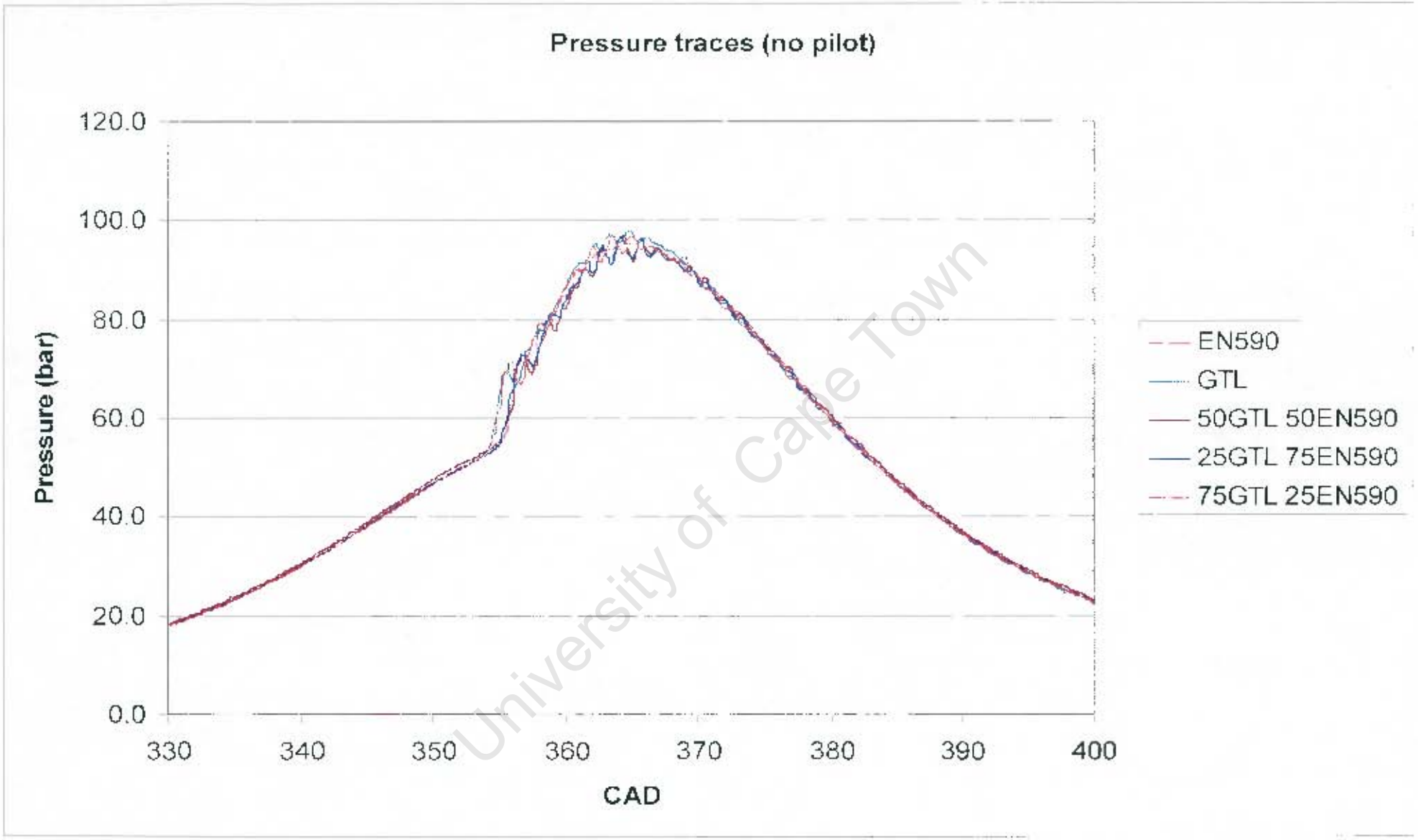

University of Cape Town

Figure F-11: Pressure traces for all test fuels without pilot injections